공학박사 학위논문

Effects of Alloying Elements and Rolling Conditions on Stretch Formability of Mg Alloys

마그네슘 합금 판재 성형성에 미치는 압연 공정 및 첨가 합금의 영향

2017년 2월

서울대학교 대학원

재료공학부

朴 重 源

Effects of Alloying Elements and Rolling Conditions on Stretch Formability of Mg Alloys

지도 교수 신 광 선

이 논문을 공학박사 학위논문으로 제출함

2017년 2월

서울대학교 대학원

재료공학부

朴 重 源

朴 重 源의 박사 학위논문을 인준함

2017년 2월

위 원 장	한 흥 남	(인)
부위원장	신 광 선	(인)
위 원	김 낙 준	(인)
위 원	김 도 향	(인)
위 원	이 경 훈	(인)

Abstract

Effects of Alloying elements and Rolling Conditions on Stretch Formability of Mg Alloys

Joong Won Park

School of Materials Science and Engineering

The Graduate School

Seoul National University

The development of formable Mg sheets is essential to meet the needs of the automotive industry for lightweight material. However, it is difficult to archive high formability due to their crystal structure. Basal slip mode and {10-12} tensile twinning are main deformation modes during deformation at room temperature. An activation of these 2 deformation modes is intricately connected with microstructures, textures, and alloying elements. Various alloys have been developed by using various rolling conditions in order to investigate effects of texture and grain size.

Microstructures and textures of by Mg-Al-Zn, Mg-Zn and Mg-Sn-Al alloys were examined, and then change of IE values through microstructures and textures were investigated. Basal pole intensity significantly decreased in Mg-Al-Zn and Mg-Sn-Al alloys, but there was the slight change in Mg-Zn alloys. In Addition, tensile tests were also performed to investigate the relationship with IE value and corresponding parameters from tensile test such as uniform elongation, the work hardening exponent (n) and the Lankford value (r-value).

To identify effects of grain size and texture on stretch formability more detailed, AZ31 alloys have been developed using various rolling conditions. Increasing rolling temperature enhances the formability of AZ31 alloys because of a weakening basal texture. Increasing annealing temperature and time increase grain size and larger grain size promotes the activation of {10-12} tensile twins. There are two roles of the tensile twinning in deformation. One is to contribute to the deformation through twin strain and another is to support to strain compatibility in grain boundaries. The tensile twins also play a critical role in Erichsen test (bi-axial tension condition).On the other hands, tensile twinning occurring in coarse grain size can decrease the IE value by acting as an origin of cracks because twin growth is so fast that the twin boundary acts as the obstacle interrupting the movement of basal dislocation.

Not only do grain size and texture affect to form $\{10\bar{1}2\}$ tensile twins at room temperature, but alloy elements determine twinning, 5 Mg-Zn alloys were fabricated and their grain size varied under different annealing conditions. The large-grain Ca-containing alloy showed the highest amount of $\{10\bar{1}2\}$ tensile twin. Tensile twinning is attributed to weak basal texture and large grain size as assessed from measurements of microstructures and VPSC calculations. The results of EBSD analysis and the small Erichsen test reveal that twinning contributes to stretch formability but the interaction between twin and slip causes cracks as grain size increases.

Keywords: Mg alloy, Stretch formability, Texture, Microstructure, Erichsen test

Student Number: 2007-22954

Contents

List of Tables

List of Figures

Chapter 1. Introduction

1.1 Introduction

There are increasing interests in developing magnesium alloys due to their excellent specific strength to reduce the weight of transportation vehicles. However, the structural application of magnesium alloys is limited because of their poor low formability at ambient temperatures [1]. It is well known that Mg has hexagonal crystal structure and cannot satisfy the von Mises requirement which requires a minimum of five independent slip modes for a grain to deform arbitrarily. In Mg, the (0002)<11-20> basal slip, which has only two independent slip systems [1], is preferentially operative because the critical resolved shear stress (CRSS) for the basal slip is much lower than those for the non-basal slips at room temperature [2]. But, basal slip and prismatic modes cannot operate in c-axis direction.

During the last decades, various methods were considered to develop magnesium alloys with good formability. Severe plastic deformation processes (SPD) were designed to fabricate ultra fine grain materials: Equal channel angular pressing (ECAP), Friction stir processing (FSP), Screw rolling etc. [3, 4, 5]. These processes weaken basal texture and reduce grain size with introducing high levels of shear. In addition, alloy design is considered to be one of the most favored and easy way to reach the goal. It is reported that an addition of Zn and Al improve both ductility and strength in Mg alloys. Although AZ alloys are commercially used due to their good mechanical properties, they have poor formability after rolling, which is required to reduce product cost. Research of alloying separates by two alloy

system: Mg-Zn and Mg-Al based alloys. Textures of Mg alloys remarkably influence their mechanical properties. Rear Earth elements (RE), Y, and Ca have been widely known that have contributed to weakening of the strong basal texture in Mg-Zn based alloys [6, 7, 8, 9, 10]. However, the effects of those kinds of alloying elements are limited in Mg-Al based alloys because Al forms intermetallic compounds with Ca and RE elements. However, Al based alloys have very attractive characterization: good corrosion resistance and good castability. Thus, many Al-based alloys are developing.

More fundamental ways are considered to improve formability of Mg; Single crystal experiment and plasticity model are adopted in order to analyze deformation modes [1, 11, 12, 13]. Basal slip and {10-12} tensile twin play critical roles in yield strength and deformation behaviors at room temperature because the stress necessary for activating these modes is so low that they form much more readily than other deformation modes such as prismatic and pyramidal slip. These deformation modes are affected by microstructure and grain size. Grain size refinement increases the yield strength of Mg and decreases twinning during deformation [14]. Hall-Petch relation can well explain strengthening mechanism with grain size. $\sigma_y = \sigma_0 + kd^{-1/2}$, where σ_y is the yield stress, σ_0 is the friction stress when dislocation move on the slip plane, d is the average grain size, and k is the stress concentration factor [15]. σ_y and σ_0 can be replaced by critical reserved shear stress (CRSS) of individual deformation mode τ_y and τ_o, respectively. Grain refinement is effective for the activation of non-basal slip mode at grain boundaries, because grain refinement creates stress concentration at grain boundaries [16]. As for other slip modes of Mg alloys, the Hall-Petch relation also can be applied to twinning [17, 18, 19, 20]. The activity of twinning increases with increasing grain size and, in turn, twinning to basal slip transition occurs at a

certain grain size [20, 21]. Moreover, texture is strongly related to the activation of certain deformation modes when plastic deformation occurs. In order to form the grain orientation most favorable for activating basal slip or tensile twin mode, various methods are being investigated that may contribute to weak basal texture [22, 23]. However, the onset and extend of twinning is more complex than those of slip modes. A proportion of twins occur against Schmid factor (SF) criterion [24, 25, 26]. Thus, understanding the role of twinning during deformation is necessary in developing Mg alloy sheets with high formability.

1.1 Characterization of Mg and Mg alloys

Magnesium, with its atomic number 12, has hexagonal close-packed (HCP) crystal structure. HCP crystal lattice and major planes of magnesium are shown in Fig. 1.1 with lattice parameters a=3.18 Å and c=5.19 A. The ideal c/a ratio of HCP metal is 1.633. An activation of slip modes and twinning is determined according to c/a ratio. For example, Cd and Zn have larger than the ideal value of c/a ratio, which means that more atoms aligned in basal plane. In this case, {0001}[11-20] basal slip mode dominantly forms during deformation. Otherwise, {10-10}[11-20] prismatic slip mode dominantly activate in Zr and Ti, with much smaller than the ideal c/a ratio value. There is a list of various HCP metals with their c/a ratios in Table 1.1 [27]. However, Mg, Co and Be do not meet the relationship between dominant deformation modes and c/a ratio. These three metals have less c/a ratio than 1.633 but basal slip mode dominantly activates in these metals. There may be other factors to affect an activation of deformation modes, such as Stacking fault energy (SFE) and characterization of metallic bond induced by electron cloud.

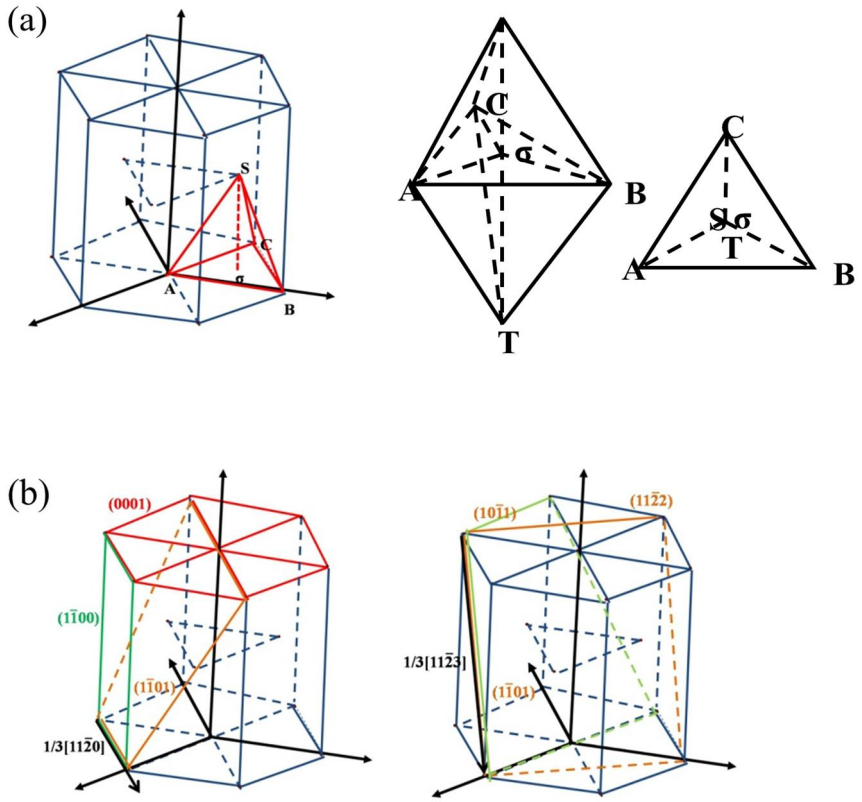

Fig. 1.1. Schematic description of (a) HCP crystal lattice and (b) major slip modes and planes

Table 1.1. Lattice parameters of various HCP metals [27]

Metal	a, A	C, A	c/a (room temp.)	Dominant slip mode
Cd	2.972	5.605	1.8859	Basal
Zn	2.659	4.936	1.8563	Basal
Co	2.502	4.601	1.623	Basal
Mg	3.203	5.200	1.623	Basal
Zr	3.231	5.147	1.593	Prism
Ti	2.950	4.683	1.587	Prism
Be	2.281	3.576	1.568	Basal

CRSS is the shear stress level where level is resolved onto that specific slip mode via Schmid factor criterion (SF), and then the dislocations on that system are activated. SF criterion shows the geometrical relationship between deformation mode and direction of applied force. Schmid's law is expressed as follows;

$$\tau_c = \sigma_y . \cos\emptyset\cos\lambda$$

Where τ_c and σ_y are CRSS of corresponding deformation mode and the uni-axial yield strength, respectively. Single crystal studies normally have used Schmid's law to observe CRSS values of deformation modes because of its simplicity of calculation [28, 29, 30]. There are some possible slip systems in Mg, and non-basal slip was reported [12, 30, 31]. It has previously mentioned that Mg cannot satisfy the von Mises criterion, so the formability of Mg is poor at room temperature. Basal slip mode and {10-12} tensile twin mostly contribute to deformation at room temperature due to their significantly low CRSS.

An activation of non-basal slip is affected by temperature, alloying elements, and grain size. Basal slip mode and {10-12} tensile twin have low CRSS values at room temperature, and their values hardly change even at high temperatures. On the other hand, CRSS of non-basal slip mode decreases with increasing temperature [30, 32]. Comparative CRSS value of deformation modes is more important than absolute CRSS value. Thus, non-basal slip easily activates with suppressing basal slip and tensile twinning. In addition, transmission electron microscopy (TEM) precisely found a movement of prismatic slip at high temperature; edge dislocation of prismatic slip mode was immobile at room temperature, but prismatic dislocation could move via double kink induced by thermally activated cross slip [33]. Alloying elements enhance an activation of non-basal slip modes. Addition of Li contributes to

the enhancement of <c+a> slip mode by visco-plastic self-consistent calculation (VPSC) and single crystal experiments [6, 30]. Grain refinement normally is effective for the activation of non-basal slip mode at grain boundaries, because grain refinement creates stress concentration at grain boundaries [16]. And preference of <c+a> slip mode was found when nano-sized grain compressed in the direction of c-axis according to molecular dynamic study [34]. Mg

Table 1.2. List of possible dislocation modes in Mg and Mg alloys

Type of dislocations	Number of systems	Burgers vector	Slip system	
a	3 (2)	1/3<11$\bar{2}$0>	Basal	{0001}<11$\bar{2}$0>
	3 (2)		Prism-I	{10$\bar{1}$0}<11$\bar{2}$0>
	6 (4)		Pyramidal-I	{10$\bar{1}$1}<11$\bar{2}$0>
c	3 (2)	<0001>	Prism-I	{10$\bar{1}$0}<0001>
	3 (2)		Prism-II	{11$\bar{2}$0}<0001>
c+a	3 (2)	1/3<11$\bar{2}$3>	Pyramidal-II	{11$\bar{2}$2}<11$\bar{2}$3>

1.2 Twinning in Mg and Mg alloys

When a number of metals are deformed, twinning, which is a catastrophic process in the form of sound, frequently occurs by shear. The cry of tin is the well-known phenomenon which is associated from the formation of twins. Twin plays important role in HCP. Five independent slips are necessary for satisfying the von Mises criterion during homogeneous deformation [35]. However, HCP metals deform by significantly limited slip modes. Interestingly twinning occurs on non-close-packed pyramidal planes, thus it is difficult in order to accommodate c-axis strain without twin modes [1].

In the crystallographic point of view, the twinned lattice is oriented to a mirror image of the untwined lattice. Fig 1.2 shows a simple example [36]. The lattice has been twinned along plane K_1 and the twinning direction η_1; the second undistorted plane is K_2, the plane containing η_1 and the normal to K_1 and K_2 is the plane of shear. The open circles are original atomic positions and black circles are moved to twinned atomic positions atomic by displacements which are equivalent to one or more inter-atomic spacing [36]. Twinning in the HCP metals frequently occurs to support limited possible slip modes. Figure 1.3 shows variation of twinning shear with c/a ratio for six possible twin modes in HCP metals [1]. In the plots, a positive slope represents contraction along the c-axis, while a negative slope represents extension [1]. For examples, there are {10-12} extension twin and {10-11} contraction twin in Mg and Mg alloys since c/a ratio of Mg crystal is less than $\sqrt{3}$. The extension twin is the resulting twin extending the crystal along the c-axis, while the contraction twin is the resulting twin shortening the crystal along c-axis. Figure 1.4 schematically shows the {10-12} extension twin and the {10-11} contraction twin.

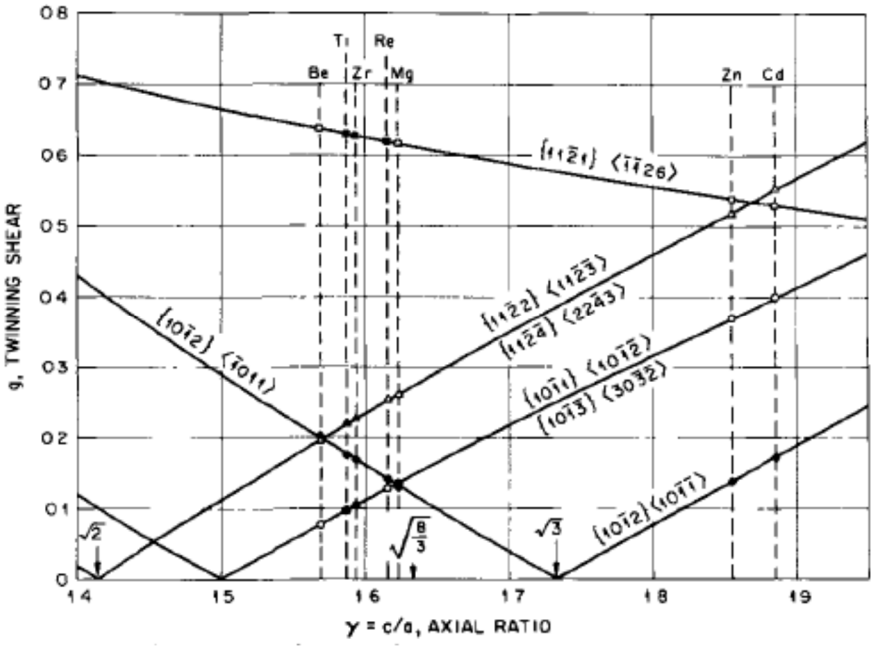

Fig. 1.2. Variation of twinning shear with the axial ratio, for the seven hexagonal metals, a filled symbol indicates that the twin mode is an active mode [1]

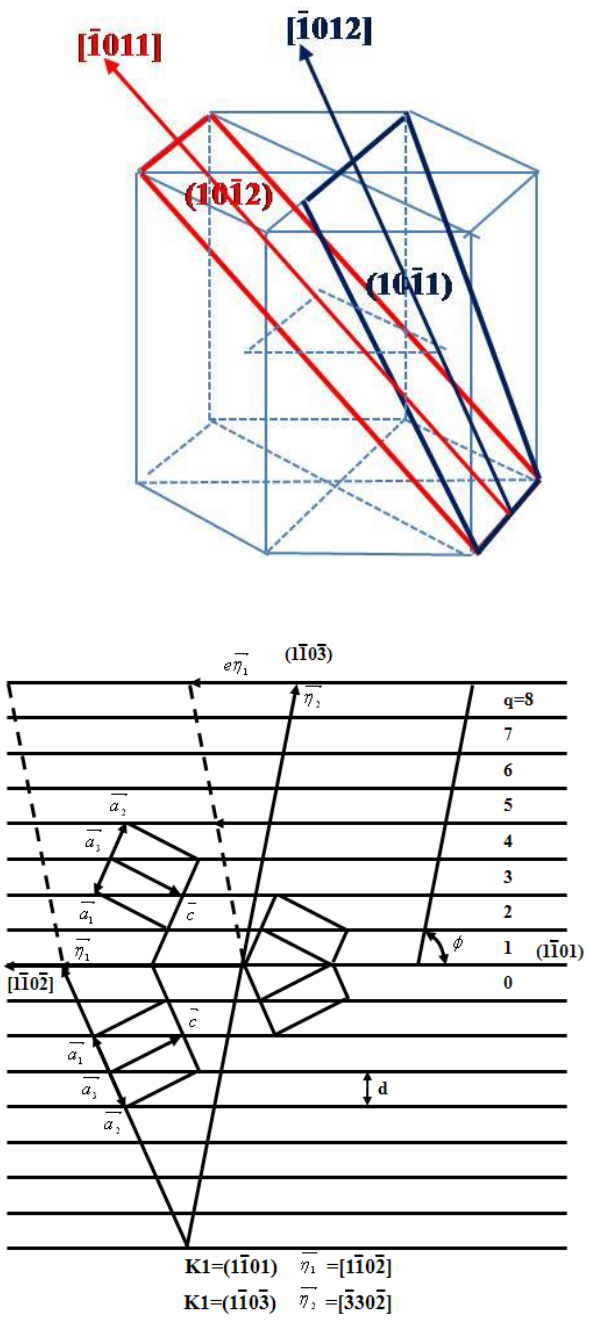

Fig. 1.3. Schematic description of (a){10-12} tensile twin, and (b) {10-11}compressive twin [44]

There are several twin modes reported in Mg and Mg alloys including the form of double twins which re-twin in the primary twin interior and the preferential alignment of primary twins [37, 38]. Table 1.3 lists detailed information regarding their misorientations between the matrix and the corresponding twin types. The CRSS value for {10-12} twin is only 2 to 3 MPa, while other twins require much larger shear stress (e.g. the second frequent one, {10-11} twin, requires in the range of 70-40 MPa) [39]. In addition to a low CRSS, {10-12} twin needs a simple atomic shuffling to form [1]. Therefore, the {10-12} twin has been far the most observed during deformation of Mg and Mg alloys.

Twinning is affected by applied conditions and microstructure during the deformation of HCP metals. The temperature, strain late and stress level are categorized as the applied conditions and the characteristics of twin can vary by processes and their conditions. Twinning in FCC metals occurs by work-hardening which helps satisfy twinning stress, because the CRSS of slip modes in FCC metals is less sensitive to temperature compared to those of BCC and HCP metals. In HCP metals, the CRSS of twinning hardly changes with temperature as in FCC and BCC metals [19, 40, 41]. Reed-hill reported that {11-21} twin is rarely found at room temperature in polycrystalline Zr but the frequency of the twin increases at 77K [19, 42]. The CRSS of slip modes with temperature varies in wide range when HCP metals are strained. As already noted in the previous section, the CRSS of slip modes are dependent of the temperature when Mg and Mg alloys are deformed [43]. The CRSS of prismatic and pyramidal slip decrease with increasing temperature, i.e. non-basal slip modes can easily activate at higher temperature. Thermally activated non-basal slip modes compete with twinning and it results in diminishing twinning with increasing temperature. Strain rate coupled with

temperature is one of the most important factors to affect on deformation behavior of metals. Generally, the combination of high strain rate and low temperature enhances twinning in metals. Even in Al alloys which are FCC metals with high stacking fault energy, twinning has occurred through shock-loading tests [19]. It seems that strain rate much affects on occurrence of twins. However, strain rate itself is not dependent function of the CRSS of twinning [19, 44]. Twinning is accompanied by the activation of slip to nucleate twins and the accommodation of local strain induced by twinning.

It has been reported that microstructures (grain size, texture, and alloy content etc.) affects frequency, shape, and width of twins. The grain size refinement normally increases yield strength of metals at low temperature. This phenomenon is well explained by the Hall-Petch relation [17, 45]; $\sigma_y = \sigma_o + k\, d^{-1/2}$ where d is the mean grain diameter, σ_y is the yield or flow stress, and σ_o is a friction stress. The dislocation pile-up model is well known and successfully applied to a number of metals. Like other deformation modes, the Hall-Petch relation also can be applied to twinning [17, 45, 46]. The Hall-Petch Slope, k, of twinning reported shows much stronger than that of the slip modes in polycrystalline Mg alloys [17, 47]. In other words, twinning can play more crucial role than slip modes in the deformation of Mg alloys with large grain size. Twinning significantly affects on the texture evolution and deformation behavior [48], but twinning itself is very dependent on strain path which is related to initial texture or orientation. Twin morphology, width of twins and frequency can be changed by strain path. The {10-12} twin results from applied extension along the c-axis, while the {10-11} twin occurs by the contraction along c-axis. Each {10-12} and {10-11} twinning has six equivalent twinning planes and specific shear direction. Like slip modes, the twin variants with the highest SF are far most

observed in Mg polycrystalline. Moreover, it is found that effects of SF on twin growth are also significant [49, 50]. When several twin variants simultaneously occur in one grain, they interrupt their growth and their widths of twins become narrow. The effects of addition elements on twinning have been studied. Crystallographically, Magee et al. explained that twinning with interstitial atoms in BCC decreases because interstitials require more energy to move right positions during twinning [19, 51]. However, it has reported that certain addition elements enhance twinning. It associated with a change of stacking fault energy. Fig. 1.4. shows a relation between the twinning stress and the measured stacking fault energy [19, 52]. Measurement of stacking fault is very difficult, thus it has been calculated by using first principles recently. Vitek introduced the concept of the generalized stacking fault (GSF) energy surface [53]. The GSF energy is a measure of the energy between two adjacent planes during shear deformation in specific slip direction on a given slip plane. This method can predict tendency of twinning by comparing reserved shear stress of twinning and slip modes [54].

Table 1.3. Twin type and corresponding misorientation angle in Mg crystal [24, 43]

Type of Twin	Misorientation Angles/Axis
$\{10\bar{1}1\}$	56.2^{o} $<1\bar{2}10>$
$\{10\bar{1}2\}$	86.3^{o} $<1\bar{2}10>$
$\{10\bar{1}3\}$	64^{o} $<1\bar{2}10>$
$\{10\bar{1}5\}$	41^{o} $<1\bar{2}10>$
$\{30\bar{3}2\}$	39.2^{o} $<1\bar{2}10>$
$\{30\bar{3}4\}$	70.8^{o} $<1\bar{2}10>$
$\{10\bar{1}1\}$-$\{10\bar{1}2\}$	37.5^{o} $<1\bar{2}10>$
$\{10\bar{1}1\}$-$\{10\bar{1}2\}$	30.1^{o} $<1\bar{2}10>$
$\{10\bar{1}1\}$-$\{10\bar{1}2\}$	66.5^{o} $<5\bar{9}43>$
$\{10\bar{1}1\}$-$\{10\bar{1}2\}$	69.9^{o} $<2\bar{4}21>$
$\{10\bar{1}2\}$-$\{10\bar{1}2\}$	7.4^{o} $<1\bar{2}10>$
$\{10\bar{1}2\}$-$\{10\bar{1}2\}$	59.9^{o} $<10\bar{1}0>$[a]
$\{10\bar{1}2\}$-$\{10\bar{1}2\}$	60.4^{o} $<\bar{8}170>$[b]
$\{10\bar{1}3\}$-$\{10\bar{1}2\}$	22.2^{o} $<1\bar{2}10>$

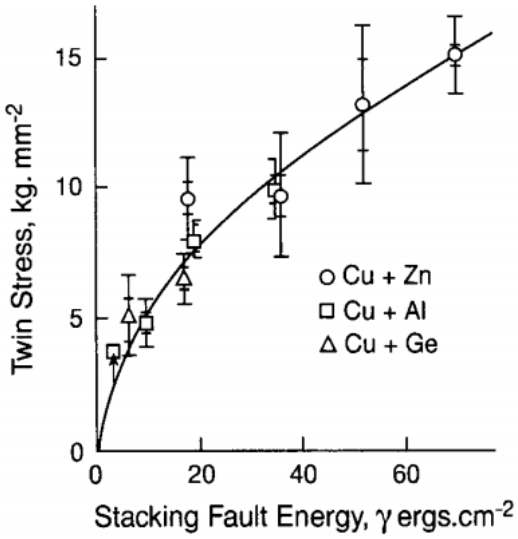

Fig. 1.4. The dependence of the twinning stress on stacking fault energy for copper-base alloys [19]

1.3 Visco-plastic self-consistent (VPSC) model

Slip mode and twinning play a critical role in deformation. However, it is difficult to investigate slip or twin behavior during deformation through experimental methods such as transmission electron microscopy (TEM), electron backscatter diffraction (EBSD), and x-ray diffraction (XRD). Plasticity model enables to predict their behaviors by using texture evolution and streee-strain curve.

Various poly-crystal plasticity models have been developed from Sachs model (iso-stress assumption of single slip in each grain) and Taylor model (iso-strain assumption of multiple slip in each grain). VPSC model was developed for application to low-symmetry materials such as Mg, Zr, and Ti by Lebensohn and Tome [55]. Not only, does predicting deformation behavior of anisotropic materials have the unique advantages, but twinning behavior can be predicted via employing twinning modes [6].

Initial texture represents grains and their orientations. Each grain is governed by a visco-plastic formulation of the inhomogeneous ellipsoidal inclusion embedded in a homogeneous effective medium (HEM). The single grain response is described by means of a rate sensitive constitutive law of the form.

$$D_{ij}^{c} = \dot{\gamma}_0 \sum_s m_{ij}^{s} \left(\frac{m^{s}:\sigma}{\tau^{s}}\right)^{n} = \dot{\gamma}_0 \sum_s \frac{m_{ij}^{s} m_{kl}^{s}}{\tau^{s}} \left(\frac{m^{s}:\sigma}{\tau^{s}}\right)^{n-1} \sigma_{kl} = M^{c}{}_{ijkl} \sigma_{kl}^{c}$$

Where D^c is the strain rate in the grain, s means each slip system, m^s is the Schmid factor, and τ^s is a threshold stress for each deformation mode. The schmid factor m^s is descriped by

$m_{ij}^{s}=1/2(n_i b_j + n_j b_i)$

Where n denote normal to slip plane, and b denote Burgers vector.

The relationship between the strain rates and stresses within the inclusion and the surrounding aggregate is given by

$(D^c - \bar{D}) = \tilde{M}^c : (\sigma^c - \bar{\sigma})$

$\tilde{M}^c$ is the accommodation tensor, which is a function of the secant compliance tensor of the HEM.

$\tilde{M}^c = n^{eff}(I - E)^{-1} : E : \bar{M}^{sec}$

I is the identify matrix and n^{eff} is a parameter related to rate sensitivity.

In VPSC model, Voce hardening law was adopted to model the hardening behavior of deformation mode.

$$\hat{\tau}^s = \tau_0^s + (\tau_1^s + \theta_1^s r)(1 - \exp(-r\left|\frac{\theta_0^s}{\tau_1^s}\right|$$

Where r is the accumulated shear in the grian, and r_0, θ_0, θ_1 are the initial CRSS, the initial hardening rate, the asymptotic hardening rate, respectively.

In Mg alloys, twinning occurs with orienting grains during deformation. VPSC model assumes that twinning is associated with a CRSS, like slip modes. And the predominant twin reorientation scheme (PTR) is used to describe texture evolution, induced by twinning.

$V^{acc,mode} = \sum_c \sum_t \frac{\gamma^{t,c}}{S^t}$

Where C is denoted as each grain, $\gamma^{t,c}$ is the amount of twinning shear, the corresponding twin mode denotes t, and volume fraction is $V^{t,c} = \frac{\gamma^{t,c}}{S^t}$

The PTR scheme uses a statistical approach because it is unable to consider each twinned fraction as a new orientation. At each

incremental step, some grains are fully reoriented when certain conditions are satisfied.

$$V^{th,mode}=A^{th1}+A^{th2}\frac{V^{eff,mode}}{V^{acc,mode}}$$

After each deformation increment, a grain is randomly chosen, and the twin system with the highest accumulated volume fraction is identified. If the latter is larger than the threshold $V^{th,mode}$ then the grain is allowed to reorient and $V^{eff,mode}$ and $V^{th,mode}$ are updated. The process is repeated until either all grains are randomly checked or until the effective twin volume exceeds the accumulated twin volume [57].

1.4 Development of wrought Mg alloys

Pure magnesium have very limited mechanical properties. Hence, numerous ways have been developed to improve them. Alloying is easy and widely used one. Aluminum, Zinc, Manganese and Zirconium are common alloying elements in the development of wrought magnesium alloys. In additions to alloying, dispersion of quasi-crystalline phase, long period stacking ordered structures, amorphous and several reinforcements in magnesium matrix can enhance the mechanical properties.

A wide range of Mg-Al-Zn extrusion alloys are commercially used like AZ31, AZ61 and AZ81 etc. Recently, high strength of Mg-Al-Zn system has been continuously developed. Park reported that Mg–6Zn–1Mn (wt%) alloys containing various Al contents exhibited excellent tensile properties because of refined precipitates by Al addition [58]. T.T. Sasaki reported that additions of Sn on Mg-Zn-Al alloy achieved high yield strength [59].

Mg-Zn based systems have been widely used to develop magnesium alloys which have high strength and reasonable ductility. Zn is an effective element to enhance solid-solution strengthening the -Mg matrix with its high maximum solubility in Mg and to increases the response of Mg alloys towards precipitation hardening. Rare-earth additions into Mg alloys have been shown to have a wide range of benefits for magnesium alloys. Recently, Mg-Gd-Y-Zn-Zr alloys have been show high strength. T. Homma reported that YTS over 470MPa has been obtained in Mg-Gd-Y-Zn-Zr alloy produced by conventional hot extrusion [60]. Ke Liu reported that YTS are 418MPa [61].

The Mg–Li systems have been investigated because these offer potential to ruduce weight of Mg alloys and improve the room temperature ductility. The BCC β-phase are partially formed with 5 to 11wt% Li content in Mg alloys and above 11 wt% Li the alloy entirely changes HCP α-phase to β-phase. Strength of Mg-Li is very low. Therefore, there are two ways to improve strength of Mg-Li systems. One is using SPD and another is adding elements. Xiangrui Meng reported that as-rolled Al and Zn additions affected on strength and elongation of Mg-8Li respectively [62]. Introducing icosahedral quasicrystal structure in Mg-Li system, the tensile strength effectively strengthened [63].

A great number of composites differ in the reinforcing components and in the production process. By incorporating reinforcement particles into Mg alloys, strength has been observed to increase since reinforcement particles act as obstacles to dislocations. Maung Aye Thein reported that AlN particles are used as reinforcement in Mg-5Al wt.% alloys and enhance the mechanical properties[64].

The alloy reveals a very high yield strength of 610MPa and elongation of 5% by using rapidly solidified powder metallurgy. Y. Kawamura reported that the

extraordinary hight strength of the RS P/M MgZnY system is caused the presence of fine grains and dispersion of long period stacking ordered structures [65].

The icosahedral phase possesses fivefold symmetry and a quasiperiodic structure, very different from those of crystalline phases. Recently there has been a great interest in Mg alloys strengthened by the icosahedral (I) phase. Bae et al. produced Mg-Zn-Y distributing quacicrystal phases finely in the alloy and achieved yield stress of 220 MPa and ultimate tensile strength of 370 MPa with 17.2% elongation in tensile tests at room temperature [66].

Among the benefits of adding carbon nanotubes are increased yield strength and stiffness. In addition to strength and stiffness, ductility of magnesium alloys can be improved due to the activation of additional slip planes. T. Honma reported that Si-CNFs were synthesized successfully and high strength possessed [67].

1.5 Research objectives

There have been many efforts to improve stretch formability of Mg at room temperature. Effects of grain size on stretch formability are dependent on texture. In the present study, AZ31 alloys have been developed using various rolling conditions in order to investigate effects of texture and grain size. Increasing rolling temperature enhances the formability of AZ31 alloys because of a weakening basal texture. Increasing annealing temperature and time increase grain size and larger grain size promotes the activation of {10-12} tensile twins. Tensile twinning contributes to enhancement of the IE value, but tensile twinning larger grain size can decrease the IE value by acting as an origin of cracks.

In addition, effects of alloying elements were covered. Alloy elements and grain size are important factors that determine formation of {10-12} tensile twins at room temperature. 5 Mg-Zn alloys were fabricated and their grain size varied under different annealing conditions. The large-grain Ca-containing alloy showed the highest amount of {10-12} tensile twin. Tensile twinning is attributed to weak basal texture and large grain size as assessed from measurements of microstructures and VPSC calculations. The results of EBSD analysis and the small Erichsen test reveal that twinning contributes to stretch formability but the interaction between twin and slip causes cracks as grain size increases.

Bibliography

1. M. H. Yoo, "Slip, Twinning, and Fracture in Hexagonal Close-Packed Metals", Metal. Trans. A, 12 (1981), pp. 409-418.
2. H. Yoshinaga and R. Horiuchi, "On the Nonbasal Slip in Magnesium Crystals", Trans. JIM., 5 (1963), pp. 14-21
3. M. Gzyl, A. Rosochowski, S. Boczkal, and L. Olejnik, "The role of microstructure and texture in controlling mechanical properties of AZ31B magnesium alloy processed by I-ECAP", Mater. Sci. Eng. A 638 (2015), pp. 20-29.
4. D. Sagapuram, M. Efe, W. Moscoso, and S. Chandrasekar, "Controlling texture in magnesium alloy sheet by shear-based deformation processing", Acta Meter., 61 (2013), pp. 6843-6856.
5. M. Diez, H. E. Kim, V. Serebryany, S. Dobatkin, and Y. Estrin, "Improving the mechanical properties of pure magnesium by three-roll planetary milling", Mater. Sci. Eng. A, 612 (2014), pp. 287-292.
6. S. R. Agnew, M. H. Yoo, and C. N. Tome "Application of texture simulation to understanding mechanical behavior of Mg and solid solution alloys containing Li or Y", Acta Mater., 49 (2001), pp. 4277-4289.
7. J. Bohlen, M. R. Nurnberg, J. W. Senn, D. letzig, and S. R. Agnew, "The texture and anisotropy of magnesium-zinc-rare earth alloy sheets", Acta Mater., 55 (2007), pp. 2101-2112.
8. T. Al-Samman, and X. Li"Sheet texture modification in magnesium-based alloys by selective rare earth alloying", Mater. Sci. Eng. A, 528 (2011), pp. 3809-3822.
9. M. Yuasa, M. Hayashi, M. Mabuchi, and Y. Chino, "Improved plastic anisotropy of Mg-Zn-Ca alloys exhibiting high-stretch formability: A first-

principles study", Acta Mater, 65 (2014), pp. 207-214.

10. H. Ding, X. Shi, Y. Wang, G. Cheng, and S. Kamado, "Texture weakening and ductility variation of Mg-2Zn alloy with Ca or RE addition", Metar. Sci. Eng. A, 645 (2015), pp. 196-204.
11. R.E. Reed-Hill and W.D. Bobertson, "Deformation of Magnesium Single Crystals by Nonbasal Slip", Trans. Metall. Soc. AIME., 209 (1957) pp. 496-502.
12. H. Yoshinaga and R. Horiuchi, "On the non-basal Slip in Magnesium Crystals", Trans. JIM., 5 (1963), pp. 14-21.
13. H. Yoshinaga and R. Horiuchi, "Deformation Mechanisms in Magnesium Single Crystals Compressed in the Direction Parallel to Hexagonal Axis", Trans. JIM., 4 (1963), pp. 1-8
14. W. Yuan, S. K. Panigrahi, J. –Q. Su and R. S. Mishra, "Influence of grain size and texture on Hall-Petch relationship for a magnesium alloy", Scripta Meter., 65 (2011), pp. 994-997.
15. R. W. Armstrong, "The influence of polycrstal grain size on several mechanical properties of materials", Metal. Mater. Trans., 1A (1970), pp. 1169-1176.
16. J. Koike, T. Kobayashi, T. Mukai, H. Watanabe, M. Suzuki, K. Maruyama and K. Higashi, "The Activity of Non-basal Slip Systems and Dynamic Recovery at Room Temperature in Fine-grained AZ31B Magnesium Alloys", Acta Mater., 51 (2003), pp. 2055-2065.
17. Yi Wang and Hahn Choo, "Influence of Texture on Hall-Petch Relationships in an Mg Alloy:, Acta Mater., 81 (2014), pp. 83-97.
18. S.G. Hong, S.H. Park and C.S. Lee, "Role of $\{10\bar{1}2\}$ twinning characteristics in the deformation behavior of a polycrystalline magnesium alloy", Acta Mater., 58 (2010), pp. 5873–5885.

19. J.W. Christian and S. Mahajan, “Deformation Twinning”, Prog. Mater. Sci., 39 (1995), pp. 1-157.
20. M.A. Meyers, O.Vohringer and V.A. Lubarda, “The Onset of Twinning in Metals: A Constitutive Description”, Acta Mater., 49 (2001), pp. 4025–4039.
21. C. M. Cepeda-Jimenez, J. M. Molina-Aldareguia and M. T. Perez-Prado “Origin of the Twinning to Slip Transition with Grain Size Refinement, with Decreasing Strain Rate and with Increasing Temperature in Magnesium”, Acta Mater. 88 (2015), pp. 232-244.
22. W.J. Kim, J.D. Park and W.Y. Kim, “Effect of Differential Speed Rolling on Microstructure and Mechanical Properties of an AZ91 Magnesium Alloy”, J. Alloys Compd., 460 (2008), pp. 289–293.
23. Q. Ma, H.E. Kadiri, A.L. Oppedal, J.C. Baird, M.F. Horstemeyer and M. Cherkaoui, “Twinning and Double Twinning Upon Compression of Prismatic Textures in an AM30 Magnesium Alloy”, Scripta Mater., 64 (2011), pp. 813–816.
24. Ming Zhe Bian and Kwang Seon Shin, “{10-12} Twinning Behavior in Magnesium Single Crystal” Met. Mater. Int., Vol. 19, No. 5 (2013), pp. 999-1004.
25. R.E. Reed-Hill and W.D. Robertson, “Additional Modes of Deformation Twinning in Magnesium”, Acta Metal., 5 (1957), pp. 717-727.
26. J.W. Christian and S. Mahajan, “Deformation Twinning”, Prog. Mater. Sci., 39 (1995), pp. 1-157.
27. P.G. Partridge, “The Crystallography and Deformation Modes of Hexagonal close-packed Metals”, Met. Rev., 12 (1967), pp. 169-194
28. 28. A.Akhtar and E.Teghtsoonian, “Solid Solution Strengthening of Magnesium Single Crystals-I Alloying Behaviour in Basal Slip”, Acta Metall., 17 (1969), pp. 1339-1349.

29. A.Akhtar and E.Teghtsoonian, “Solid Solution Strengthening of Magnesium Single Crystals-II The effects of Solute on the Ease of Prismatic Slip”, Acta Metall., 17 (1969), pp. 1351-1356.
30. A.Akhtar and E.Teghtsoonian, “Substitutional Solution Hardening of Magnesium Single Crystals”, Phil. Mag., 25 (1972), pp. 897-916.
31. S. Ando, N. Harada, M. Tsushida,H. Kitahara and H. Tonda, “Temperature Dependence of Deformation Behavior in Magnesium and Magnesium Alloy Single Crystals”, Key Eng. Mater., 345-346 (2007), pp. 101-104.
32. R.E. Reed-Hill and W.D. Bobertson, “Deformation of Magnesium Single Crystals by Nonbasal Slip”, Trans. Metall. Soc. AIME., 209 (1957) pp. 496-502.
33. T. Obara, H. Yoshinga and S. Morozumi, “$\{11\bar{2}2\}\langle 11\bar{2}3\rangle$ Slip System in Magnesium”, Acta Metall., 21 (1973), pp. 845-853.
34. A. Couret, and D. Caillard, “An in situ study of prismatic glide in Mg-II. Microscopic activation parameters”, Acta metal, 33 (1985), pp. 1455-1461.
35. Y.F. Guo, S. Xu, X.Z. Tang, Y.S. Wang, and S. Yip, “Twinnability of hcp metals at the nanoscale”, J. App. Phys., 115 (2014), pp.224902.
36. Taylor, S., “Plastic Strain in Metals”, J. Inst. Met., 62 (1938), pp.307-324.
37. R. W. K. Honeycombe, “The Plastic Deformation of Metals”, Edward Arnold
38. M.R. Barnett, Z. Keshavarz, A.G. Beer and X. Ma, “Non-Schmid Behaviour during Secondary Twinning in a Polycrystalline Magnesium Alloy”, Acta Mater., 56 (2008), pp. 5-15.
39. L. Jiang, J.J. Jonas, A.A. Luo, A.K. Sachdev and S. Godet, “Influence of $\{10\bar{1}2\}$ Extension Twinning on the Flow Behavior of AZ31 Mg Alloy”, Mater. Sci. Eng. A, 445-446 (2007), pp. 302-309.
40. J. Koike, “Enhanced Deformation Mechanisms by Anisotropic Plasticity in Polycrystalline Mg Alloys at Room Temperature”, Metall. Mater. Trans. A,

36 (2005), pp. 1689-1696.

41. K. Ishikawa and H. Watanabe, “High Temperature Compressive Properties over a wide Range of Strain Rates in an AZ31 Magnesium Alloy”, J. Mater. Sci., 40 (2005), pp. 1577-1582.
42. Barnett M. R., “A Taylor Model Based Description of the Proof Stress of Magnesium AZ31 during Hot Working”, Metall. Mater. Trans. A, 2003, 34(9), pp. 1799-1806.
43. L. Capolungo, P. E. Marshall, R. J. McCabe, I. J. Beyerlein, and C. N. Tome, “Nucleation and growth of twins in Zr: A statistical study”, Acta Mater., 57, 20 (2009), pp. 6047-6056.
44. Ming Zhe Bian, “Plastic deformation behavior of magnesium single crystals”, Seoul National Univ., (2012).
45. I. Ulacia, N. V. Dudamell, F. Galvez, S. Yi, M. T. Perez-Prado, and I. Hurtado, “Mechanical Behavior and Microstructural Evolution of a Mg AZ31 Sheet at Dynamic Strain Rates” Acta Mater., 58, (2010), 2988-2997.
46. R. W. Armstrong, “The influence of polycrstal grain size on several mechanical properties of materials”, Metal. Mater. Trans., 1A (1970), pp. 1169-1176.
47. C. M. Cepeda-Jimenez, J. M. Molina-Aldareguia and M. T. Perez-Prado “Origin of the Twinning to Slip Transition with Grain Size Refinement, with Decreasing Strain Rate and with Increasing Temperature in Magnesium”, Acta Mater. 88 (2015), pp. 232-244.
48. M. R. Barnett, Z. Keshavarz, A. G. Beer, and D. Atweel, “Influence of grain size on the compressive deformation of wrought Mg-3Al-1Zn”, Acta mater. 52 (2004), pp., 5093-5103.
49. S.H. Park, S.G. Hong and C.S. Lee, “Role of {10-12} twinning characteristics in the deformation behavior of a polycrystalline magnesium alloy”, Scripta

Mater., 62 (2010), pp. 202–205.

50. L. Jiang, J. J. Jonas, R. K. Mishra, A. A. Luo, A. K. Sachdev, and S. Godet, “Twinning and texture development in two Mg alloys subjected to loading along three different strain paths”, Acta Mater., 55 (2007), pp., 3899-3910.
51. S. G. Hong, S. H. Park, and C. S. Lee, “Role of {10-12} twinning characteristics in the deformation behavior of a polycrystalline magnesium alloy”, Acta Mater., 58 (2010) pp., 5873-5885.
52. D.W. Shin and C. Wolverton, “First-principles Density Functional Calculations for Mg Alloys: A Tool to Aid in Alloy Development”, Scripta Mater., 63 (2010), pp. 680-685.
53. Tenckhoff, “Deformation Mechanisms in Zirconium and Zircaloy”, (1988), pp. 9-9.
54. V. Vitek, “Intrinsic Stacking Faults in Body-centred Cubic Crystals”, Phil. Mag., 18 (1968), pp. 773-786.
55. S. L. Shang, W. Y. Wang, B. C. Zhou, Y. Wang, K. A. Darling, L. J. Kecskesf, S. N. Mathaudhu and Z. K. Liu, “Generalized stacking fault energy, ideal strength and twinnability of dilute Mg-based alloys: A first-principles study of shear deformation”, Acta Mater., 67 (2014), pp., 168-180
56. R.A. Lebensohn, and C.N. Tome, “A self-cosistent anisotropic approach for the simulation of plastic deformation and texture development of polycrystals: application to zirconium alloys”, Acta Metall., 41 (1993), pp. 2611-2624.
57. C.N. Tome, and R.A. Lebensohn, “Manual for code visco-plastic self-consistent (VPSC)”, LosAamos National Laboratory (USA) and Universidad Nacional de Rosario (Argentina), 6 edition, 2003.
58. S.S. Park, G.T. Bae, D.H. Kang, I.H. Jung, K.S. Shin and N.J. Kim, "Microstructure and tensile properties of twin-roll cast Mg-Zn-Mn-Al alloys", Scripta Mater. 57 (2007), pp. 793-796.

59. T.T. Sasaki, K. Yamamoto, T. honma, S. kamado and K. Hono, "A high-strength Mg-Sn-Zn-Al alloy extruded at low temperature", Scripta Mater. 59 (2008) pp. 1111-1114.
60. T. Homma, N. kunito and S. Kamado, "Fabrication of extraordinary high-strength magnesium alloy by hot extrusion", Scripta Mater. 61 (2009) pp. 644-647.
61. K. Liu, L.L. Rokhlin, F.M. Elkin, D. Tang and J. Meng, "Effect of ageing treatment on the microstructures and mechanical properties of the extruded Mg–7Y–4Gd–1.5Zn–0.4Zr alloy", Mater. Sci. Eng. A 527 (2010) pp. 828-834.
62. X. Meng, Ruizhi W, M. Zhang, L. Wu and C. Cui, "Microstructures and properties of superlight Mg–Li–Al–Zn wrought alloys", Jol. Ally. Compds. 486 (2009) pp.722-725.
63. D.K. Xu, L. Liu, Y.B. Xu and E.H. Han, "D.K. Xu, L. Liu, Y.B. Xu and E.H. Han, Scripta Mater. 57 (2007) p.285.", Scripta Mater. 57 (2007) pp. 285-288.
64. M. A. Thein, L. Lu and M.O. Lai, "Maung Aye Thein, L. Lu and M.O. Lai, Composite Structures 75 (2006) p. 206.", Composite Structures 75 (2006) pp. 206-212.
65. Y. Kawamura, K. Hayashi, A. Inoue and T. Masumoto,"Rapidly Solidified Powder Metallurgy Mg97Zn1Y2Alloys with Excellent Tensile Yield Strength above 600 MPa", Mater. Trans. JIM 42 (2001) p. 1172-1176.
66. D.H. Bae, S.H. Kim, D.H. Kim and W.T. Kim, "Deformation behavior of Mg–Zn–Y alloys reinforced by icosahedral quasicrystalline particles", Acta Mater. 50 (2002) pp.2343-2356.
67. T. Honma, K. Nagai, A. Katou, K. Arai, M. Suganuma and S. Kamado, "Synthesis of high-strength magnesium alloy composites reinforced with Si-coated carbon nanofibres", Scripta Mater. 60 (2009) pp. 451-454.

Chapter 2. Experimental procedure

2.1 Sample preparation

2.1.1 Strip casting and extrusion conditions

Materials were prepared by two processes before rolling; twin roll strip casting and indirect extrusion were used to fabricate Mg alloys. Firstly, AZ31 alloys were prepared by strip casting with a nominal composition of 3 wt.% Aluminum and 1 wt.% Zinc. Materials were melted with protective gas containing mixture of SF_6 and CO_2, and then stabilized at 700^{o}C for 30min. Twin roll strip casting was conducted with 4mm roll gap and 3.0 mpm roll speed. Secondly, Mg-Zn and Mg-Sn alloys were fabricated by extrusion process. Various alloys were melted at 720^{o}C to prepare billets for extrusion. Extrusion carried out at 340^{o}C with a plate shape die (extrusion ratio 56:1). Extruded specimens have 30mm width (Fig 2.1). But the length is not enough for Erichsen test, thus rolling was conducted in transverse direction.

2.2.2 Rolling and annealing conditions

The strip casted specimens were preheated at 150^{o}C, 250^{o}C, 350^{o}C or 450^{o}C for 20min before rolling. Rolling was performed at a rolling reduction of 50% per pass until a thickness of 1mm was obtained with 150^{o}C hot rolls for the specimens preheated at 150^{o}C and 200^{o}C hot rolls for the specimens preheated at 250^{o}C and 450^{o}C. Specimens with different average grain sizes were prepared at temperatures ranging from 350^{o}C to 450^{o}C and annealing times

from 1 to 144 hrs. The compositions and rolling conditions are listed in Table 2.1.

The extruded specimens were preheated at various temperatures ranging from 250^{o}C to 550^{o}C for 20min before rolling. Rolling was performed with rolling reduction of 50% per pass until a thickness of 1mm was obtained with 200^{o}C hot rolls. Specimens with different grain sizes were prepared at various temperatures ranging from 250^{o}C to 550^{o}C and annealing times varying from 1 to 48hrs. The compositions and rolling conditions are listed in Table 2.1.

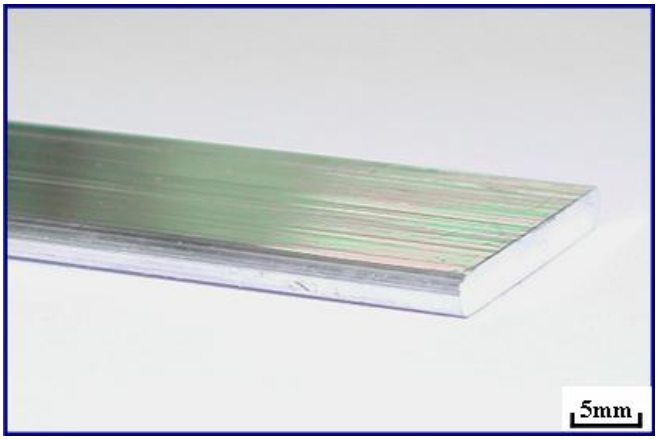

Fig. 2.1. Extruded Mg alloys with plate shape die (30w x 3t)

Fig. 2.2. Images of Xpert Pro MRD and Su-70(EBSD)

Table 2.1. Rolling conditions of strip cated and extruded Mg alloys

Compositions (wt.%)	Fabrication process	Preheat temperature (^{o}C)	Roll temperature (^{o}C)	Annealing temperature (^{o}C)
Mg-3.0Al-1.0Zn	Strip casting	150 – 450	150 - 200	250 - 450
Mg-3.0Zn	Extrusion	250	200	250-350
Mg-6.0Zn	Extrusion	250	200	250-350
Mg-6.0Zn-0.2Ca	Extrusion	250	200	250-350
Mg-6.0Zn-0.2Y	Extrusion	250	200	250-350
Mg-6.0Zn-1.0Al	Extrusion	250	200	250-350
Mg-3.0Sn-3.0Al	Extrusion	350-550	200	350-550

2.2 Characterization of rolled Mg alloys

2.2.1 Mechanical property

Tensile and compressive tests were conducted to elucidate relationship between parameters from tests and stretch formability. Tensile specimens with a 20mm gauge length, 4mm gauge width and 1mm thickness were machined from rolled alloys and compressive specimens were cut into rectangular shape (2x2x4 mm). Tensile and compressive tests with loading in the rolling direction were carried out at room temperature with a nominal strain rate of 2 x 10-4 s-1. Erichsen tests were carried out using a hemispherical punch with a diameter of 20mm and a 5mm/min punch speed. Each condition conducted 3 times and computed the average.

2.2.2 Microstructure and texture analysis

The microstructure was taken by optical microscopy. Specimens were mechanically polished with sandpapers from #400 to #4000 and then micro-polished with 0.3, 0.05㎛ alumina powder. And, Specimens were chemically etched with acetic – picral (4.2 g picric acid, 10 ml acetic acid, 10 ml H_2O, and 70 ml ethyl alcohol).

Textures were measured by X-ray diffraction (XRD) using a PANalytical X'Pert PRO X-ray diffractometer with a Cu Kα source. Pole figures were obtained from the normal direction planes of the rolled sheets and then data were calculated using the arbitrarily defined cells (ADC) method with LaboTex 3.0 software [1].

Measurements of microstructures and textures were carried out by EBSD

using FE-SEM (Su-70, HITACHI) fitted with a TSL EBSD camera operating at 20 kV, 70o tilting angle. Specimens were prepared by mechanical polishing using sand papers and alumina powder, followed by chemical etching with acetic – picral (4.2 g picric acid, 10 ml acetic acid, 10 ml H2O, and 70 ml ethyl alcohol). Data with a confidence index >0.1 were used for texture and twin analysis.

2.2.3 Small Erichsen test

In order to investigate fracture behavior during the Erichsen test, the small Erichsen test in which size is reduced by one tenth was carried out. There are two steps to take fracture images. First, the EBSD technique was used to confirm initial orientation for specimens. Second, small Erichsen device is put into SEM chamber. There is a schematic description of small Erichsen device in Fig. 2.3. Third, twinning and crack propagation is observed with successive punch displacements of 1/3mm, 2/3mm, and 1mm.

2.2.4 Bi-axial tension test

Sheet forming is a critical issue to promote wider use of Mg alloys in the industry. Physical properties are commonly evaluated by various uniaxial tests but these ways are limited to reflect materials' formability. Particularly, Mg alloys exhibit disagreement between properties from the unaxial tests and stretch formability due to the anisotropy of Mg [2]. Therefore, many researchers have designed various test methods under bi-axial tension condition to investigate precisely the stretch formability of materials [3]. Cupping tests widely used can exam formability under the bi-axial tension

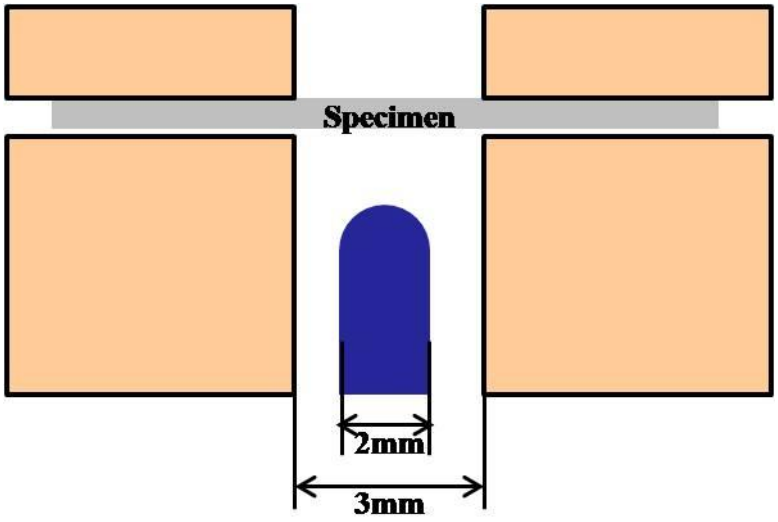

Fig. 2.3. Design for small Erichsen test device

condition but there are a lot of problems to investigate texture and microstructure evolution during the tests. In the present study, bi-axial tension test are carried out with a cross shaped specimen shown in Fig. 2.4 [3].

There are two types of bi-axial tensile test machines. One is controlled by load and another is controlled by displacement. The apparatus controlled by load has many benefits to investigate mechanical behavior under the bi-axial tension condition but it is very complicated since two different tension axis should be synchronized during bi-axial tension test. On the other hand, the apparatus controlled by displacement is simpler and more effective way to carry out the bi-axial tension test. The apparatus can set on a uniaxial testing machine. The pantograph connects four wings of the specimen to stretch it in the two directions at the same time when compression is applied on the top of it [4] (shown in Fig. 2.4).

Another reason to use the method is that it makes possible to investigate texture and microstructure evolution with EBSD analysis. To obtain EBSD image, sample should be flat and small. Fig. 2.5 exhibits a drawing of the cross specimen. The center of the specimen has 0.5mm thickness to lead the strain at the center.

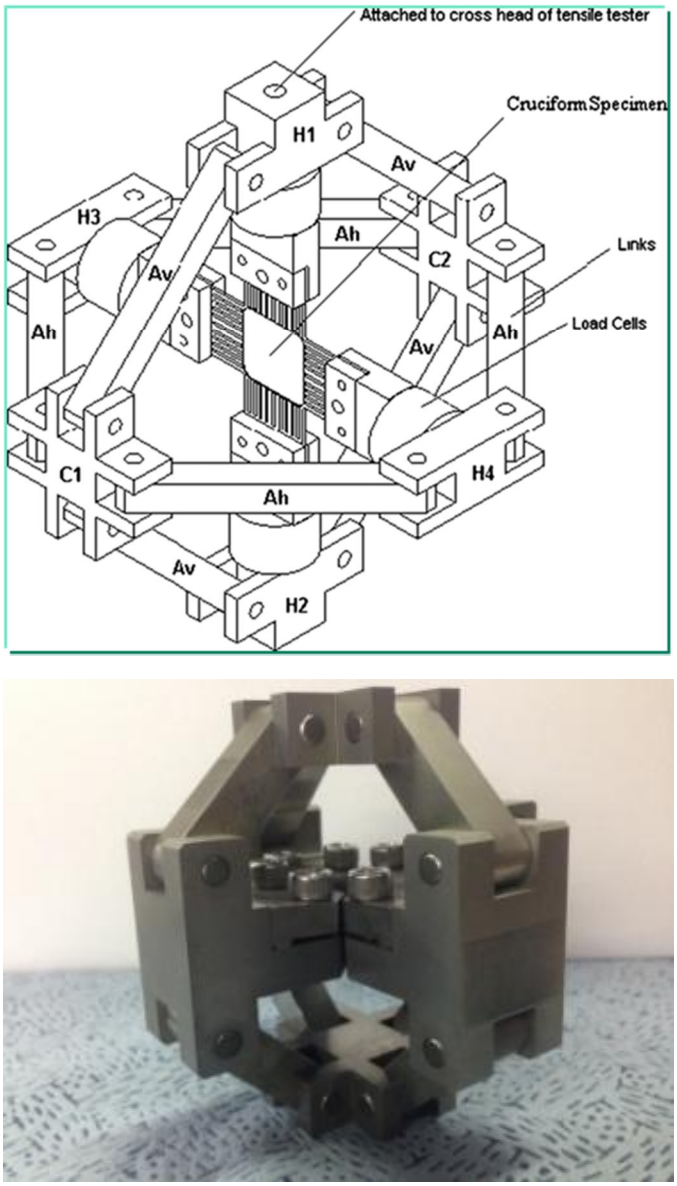

Fig. 2.4. Design for bi-axial tension test device [4]

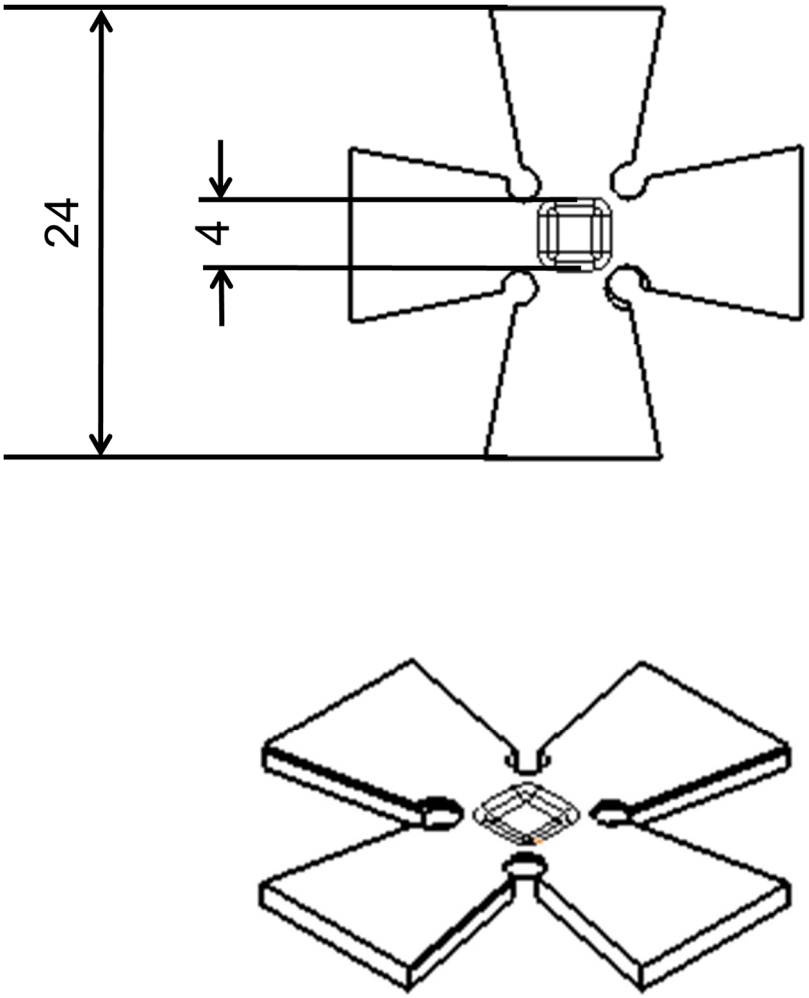

Fig. 2.5. Drawing of cross shaped specimen

Bibliography

1. J.J. Jonas, S. Mu, T. Al-Samman, Gunter Gottstein, L. Jiang, and E. Martin, “The role of strain accommodation during the variant selection of primary twins in magnesium”, Acta Mater. 5 (2011), pp. 2046-2056.
2. B. C. Suh, M. S. Shim, K. S. Shin, and Nack J. Kim, “Current issues in magnesium sheet alloys: Where do we go from here”, Scripta Mater. 84-85, (2014), pp. 1-6.
3. J. G. Park, D. C. Ahn, J. B. Nam, Y. S. Kim, “State of art for biaxial tensile test systems”, Trans. Mater. Proc. 20 (2011), pp. 222-228
4. G. Ferron, and A. Makinde, “Design and development of a biaxial strength testing device”, J. Test. Eval., 16 (1988), pp. 253-256.

Chapter 3. Effects of rolling and annealing conditions on stretch formability of Mg alloys

3.1 Introductions

The structural applications of Mg alloys are limited because of their poor formability at ambient temperatures. During the last decades, various methods were considered to develop Mg alloys with good formability. Changing rolling and annealing conditions are effective ways to modify microstructures and textures of Mg sheets, which strongly affect their mechanical properties. Asymmetric rolling was adopted to apply force throughout the thickness of specimens. This technique showed weak basal texture and refined grains [1]. High rolling ratio, which leads to high strain and strain rate, decreased typical basal texture via enhancement of shear band and {10-11}compressive twin [2, 3]. Rolling temperature affects an activation of deformation modes during rolling; non-basal slip mode more frequently occurs instead of basal slip mode and tensile twin [4, 5]. {10-12} tensile twin plays important role to enhancement of strong basal texture but an activation of non-basal slip suppressed reorientation of grains by tensile twinning. Mg-Zn and Mg-Al alloys are most widely used as structure material. A character of each alloys are different thus a usage of each alloys are various. And effects of applied rolling conditions vary by alloys as well.

In this study, Mg alloys have been developed with various rolling and annealing conditions. Comparative microstructures and textures were examined in order to investigate the effects of rolling and annealing conditions on the formability by Mg-Al-Zn, Mg-Zn and Mg-Al-Sn alloys. In

Addition, tensile tests were also performed to investigate the relationship with IE value and corresponding parameters from tensile test such as uniform elongation, the work hardening exponent (n) and the Lankford value (r-value).

3.2 Results and discussion

3.2.1 Stretch formability vs Rolling conditions

Erichsen tests were carried out in Mg-Al-Zn, Mg-Zn and Mg-Sn-Al alloys with the various preheat and annealing conditions. The IE values were plotted by rolling and annealing temperatures in order to identify effects on stretch formability (shown in Fig. 3.1, 3.2, and 3.3). The IE values increase with increasing both annealing and preheat temperatures, while the effects of annealing conditions are uncertain in Mg-Sn-Al alloys. IE values of TA33 and TA63 increase and then decrease with increasing annealing temperature. This phenomenon is associated with grain size distribution. It will cover in chapter 6. The change of IE values via different rolling and annealing conditions indicates that increasing rolling temperature is more effective to improve formability than annealing temperature and also can be assumed that these two conditions have different effects on the microstructure Mg alloys.

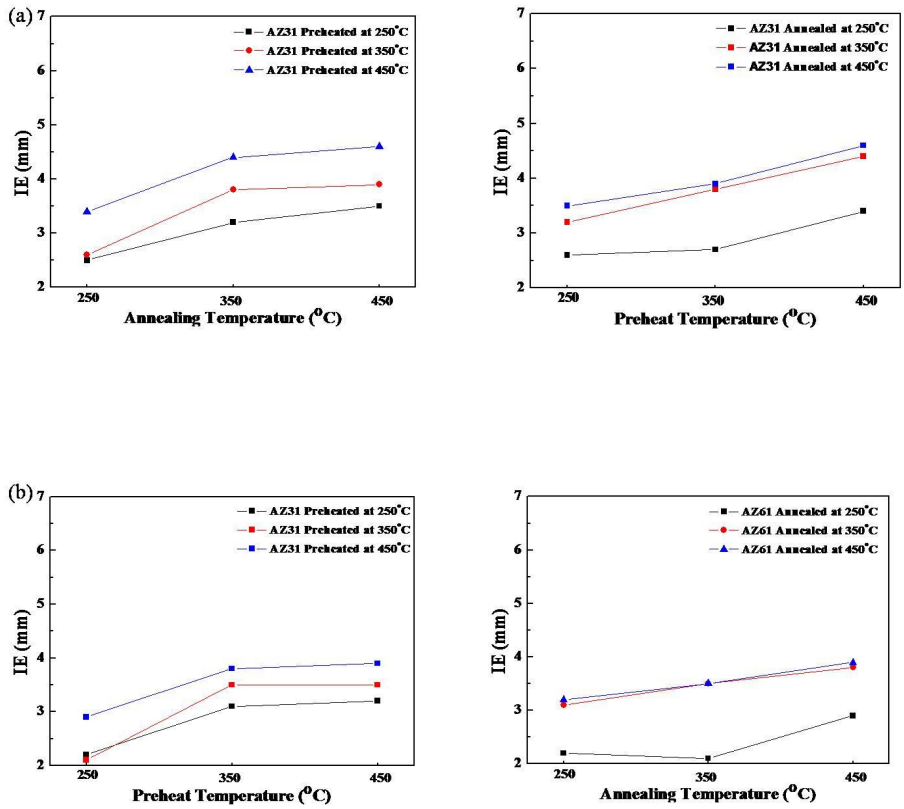

Fig. 3.1. Relationships between IE value and annealing and preheat temperature, which are obtained from (a) AZ31 and (b) AZ61

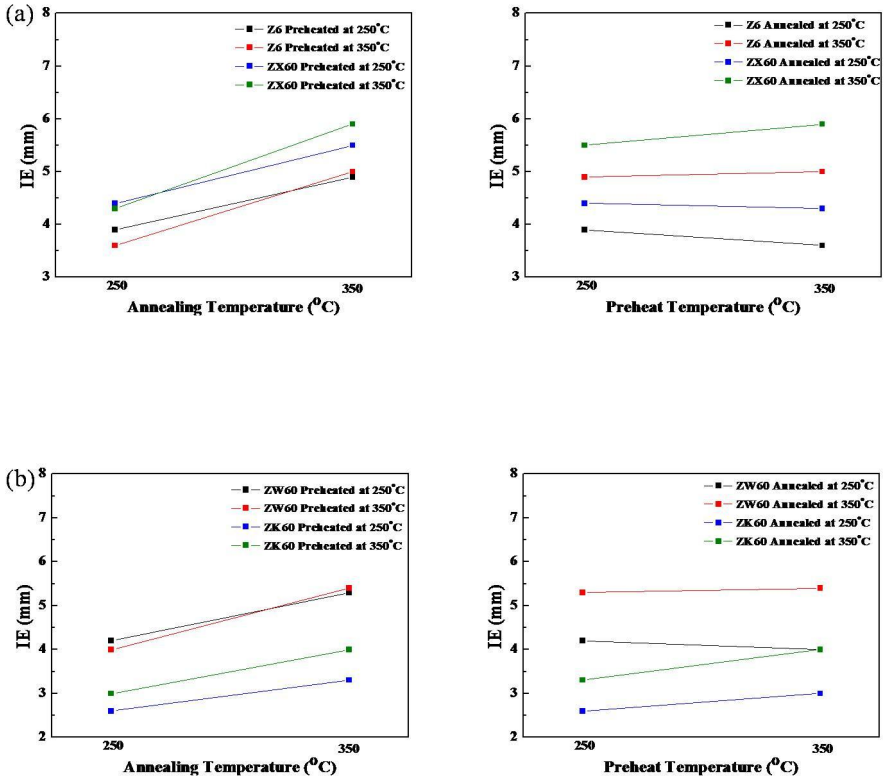

Fig. 3.2. Relationships between IE value and annealing and preheat temperature, which are obtained from (a) Z6 and ZX60 and (b) ZX60 and ZK60

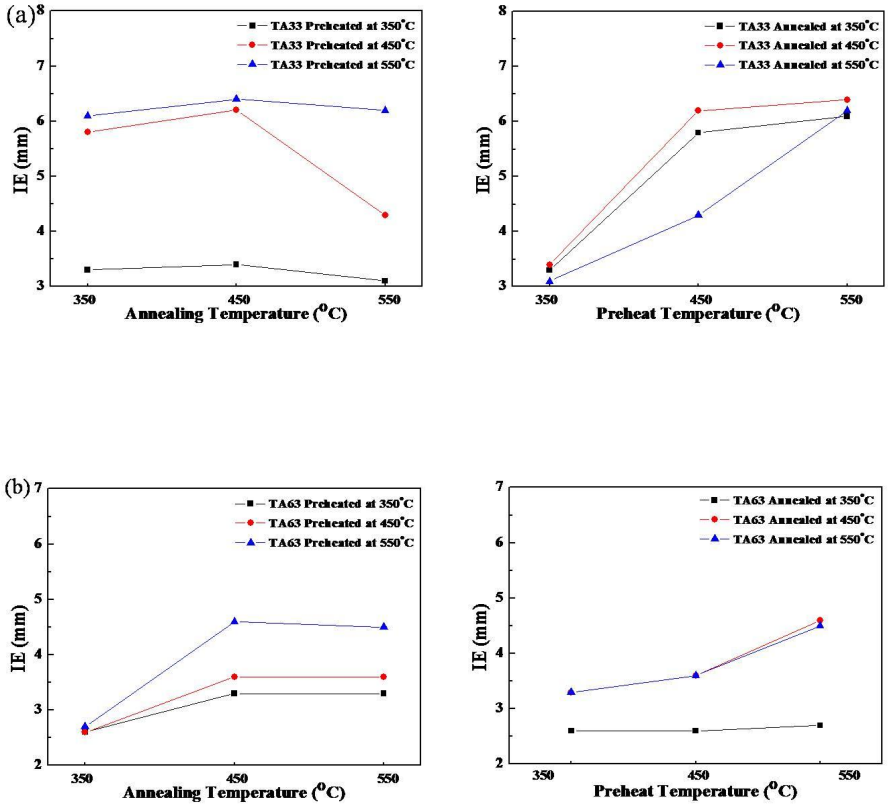

Fig. 3.3. Relationships between IE value and annealing and preheat temperature, which are obtained from (a) TA33 and (b) TA63

3.2.2 Characterization of microstructure and texture

Microstructures were taken from ND planes by a optical microscope (Fig. 3.3). All the microstructures have recrystallized grain structures with equiaxial grains and homogenously distributed grain sizes (shown in Fig. 3.4, 3.5). Annealing temperature obviously affected grain size. However, effects of rolling temperature were different by Mg alloys; high rolling temperature increases the grain size of Mg-Al-Zn and Mg-Sn-Al alloys, while Mg-Zn alloys with different rolling temperature and the same annealing temperature have similar grain size. Mobility of grain boundary during annealing is associated with misorientaion angle between grains [6, 7]. Rolled Mg sheets typically show strong basal texture, which have smaller misorietnation angle than weak basal texture due to the crystallographic reason. According to (0002) basal pole figures of Mg-Al-Zn and Mg-Sn-Al alloys, increasing rolling temperature significantly decrease basal pole intensity, while Mg-Zn alloys shows a slight decrease in basal pole intensity. Increasing rolling temperature affects texture evolution and it also lead to increase grain growth rate. In addition, Mg-Sn-Al alloys show abnormal grain growth with annealing at 550^{o}C, which have bimodal grain size distribution (Fig. 3.4 (b)). Stretch formability of TA33 deteriorates because heterogeneous grain distribution interrupts homogeneous strain during deformation.

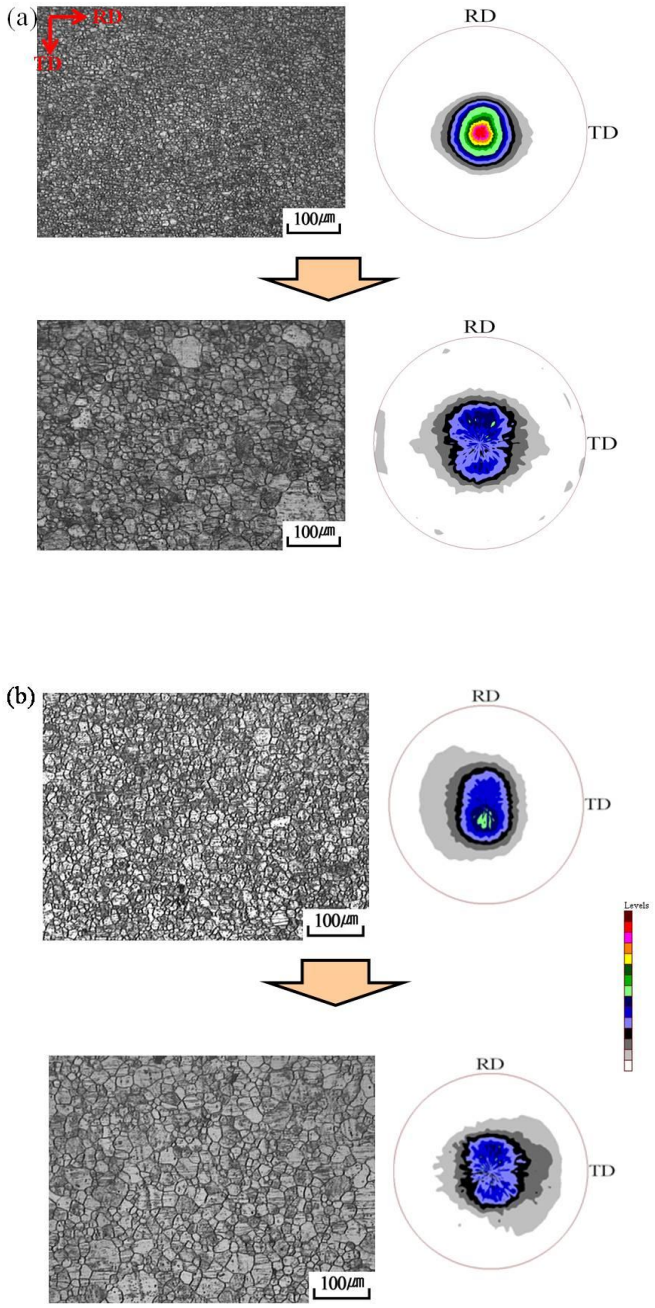

Fig. 3.4. Microstructures and textures obtained in ND planes of (a) AZ31 and (b) TA33

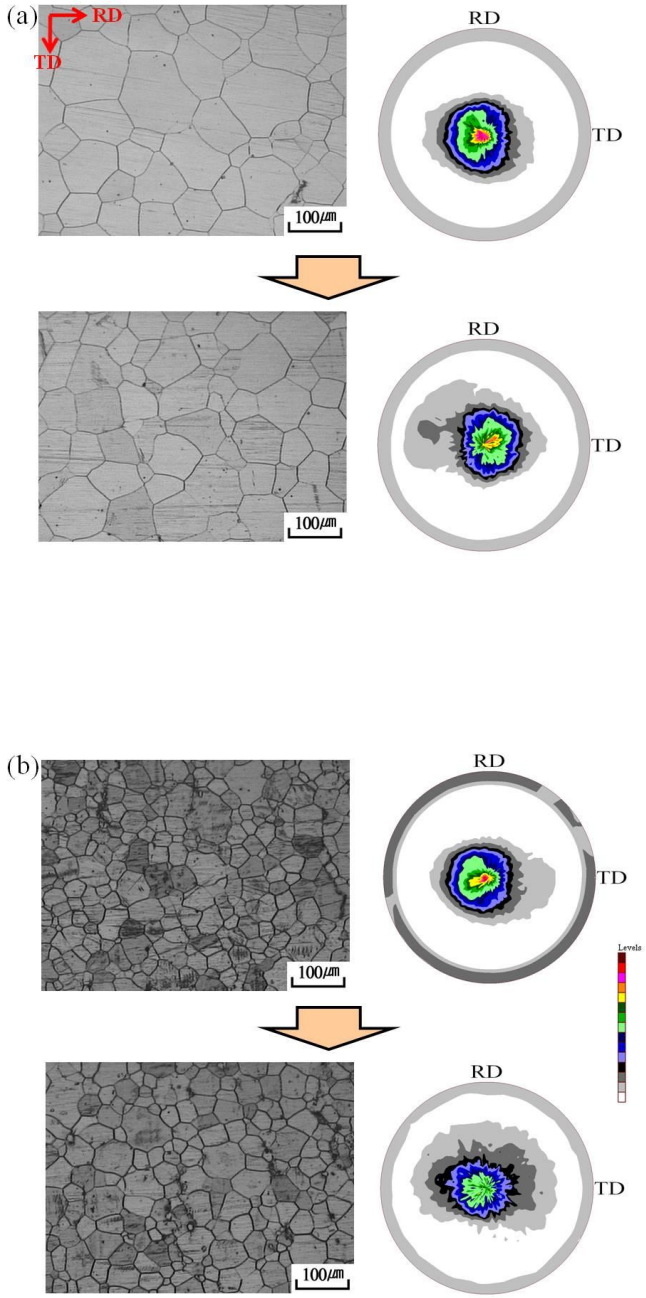

Fig. 3.5. Microstructures and textures obtained in ND planes of (a) Z6 and (b) ZX60

3.2.3 Relationship between tensile tests and stretch formability

Uniaxial tensile tests were carried out at room temperature and nominal strain rate of 2 x 10-4 s-1 in Fig. 3.6 and Fig. 3.7. Yield stress of AZ31 and TA33 decrease with increasing rolling temperature and annealing temperature. However, the effect of both conditions is different by alloys; yield stress of AZ31 more decrease with increasing rolling temperature, while yield stress of TA33 is more dependent on annealing temperature. In the last section, AZ31 and TA33 are more affected by rolling temperature, which decreases basal pole intensity. Yield stress is dependent on an activation of deformation modes. Basal slip mode and {10-12} tensile mode, in particular, play a critical role in determination of yield stress. And grain size and texture determine prefer deformation mode [8, 9, 10]. In addition, TA33 alloy have heterogeneous grain distribution, so stress concentration on grain boundaries easily occurs during deformation. Compared to AZ31 and TA33, increasing rolling temperature slightly decrease yield stress in Z6 and ZX60 alloys. This result is associated with evolution of texture. Work hardening exponent (n-value) is the parameter to show work hardening during tensile test. It can be described by the Ludwik-type power-law strain-hardening equation: $\sigma = K\varepsilon^n$, where σ is stress, ε is strain, K is constant and n is work hardening exponent[11]. High n-value found to be related to high stretch formability [12]. Twinning via large grain size decreases yield stress and develop an interaction between twinning and basal slip. The effect of grain size will cover in the next chapter. r-value are correlated well with texture induced by the rolling condition; when basal slip mode can move in the direction via

thickness, r-value is low. Uniform elongation is also affected by an activation of basal slip mode and twinning. Weak basal texture contributes to homogeneous deformation by basal dislocations. On the contrary, twinning orients grains into hard orientation and suppresses ductility. The activation of these two deformation mode is related to grain size, texture, and alloying elements. The next chapters will cover the effects of them.

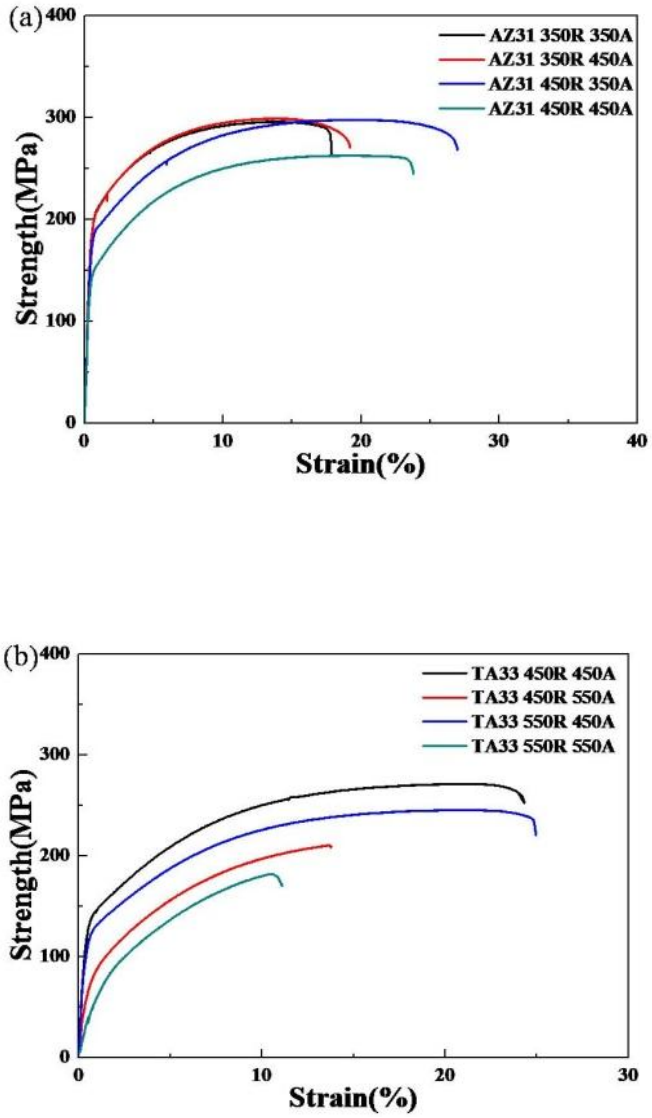

Fig. 3.6. Stress-Strain curves, tensile loading in Rolling direction, of (a) AZ31 and (b) TA33

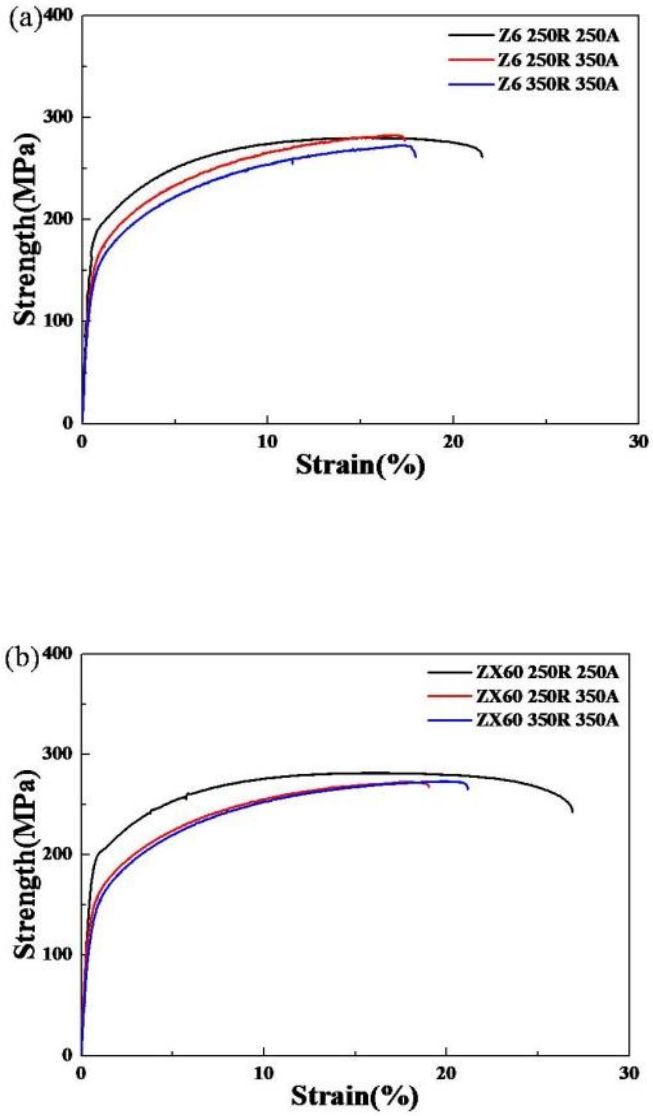

Fig. 3.7. Stress-Strain curves, tensile loading in Rolling direction, of (a) Z6 and (b) ZX60

3.3 Conclusion

The influence of rolling temperature and annealing temperature on the stretch formability was investigated in the present study. The conclusions are summarized below:

1. An increase in rolling temperature is more effective to improve IE value than annealing temperature.

2. Basal texture in AZ31 and TA33 more weakened with increasing rolling temperature, and it might lead to increase grain growth rate.

3. Results of tensile test showed that parameters of AZ31 and TA33 were differently affected by rolling temperature and annealing temperature; yield stress and n-value of AZ31 were more dependent on rolling temperature, while those of TA33 and Z6 alloys were changed by annealing temperature.

Bibliography

1. W.J. Kim, J.D. Park and W.Y. Kim, “Effect of Differential Speed Rolling on Microstructure and Mechanical Properties of an AZ91 Magnesium Alloy”, J. Alloys Compd., 460 (2008), pp. 289–293.
2. J.A. del Valle, M.T. Perez-Prado, and O.A. Ruano, “Texture evolution during large-strain ot rolling of the Mg AZ61 alloy”, Mater. Sci. Eng. A 355 (2003), pp. 68-78.
3. Y.B. Chun, C.H.J. Davies, “Texture effects on development of shear bands in rolled AZ31 alloy”, Mater. Sci. Eng. A 556 (2012), pp. 253-259.
4. Ming Zhe Bian, “Plastic deformation behavior of magnesium single crystals”, Seoul National Univ., (2012).
5. X.S. Huang, K. Suzuki, Y. Chino, and M. Mabuchi,” Influence of initial texture on rolling and annealing textures of Mg-3Al-1Zn alloy sheets processed by high temperature rolling”, J. Alloys Comp. 537 (2012), pp. 80-86.
6. M. T. Perez-Prado, O. A. Ruano, “Texture evolution during grain growth in annealed Mg AZ61 alloy”, Scripta Mater. 48 (2003), pp. 59-64
7. J. J. Bhattacharyya, S. R. Agnew, and G. Muralidharan, “Texture enhancement during grain growth of magnesium alloy AZ31B”, Acta Mater. 86 (2015), pp. 80-94.
8. Yi Wang and Hahn Choo, “Influence of Texture on Hall-Petch Relationships in an Mg Alloy:, Acta Mater., 81 (2014), pp. 83-97.
9. M.R. Barnett, “Twinning and the ductility of magnesium alloys Part I: Tension twins”, Mater. Sci. Eng. A,. 464 (2007) pp. 1-7.
10. L. Jiang, J.J. Jonas, R.K. Mishra, A.A. Luo, A.K. Sachdev, and S. Godet,

"Twinning and texture development in two Mg alloys subjected to loading along three different strain paths", Acta Mater., 55 (2007), pp. 3899-3910..

11. B. Dodd, and Y. Bai, "Ductile fracture and ductility with applications to metalworking", Academic press INC.
12. D. H. Kang, D. W. Kim, S. Kim, G. T. Bae, K. H. Kim and Nack J. Kim, "Relationship between stretch formability and work-hardening capacity of twin-roll cast Mg alloys at room temperature", Scripta Mater. 61 (2009), pp. 768-771.

Chapter 4. Effects of grain size and texture on mechanical properties of AZ31

4.1 Introductions

There is increasing interests in developing magnesium alloys due to their excellent specific strength to reduce of transportation vehicles. However, the structural application of Mg alloys is limited because of their low formability. It is well known that Mg has a hexagonal crystal structure and a strong basal texture is easily generated during conventional thermo-mechanical processing, which induces limited formability. During the past decades, various methods have been considered to develop Mg alloy sheets with good formability.

Controlling grain size and texture enhances the formability of Mg alloys at room temperature. Weakening basal texture is obviously effective to enhance stretch formability of Mg alloys. Effect of grain size on stretch formability is different by texture [1, 2]. Basal slip and {10-12} tensile twin play critical roles in yield strength and deformation behaviors at room temperature because the stress necessary for activating these modes is so low that they form much more readily than other deformation modes such as prismatic and pyramidal slip. Grain size refinement normally increases the yield strength of Mg and decreases twinning during deformation [3]. This phenomenon is well described by the Hall-Petch relation. Grain refinement is effective for the activation of non-basal slip mode at grain boundaries, because grain refinement creates stress concentration at grain boundaries [4]. As for other slip modes of Mg alloys, the Hall-Petch relation also can be applied to twinning [5, 6, 7, 8]. The activity of twinning increases with increasing grain

size and, in turn, twinning to basal slip transition occurs at a certain grain size [9, 10]. Moreover, texture is strongly related to the activation of certain deformation modes when plastic deformation occurs. In order to form the grain orientation most favorable for activating basal slip or tensile twin mode, various methods are being investigated that may contribute to weak basal texture [11, 12, 13, 14]. However, the onset and extend of twinning is more complex than those of slip modes. A proportion of twins occur against Schmid factor (SF) criterion [8, 15, 16]. Thus, understanding the role of twinning during deformation is necessary in developing Mg alloy sheets with high formability.

In the present study, AZ31 sheets fabricated with various rolling conditions were studied to identify factors that improve the stretch formability of Mg alloys. The electron back scattered diffraction (EBSD) technique was employed to investigate the influence of grain size and texture on the Erichsen test and tensile test. The small Erichsen test was designed in an attempt to investigate the relationship between twinning and fracture behavior.

Table 4.1 Rolling conditions, average grain diameters, and Erichsen values of AZ31 alloys with the preheat-treatment 150°C and 250°C

Specimens	Preheat Temp. (°C)	Annealing Temp. (°C)	Annealing Time	Grain Size (μm)	Erichsen Value (mm)
150R350A	150	350	1	3.03	3.0
150R450A	150	450	1	7.63	3.35
150R450A24H	150	450	24	11.43	3.5
150R450A48H	150	450	48	13.72	3.6
150R450A96H	150	450	96	17.24	3.7
150R450A144H	150	450	144	21.23	3.7
250R350A	250	350	1	3.92	3.2
250R450A	250	450	1	6.32	3.5
250R450A24H	250	450	24	13.17	3.7
250R450A48H	250	450	48	15.75	3.8
250R450A96H	250	450	96	18.49	3.8
250R450A144H	250	450	144	23.18	3.8

Table 4.2 Rolling conditions, average grain diameters, and Erichsen values of AZ31 alloys with the preheat-treatment 150°C and 250°C

Specimens	Preheat Temp. (°C)	Annealing Temp. (°C)	Annealing Time	Grain Size (μm)	Erichsen Value (mm)
350R350A	50	350	350	1	3.62
350R450A	50	350	450	1	7.82
350R450A24H	50	350	450	24	12.59
350R450A48H	50	350	450	48	18.36
350R450A96H	50	350	450	96	22.22
350R450A144H	50	350	450	144	28.32
450R350A	450	350	1	4.80	4.4
450R450A	450	450	1	6.92	4.6
450R450A24H	450	450	24	14.16	5.2
450R450A48H	450	450	48	17.92	5.2
450R450A96H	450	450	96	26.02	4.8
450R450A144H	450	450	144	34.36	4.3

4.2 Results and discussion

4.2.1 Results of Erichsen tests

Erichsen tests were carried out in AZ31 alloys with the various preheat and annealing conditions shown in table 4.1 and 4.2. IE values of 450R specimens increase up to 450R450A48H and then decrease again with increasing annealing time. However, those of other specimens gradually increase as annealing time increases. In addition, we found that the IE values of 450R specimens are the highest of all samples tested (Fig. 4.3(b)). 150R and 250R specimens have similar IE values and 350R specimens have little higher than those of 150R and 250R specimens.

4.2.2 Microstructures

Inverse pole figure maps (IPF) were obtained in ND planes (Fig. 4. 1). All the microstructures have recrystallized grain structures with equiaxial grains and homogenously distributed grain sizes. Grain size varies from 3.03 μm to 21.23 μm, from 3.92 μm to 23.18 μm and from 4.80 μm to 34.36 μm for 150R, 250R and 450R specimens, respectively, with increasing annealing temperature and time. This grain size change plots in Fig 4.2. Grain growth rates vary by preheat temperatures; 450R specimens are the fastest of all specimens. The relationship between grain size and IE value in each condition are presented in Fig. 4.4 (a). The IE values of all conditions increase with increasing grain size, except that those of 450R begin to decrease at high grain size. It has been reported that the relationship between IE values and grain

size is affected by texture. The stretch formability of specimens with weak basal texture deteriorated with grain coarsening, while that of specimens with strong basal texture improved [1, 2]. As has been shown in other studies, the change in IE values by grain size seems to be strongly related to texture.

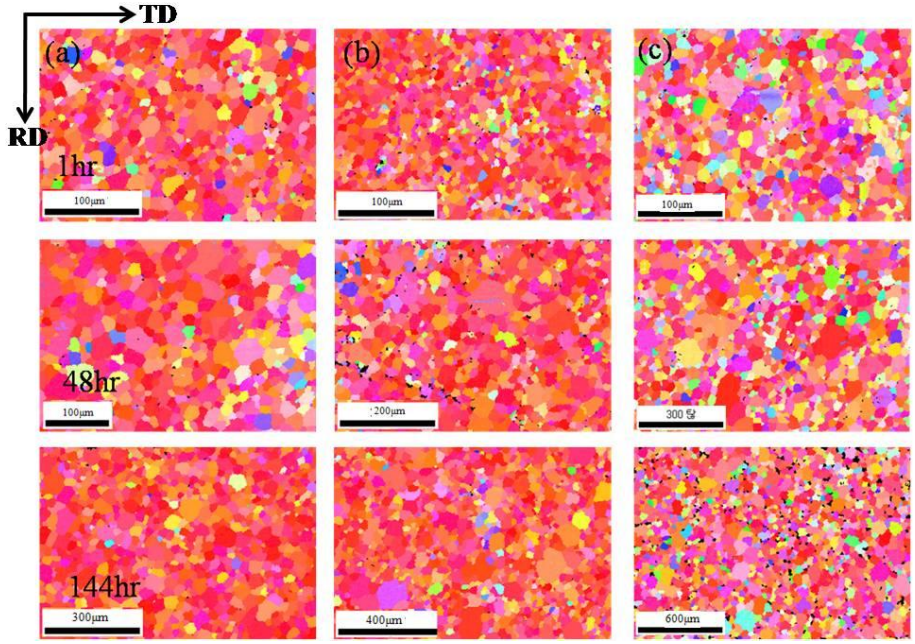

Fig. 4.1. IPF maps obtained under various rolling and annealing conditions: (a), (b) and (c) correspond to the microstructures of 150R, 250R, and 450R, respectively

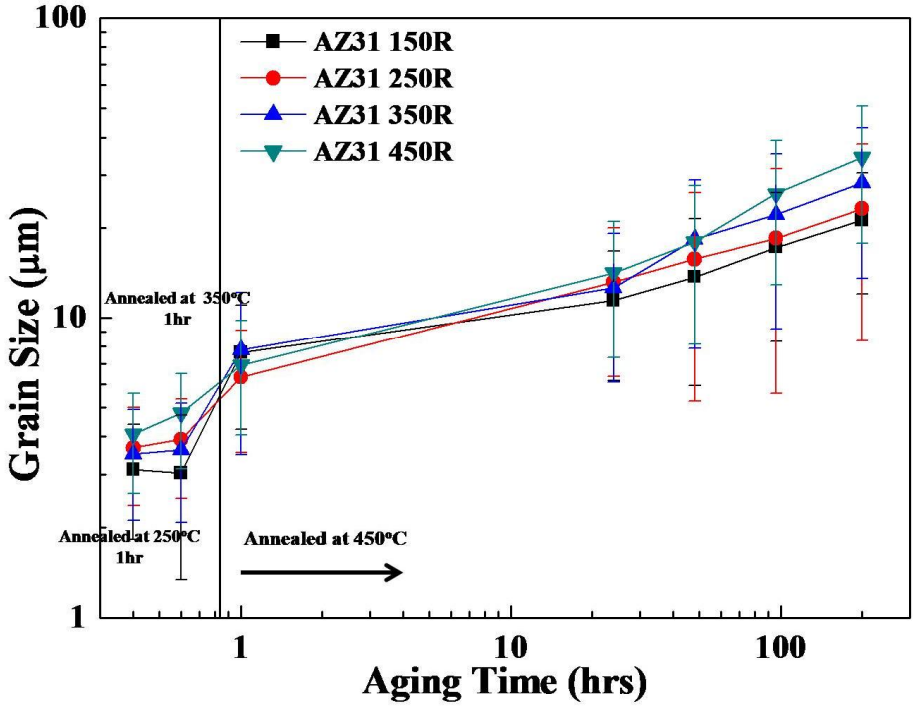

Fig. 4.2. Grain growth with different annealing conditions

4.2.3 Texture

Basal pole figures were also observed in order to investigate the texture under different rolling conditions and the effect of texture on formability. The typical rolling texture in AZ31 has the basal planes oriented parallel to the normal direction. The maximum basal pole peak appears in the normal direction in 150R and 250R specimens, while the basal pole in 450R splits and is inclined at around 20 degrees toward the rolling direction (Fig. 4.3 (b), (d) and (f)). In addition, the maximum pole intensity in 450R significantly less than that in the other specimens. It is widely known that the evolution of texture during rolling is highly dependent on applied temperature [1, 17]. A decrease in the critical rsolved shear stress (CRSS) of non-basal slip systems at elevated temperatures has been shown in single crystal studies and VPSC simulations [18, 19]. Deformation in the c-axis can be enhanced by activating non-basal slip modes, which weakens the basal texture of Mg alloys during rolling at high temperatures [11]. The relationship between basal pole intensity and IE value is presented in Fig.4.4 (b). The IE values of 450R are higher than those of other conditions. Weak basal texture with more tilted c-axes favors basal slip and tensile twinning which can contribute to deformation through thickness. On the other hand, the texture evolution seems to be independent of annealing conditions. Many reports state that basal texture hardly changed during annealing after rolling [7, 20].

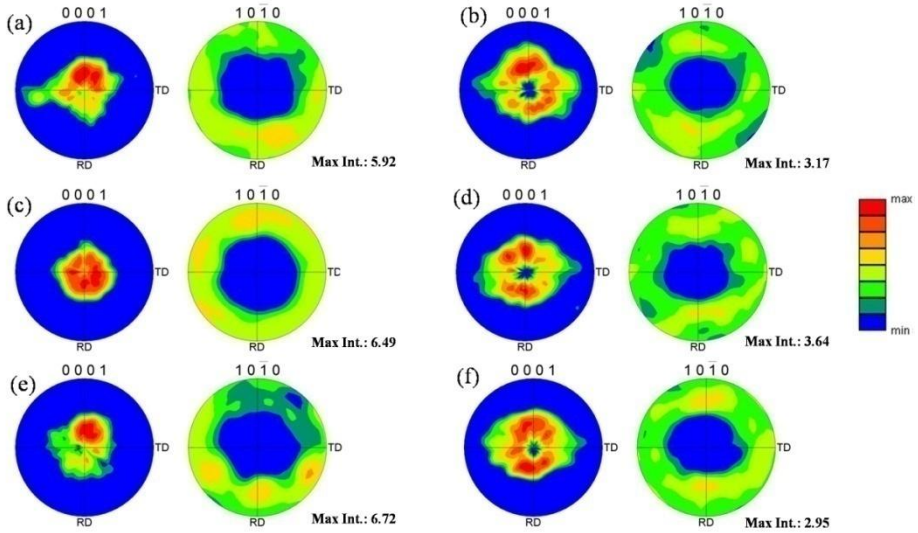

Fig. 4.3. Texture measurements (a), (c) and (e) correspond to the pole figures of 150R450A, 150R450A48hr and 150R450A144hr, respectively; the pole figures shown in (b), (d) and (f) were obtained from 450R450A, 450R450A48hr and 450R450A144hr, respectively

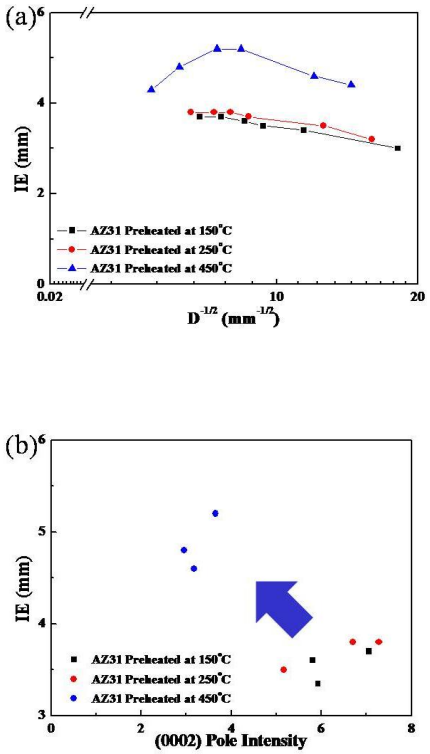

Fig. 4.4. (a) Relationship between IE value and grain size; (b) Relationship between IE value and basal pole intensity

4.2.4 Parameters from tensile tests

Uniaxial tensile tests were carried out on AZ31 at room temperature with a nominal strain rate of 2 x 10^{-4} s^{-1}. The variations in 0.2% yield strength, work hardening exponent, r-value, and uniform elongation versus grain size for AZ31 tested in RD are plotted in Fig. 4.4 (a), (b), (c), and (d), respectively. The parameters of 450R specimens were found to be significantly different from those of other specimens. 450R specimens have low yield strength and r-value, and high work hardening exponent and uniform elongation. These unique results are attributed to the texture evolution during rolling at high temperatures. D. H. Kang et al. found that Mg alloys containing Y or Rare Earth (RE) elements had high work hardening exponents and high IE values since they had weak basal textures [21, 22]. A decrease in yield strength is associated with a decrease in CRSS of deformation modes. Hall-Petch relation explains the relationship between CRSS of deformation modes and grain size (Fig. 4.6 (a)). In large grain size, a slip occurs more easily because there are enough length for dislocations to pile up in grain boundary. Interestingly, twinning also follows h-p relation. In order to analyze the effects of grain size in more detail, the CRSS values of deformation modes and their relative activity were calculated by using VPSC modeling. This approach was used to predict the stress-strain curves against various CRSS values of the 3 possible deformation modes (basal slip, prismatic slip and tensile twin) [7, 12]. The CRSS values of the 3 deformation modes were calculated in 450R specimens with various grain sizes; the associated Hall-Petch relations are shown in Fig. 4.6 (a). Slope (k) represents the sensitivity of grain size. The slope of tensile twin mode is higher than that of basal slip mode, which indicates that tensile twin mode is more sensitive to grain size. Twin volume fraction at the final

stage of uniform elongation was also calculated. And graphs, which plots relative activity of deformation modes during tensile tests, shows that tensile twinning increases with increasing grain size (Fig. 4.6 (c)). Fig. 4.6 (d) shows that relative contribution to deformation; an activation of prismatic slip increases in strong basal texture. In addition, calculated twin volume fraction increased as basal pole intensity grew weaker and grain size increased (Fig. 4.6 (b, c)). These results are in agreement with earlier studies [6, 7]. It means $\{10\bar{1}2\}$ tensile twinning decreases yield strength but increases hardening rate ($h=d\sigma/d\epsilon$) by interaction between tensile twins and basal dislocations (Fig 4.6 (e, f)). This leads to increase work hardening exponent. Work hardening coefficient increases when an activation of tensile twin increases. Weak basal texture and large grain size are key factors to enhance an activation of tensile twin. Lankford value (r-value) is a ratio of a strain in TD to a strain through thickness. Low r-value means low resistance to deformation via thickness. It relates to texture because basal slip mode, main deformation mode in Mg alloys, brings about a plastic anisotropy. One of ways to overcome the anisotropy is to randomize texture. 450R specimens show lower basal pole intensity in Fig. 4.4 (b). This can be described how much basal slip mode operates by Schmid factor of basal slip. 450R specimens have higher average Schmid factor values for basal slip mode than those of 150R and 250R specimens. The weak basal texture and the deformation at high temperatures can enhance deformation through thickness of Mg sheets [23]. As shown in Fig. 4.5 (c) and (d), yield stress and work hardening vary with grain size, while r-value and uniform elongation are independent of grain size. Twinning depends greatly on texture and grain size during deformation. In polycrystalline Mg and Mg alloys, the grain size when a transition from twinning to basal slip occurs decreases during deformation at low

temperatures and high strain rates [9]. n-value and r-value are useful parameters, obtained from tensile tests, to exam stretch formability of other metals such as Aluminum, Copper, and. Steel; a material with high n-value and r-value has high stretch formability. However, Mg alloys, which have HCP structure, shows different relation between the parameters and stretch formability. n-value is related to high formability in some range of grain size. And Mg alloys with low r-value can have high formability. According to results of microstructure and tensile tests, tensile twinning may play a critical role in stretch formability of Mg alloys.

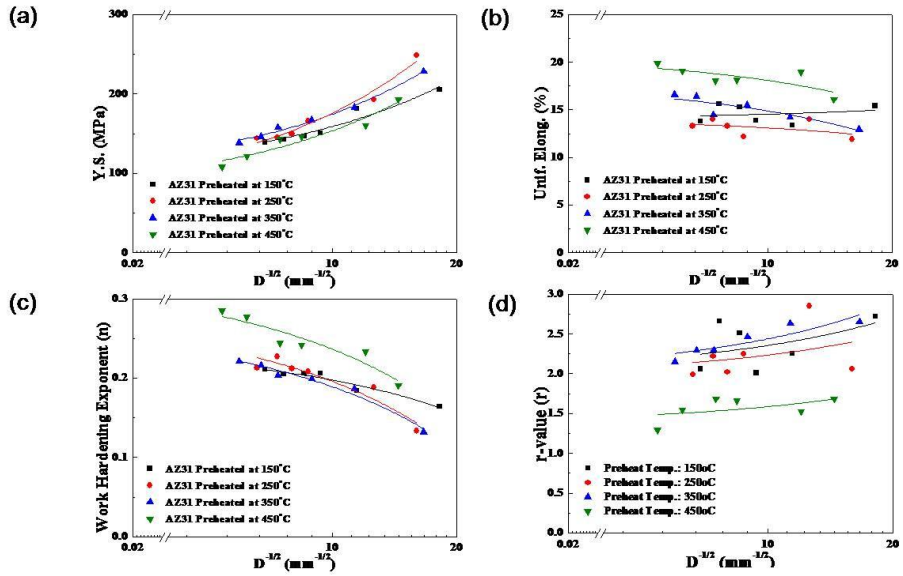

Fig. 4.5. (a) Relationship between grain size and yield strength, (b) uniform elongation, (c) work hardening exponent, and (d) r-value

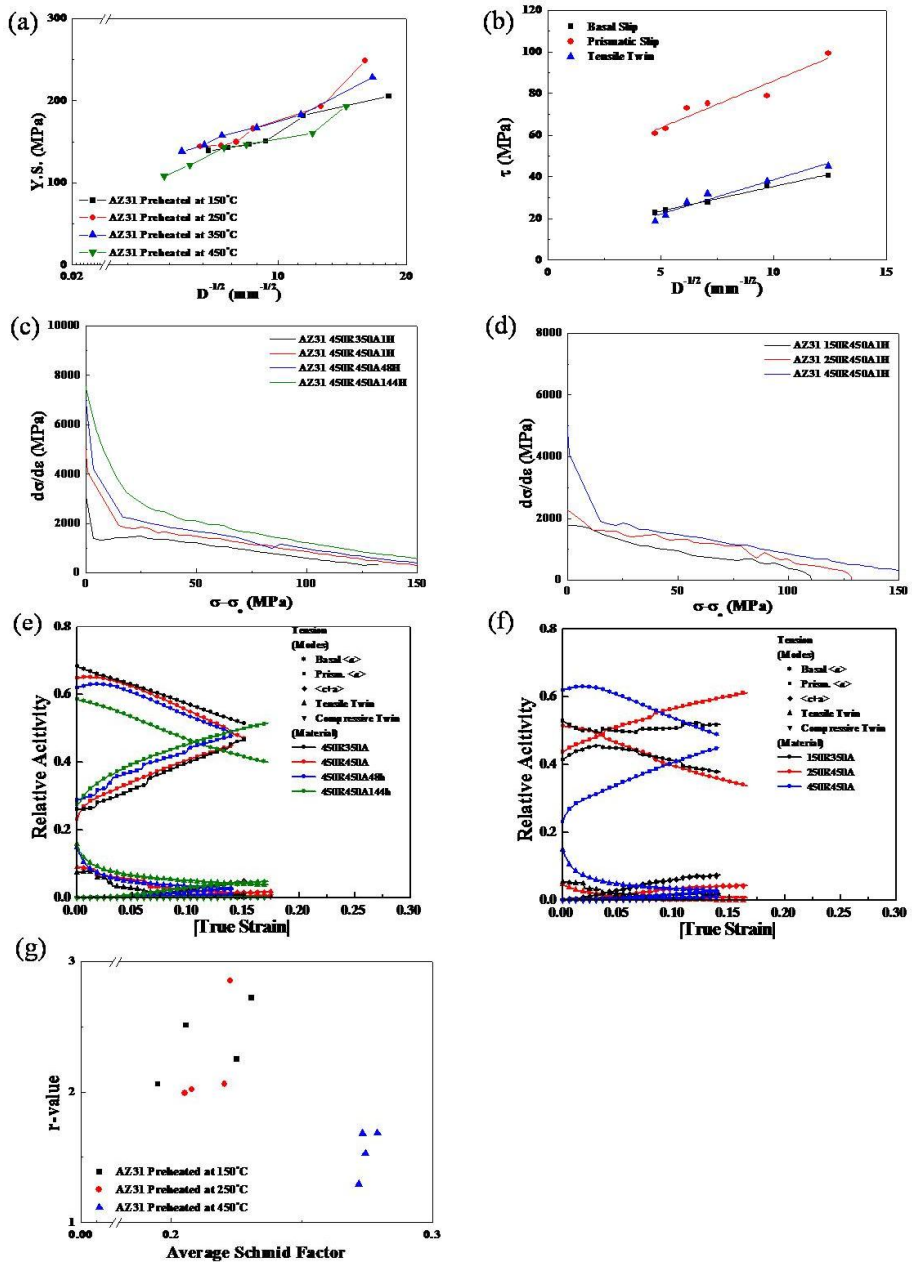

Fig. 4.6.. (a) H-P relation of 450R specimens calculated by VPSC, (b) volume fraction change during tensile loading in the rolling direction, (c, d) relative activity of deformation modes change with grain size obtained from VPSC calculations, (e,f) hardening rate as a function of flow stress from tensile tests, and (g) relationship between r-value and Schmid factor

Table 4.3. Hall-Petch parameters of 450R specimens

	τ_o (MPa)	k (MPa $mm^{1/2}$)
Basal Slip	11.696	2.365
Prismatic Slip	40.968	4.503
Tensile Twin	5.688	3.288

4.2.5 The role of tensile twin during uniaxial tensile test

Tensile twining behavior is investigated in order to improve the stretch formability of Mg alloys. The electron back scattered diffraction (EBSD) technique was employed to investigate different tensile twin behaviors during tensile test through varying grain size. Change in basal pole figures and inverse pole figures (IPF) were also observed from 0%, 2%, 5%, and 10% strained A and B specimens (shown in Fig. 4.7 (a - h). At 0% strain of both specimens, strong basal poles spread away from ND by from 20 to 45 degrees. As deformation proceeds, basal poles parallel to TD gradually strengthen in the A, while those in the B are relatively weak in Fig. 4.7 (d) and (h). Its distinctions in the evolution of the textures are associated with different tensile twin behaviors in the A and the B. Fig. 3 (a) and (b) show the distribution of orientations of all the matrix grains in which tensile twinning occurs (blue) and those of their twinned grains (red). The tensile twins resulting in the basal planes orienting toward TD, likely play a critical role in the texture evolution during the tension along RD. Especially in the A, the tensile twins occur more and it causes the basal planes tilt toward TD at 5% strain.

Given that uniaxial tension along RD causes the specimens to be elongate in RD and to be compressed in TD and ND, there are two possible tensile twins predicted in the two specimens. According to Schmid law, the tensile twins turn the orientation of the matrix grains (M2) into those of T1 and T2 in Fig. 4.8(c). However, most of the grains where twinning occurs are the grains whose basal poles are tilted 20 to 45 degrees toward RD (M1). Although the tensile twins occur in all of the grains having the M2 orientation, the texture evolution is more attributed to the tensile twinning in the M1 grains (shown in

Fig. 4.8(a) and (b)). The M2 grains fulfilling Schmid law are less than 1% of the total area in both of the specimens. The number of the tensile twins occurring in the A increases faster than that in the B, which indicates that the M2 grains are much affected by grain size. Unlike in the A, some $\{10\bar{1}1\}$ compressive twins occur in the orientations with basal poles perpendicular to RD in the B (M3). Its orientations restrain both of strains along TD and through thickness since Schmid factors of tensile twin and basal slip are high. The compressive twins are very thin and their twin boundaries do not move as the deformation undergoes. The compressive twins seem to be the crack initiation like researches reported, as the grains with the compressive twins cannot identify in IPF from 18% strained the B specimen [29].

The r-value is the ratio of a strain in TD to a strain through thickness. Thus, low r-value means low resistance to deformation via thickness. Basal slip mode more easily generate through thickness with weakening basal texture because many basal planes tilt to the RD. Also the r-value decreases with increasing grain size. It is known that thermally activated non-basal slip responsible for the deformation along c-axis in Mg crystal [23]. Two ratios of the CRSS of non-basal slips to the CRSS of basal slip mode rises as the grain size increase, which indicates it is more difficult to activate non-basal slip modes in coarser grain size (shown in Fig. 4.9 (b)). On the other hand, tensile twinning occurs more easily with increasing the grain size. A positive strain in the loading direction (c-axis of parent lattice) leads to a positive strain by 6.6% and a negative strain is formed in a direction perpendicular to the loading direction. Thus, the strong basal texture forms by activating the tensile twinning in the M1 grains, which follows the strain through thickness and the decrease r-value. However, more tensile twins appear in the M2, resulting in the compression along TD but the tension through the thickness. Particularly,

such tensile twinning appears more in the A specimen. The M2 grains have a favorable orientation for activating basal slip to compress through thickness and elongate them along RD. However, from the graph plotted with true strain in TD as a function of strain in RD, the curve of A begins to decrease around from 5% strain where the a number of tensile twins begin to occur (Shown in Fig. 4.9 (c)). Its phenomenon indicates the role of tensile twinning here likely contribute to the deformation by releasing stress concentration rather than by forming the strain induced by changing the orientation. The results here correspond with Ando's research the tensile twinning during the tensile test play an important role to increase in the ductility by releasing local stress [27]. In addition, Fig. 4.10 shows twin growth proceeds in the two different sized grains. The coarser grain size enhances the twin growth and ends up being overtaken. Such rapid orientation change by the tensile twin can cause the deterioration of the ductility and formability.

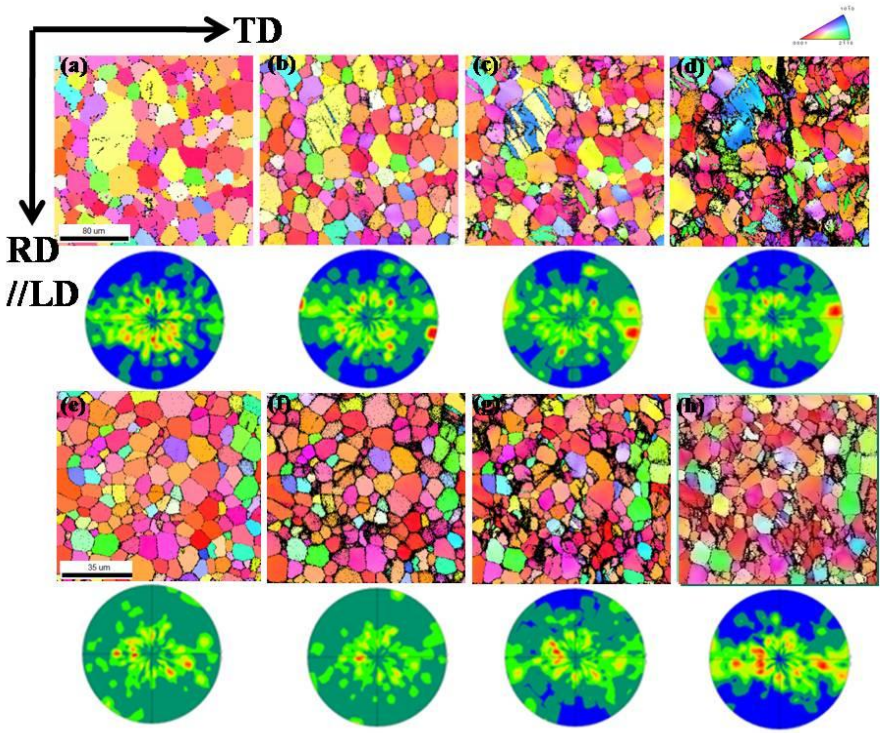

Fig. 4.7. IPF and (0002) basal pole figures obtained from 0, 2, 5, and 10% strain of A (a - b), and B (e - h) specimens

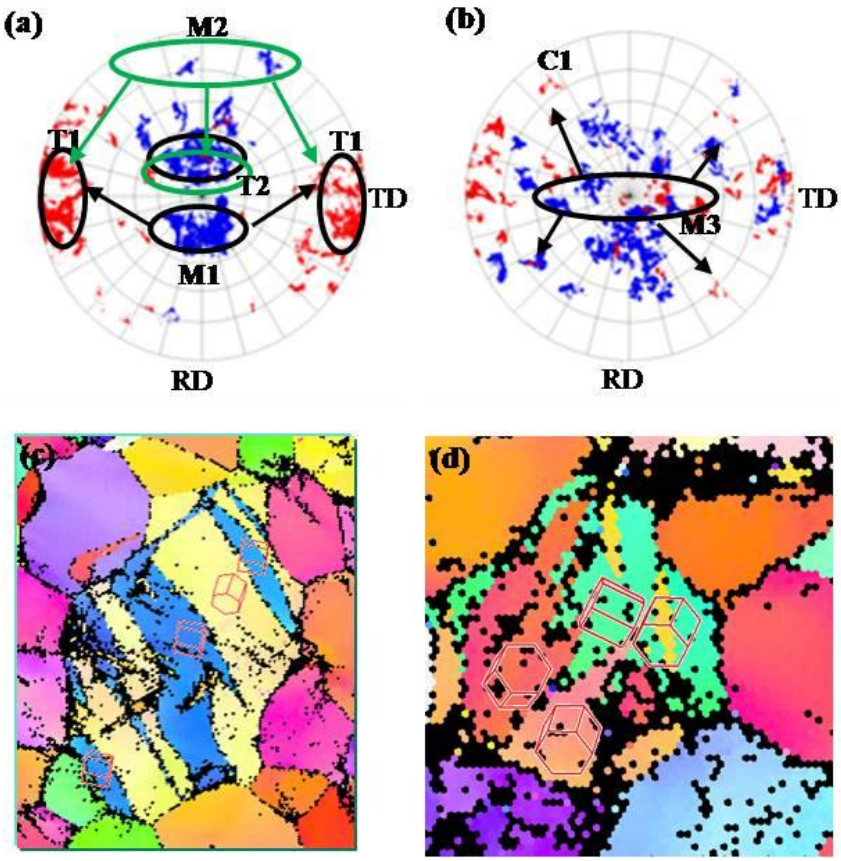

Fig. 4.8. (0002) pole figures of the matrix grains and their tension twinned grains in the A specimen (a) and the B specimen (b), IPF map of changing the M1 into the T1 (c), and the M2 into T1 and T2 by the tensile twins (d)

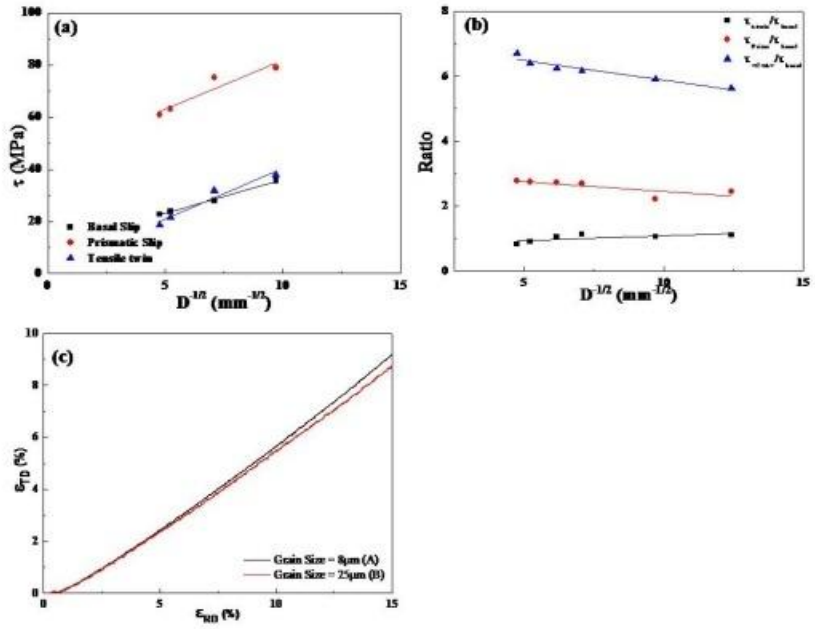

Fig. 4.9. (a) H-P relation of the AZ31 specimens calculated by VPSC and (b) the ratios of the deformation modes to the basal slip mode as a function of grain size, and (c) the graph plotted the variation of true strain in TD as a function of true strain in RD

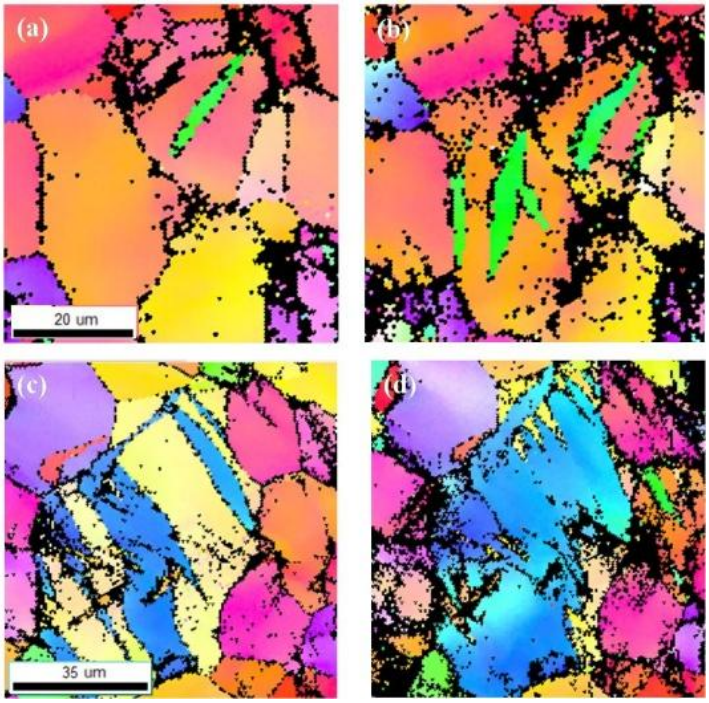

Fig. 4.10. IPF map of twinning growth obtained from the grain with less than 35 μm diameter (a) and (b), and with over 71 μm diameter (c) and (d)

4.2.6 The role of tensile twin during bi-axial tension test

The coarse grain size likely contributes to the high stretch formability. Erichsen tests are used to exam the stretch formability of material. However, it is difficult to investigate the texture evolution due to its curved surface during the test. Some research obtained the texture evolution from the cross section but the method could damage the sample cutting it []. The bi-axial tension test make possible to investigate the role of tensile twin due to its flat specimen. Three different grain sized specimens are prepared to exam the grain size effects on the stretch formability: A, B and C specimen have average grain size 6, 24 and 45μm, respectively. The bi-axial tension device was set on the uniaxial testing machine and then applied compression on the top of the device until displacement reached at 0.8mm (around 0.8mm displacement occurred along RD and TD in the cross specimens).

More tensile twinning occurs with increasing the grain size in Fig. 11. The distribution of misorientation angle increases as the grain size rise which well agrees with the result from uniaixal tension tests. Most of the tensile twinning occurred in the orientation that the c-axis is closely perpendicular to ND. It is natural that tensile twinning occurs when tension applies along RD or ND since such tensile twin leads to the strain through thickness and the strain along RD or ND. A lot of tensile twins are found even in small sized grains. The tensile twins grow and occupy large portion of their matrix grains in Fig. 4.12 (d) (A tensile twin). Meanwhile, tensile twinning sometimes occurs in hard orientation (the c-axis is parallel to ND, B tensile twin). These tensile twinning tends to occur in coarse grains. Since the textures of the three specimens are similar each other, grain size likely affects more on tensile

twinning. Particularly, the tensile twin in hard orientation increase with increasing grain size. Fig. 4.12 shows clearly the effects of grain size on tensile twinning. In the A specimen with fine grain size, blue points (matrix grain's orientation) are distributed near RD or TD and red points (twinned grain's orientation) are placed in the center of pole figure. However, it can e found in the B and C specimens that blue points are also distributed in the center the pole figures.

In the all the samples, tensile twinning mainly occurs in the orientation with high Schmid factor for tensile twins when applying tensile force along RD or TD. On the other hand, tensile twinning occurs in the hard orientation with thinner shape. It is unlikely to grow due to its unfavorable orientation. M Z Bian from his experiments suggests tensile twin in the unfavorable orientation initiated in the twin boundaries [15]. It is hard to prove the role of tensile twin in the formability. Most of the cracks initiate at grain boundary, which is attributed to the anisotropy of HCP structure. Therefore, cleavage resulted from interaction between dislocations is hardly found in measured fracture surface [28]. Tensile twins occurring in grain boundary seem to play an essential role to relax stress concentration. In the next section, the influence of tensile twin on fracture will be covered through small Erichsen test newly designed here.

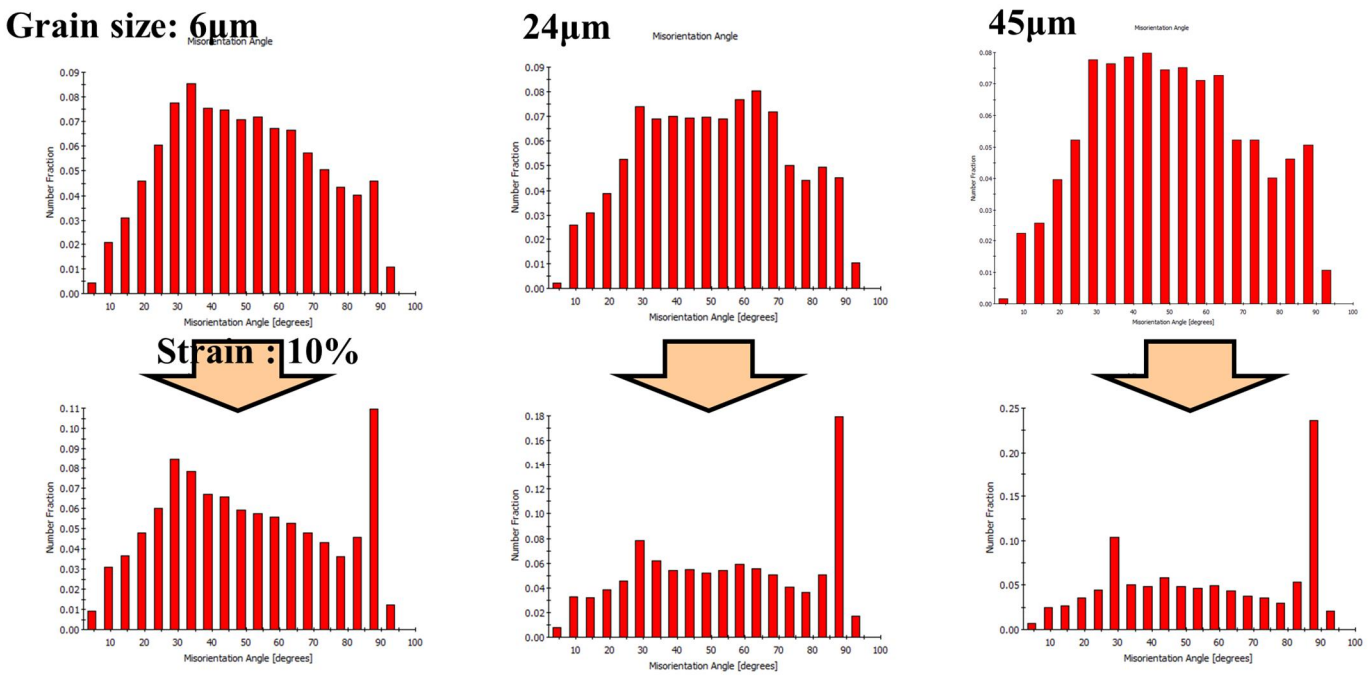

Fig. 4.11. Evolution of misorientation angle distribution after bi-axial tension

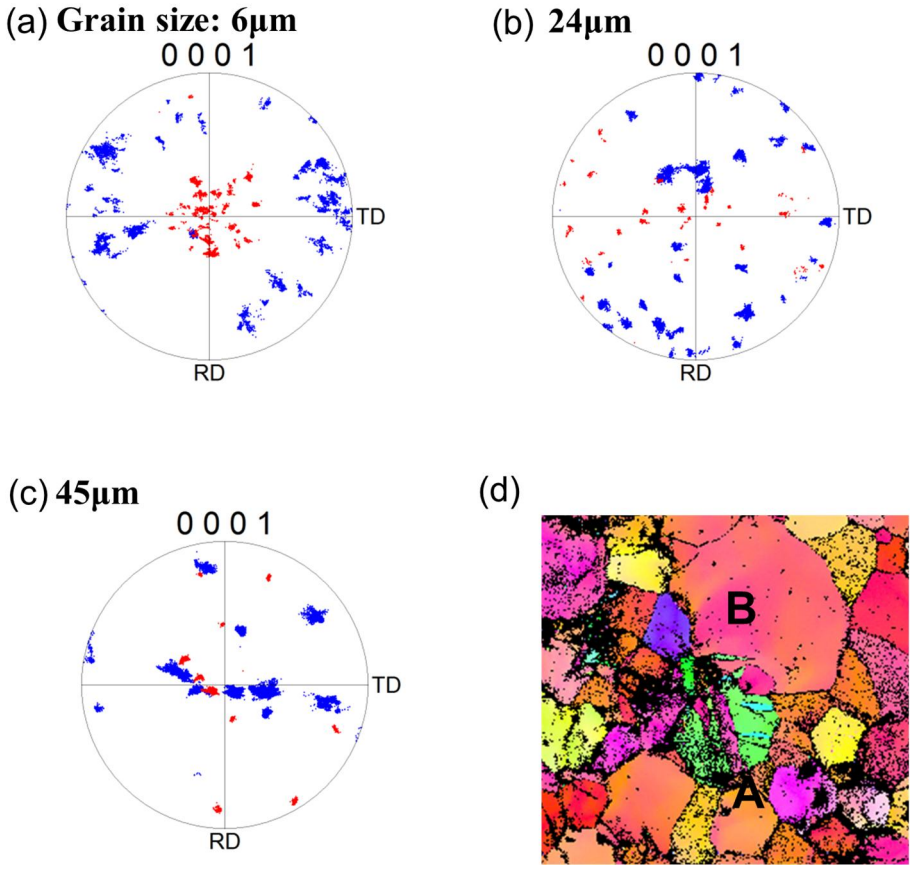

Fig. 4.12. (0002) Pole figure of the matrix grain and their twinned grian (a), (b), (c) and two different tensile twins occurring favorable and unfavorable orientation (d)

4.2.7 Fracture analysis

In order to investigate fracture behavior during the Erichsen test, the small Erichsen test in which size is reduced by one tenth was carried out. Firstly, the EBSD technique was used to uncover the influence of orientation on activation of twinning in 450R specimens under 3 different annealing conditions. Also, SEM images were obtained from ND planes to observe twinning and crack propagation with successive punch displacements of 1/3mm, 2/3mm, and 1mm in (Fig.4.13)

In 450R450A1H specimens, cracks originate at the grain boundaries of the basal planes (c-axis parallel to normal direction) and twinning is not found. The red circles in Fig. 4.14 indicate the spots where cracks initiated. Small grain size seems to suppress twinning even if the grains are favorably oriented for twinning. In the 450R450A48H specimen, which has the highest IE value, cracks initiated at the grain boundaries of the basal plane and then propagated along the black lines shown in Fig. 4.15. Many twins were present but the blue circles where twins occurred do not correspond to the black lines. The 450R450A144H specimen has the largest grain size but a lower IE value than 450R450A48H. The black lines in this specimen encounter a red circle and blue circles. This result indicates that twinning also contributes to fracture in 450R450A144H (Fig. 4.16). H. Yan et al. suggested that the high ductility was attributable to the prevalence of tensile twin mode and basal slip mode during tensile tests [24]. However, twinning has been pointed out as an origin of cracks. The interaction between basal dislocation and {10-12} twin is repulsive in Mg, so a local stress concentration is formed by a dislocation pile-up at the interface, which can initiate a crack [25]. In AZ31 alloys with large grains, the accumulated strain at twin boundaries formed cracks that

propagated along these boundaries during fracture toughness tests [26]. Ando et al. suggested that the activation of basal dislocations was suppressed in grains with tensile twins due to strain accommodation with neighboring grains [27]. Large grain size and weak basal texture enhance the activation of tensile twins and in turn, may inhibit strain incompatibility induced by basal dislocations. There is the relationship between the results of Erichsen tests and small Erichsen tests in Fig. 4.17. The both trends are same; the stretch formability increases and decreases again as a function grain size ($D^{-1/2}$). The graph shows that twinning plays critical roles in change of stretch formability; twinning enhances stretch formability of AZ31 in small grain size but it deteriorates stretch formability in larger grain size.

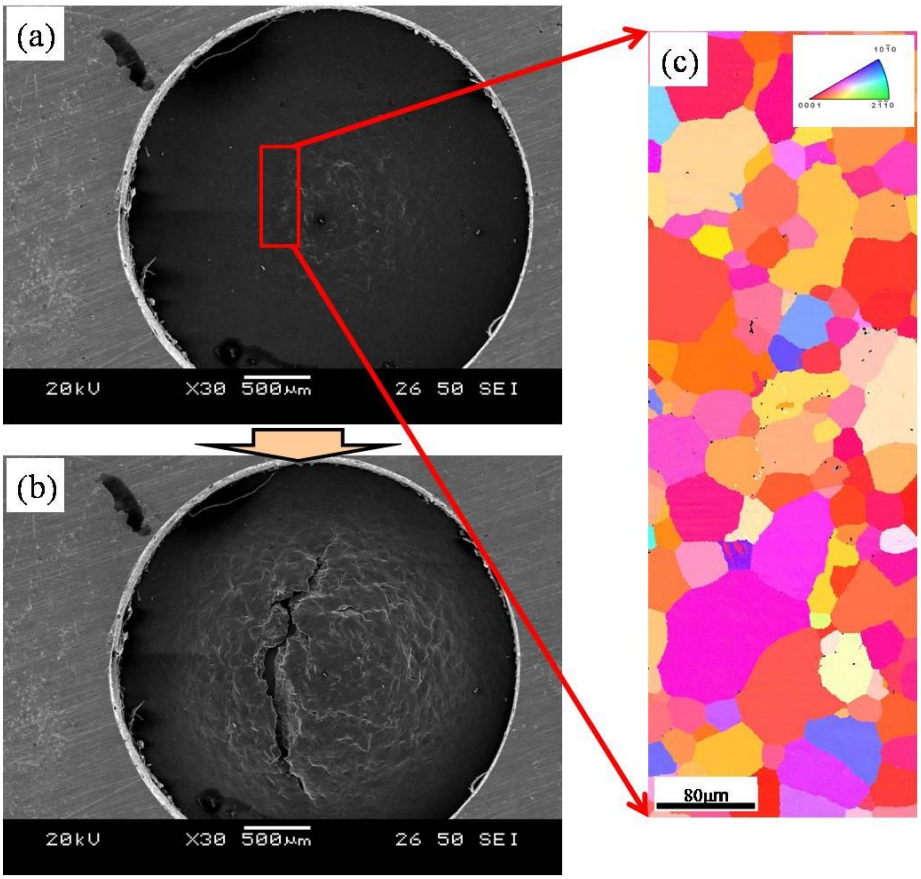

Fig. 4.13. SEM images of the small Erichsen test (a) before the test, and (b) after fracture; (c) IPF map before the test

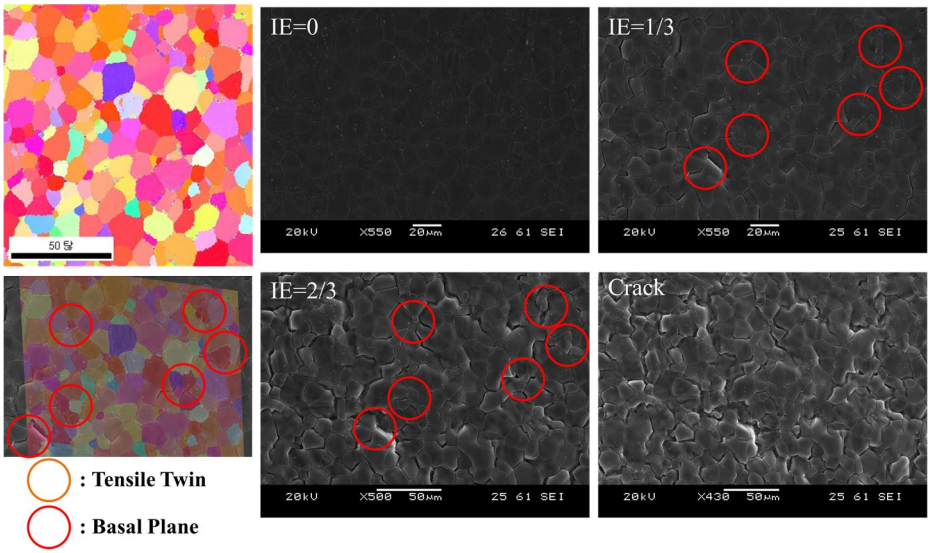

Fig. 4.14. Origin of crack and propagation during the small Erichsen test: SEM images of 450R450A1H

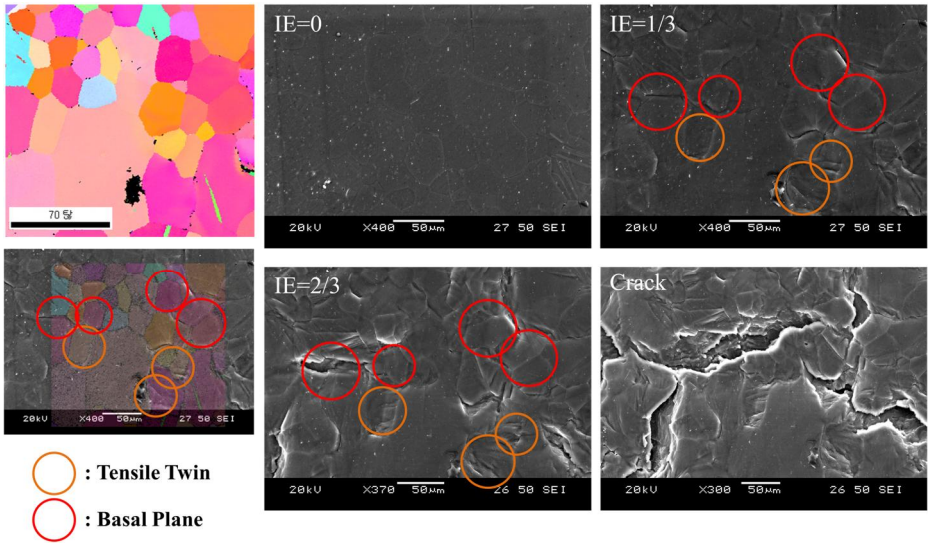

Fig. 4.15. Origin of crack and propagation during the small Erichsen test: SEM images of 450R450A48H

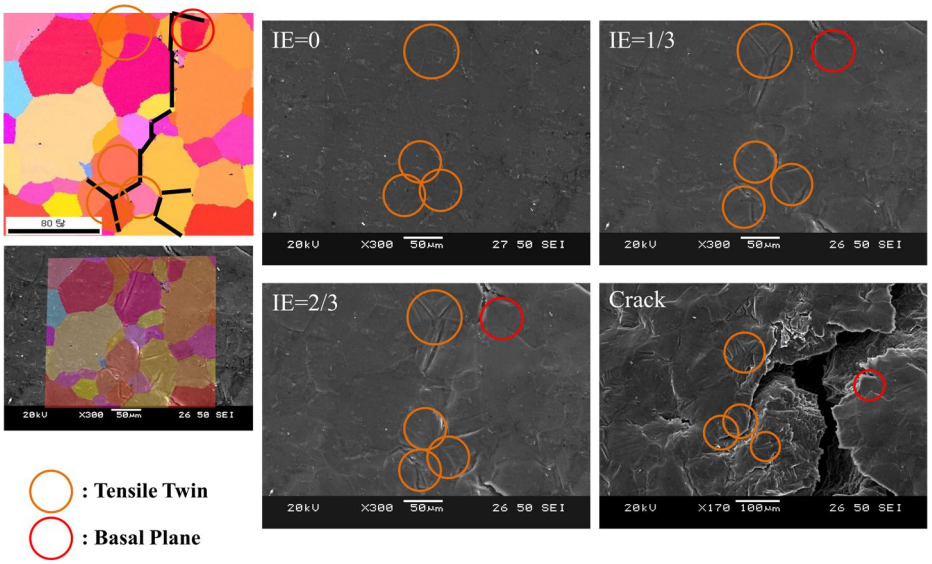

Fig. 4.16. Origin of crack and propagation during the small Erichsen test: SEM images of 450R450A144H

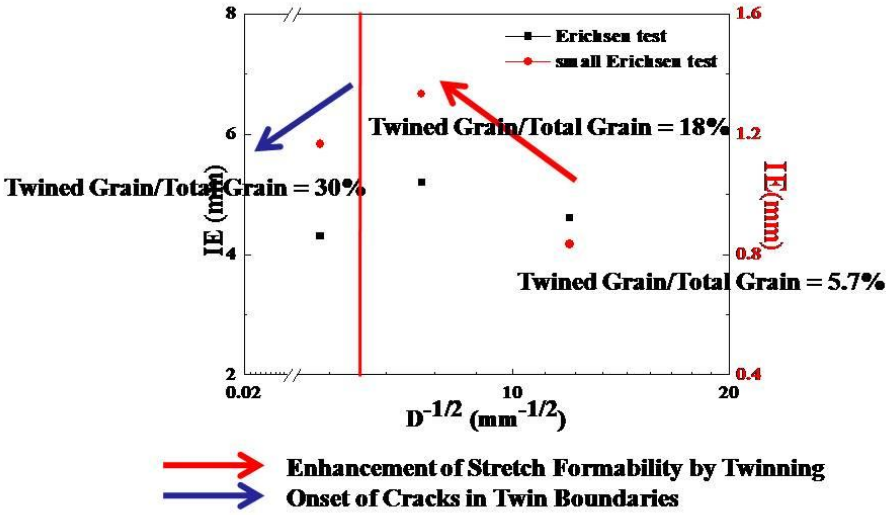

Fig. 4.17. Schematic illustration of IE value change by twinning

4.3 Conclusion

The influence of rolling conditions on the stretch formability of AZ31 was investigated in the present study. The conclusions are summarized below:

1. An increase in rolling temperature weakened basal texture and an increase in annealing temperature and time increased grain size.

2. The results of tensile tests showed that weak basal texture decreased yield strength and r-value, and increased work hardening exponent and uniform elongation.

3. In specimens with weak basal texture, the stretch formability increased with grain size up to a certain point and then decreased. It can be inferred that microstructures with large grains activated more tensile twin and tensile twins, which became origins of cracks.

4. According to VPSC calculations, tensile twin mode is more prevalent in specimens with weaker basal texture and larger grains. The increase in the Erichsen value is associated with tensile twinning.

5. Tensile twin occurring in unfavorable orientation plays a critical role to enhance the stretch formability: such tensile twin lead to grain accommodation during the deformation.

6. A small Erichsen test was carried out to explain changes in IE value with grain size. It showed that cracks initiated at grain boundaries of the basal planes and twinning did not become an origin of cracks in specimens with small grain size. However, cracks originated at either grain boundaries or twins in specimens with large grain size.

Bibliography

1. X. Huang, Y. Chino, M. Mabuchi, and M. Matsuda, “Influences of grain size on mechanical properties and cold formability of Mg-3Al-1Zn alloy sheets with similar weak initial textures”, Mater. Sci. Eng. A 611, (2014), pp. 152-161.
2. Y. Chino, K. Kimura, and M. Mabuchi, “Deformation characteristics at room temperature under biaxial tensile stress in textured AZ31 Mg alloy sheets”, Acta Mater. 57, 1476 (2009), pp. 1476-1485.
3. M. R. Barnett, M. D. Nave, and Alireza Ghaderi, “Yield point elongation due to twinning in a magnesium alloy”, Acta Mater. 60, (2012), pp. 1433-1443.
4. J. Koike, T. Kobayashi, T. Mukai, H. Watanabe, M. Suzuki, K. Maruyama and K. Higashi, “The activity of non-basal slip systems and dynamic recovery at room temperature in fine-grained AZ31B magnesium alloys”, Acta Mater. 51, (2003), pp. 2055-2065.
5. R. W. Armstrong, “The influence of polycrstal grain size on several mechanical properties of materials”, Metal. Mater. Trans., 1A (1970), pp. 1169-1176.
6. W. Yuan, S. K. Panigrahi, J.-Q. Su, and R. S. Mishra, “Influence of grain size and texture on Hal-Petch relationship for a magnesium alloy”, Scripta Mater. 65, (2011), pp. 994-997.
7. Y. Wang and H. Choo, “Influence of texture on Hall-Petch relationships in an Mg alloy”, Acta Mater. 81, (2014), pp. 83-97.
8. J.W. Christian and S. Mahajan, “Deformation Twinning”, Prog. Mater. Sci., 39 (1995), pp. 1-157.
9. C. M. Cepeda-Jimenez, J. M. Molina-Aldareguia, and M. T. Perez-Prado, “Origin of the twinning to slip transition with grain size refinement, with decreasing strain rate and with increasing temperature in magnesium”, Acta

Mater. 88, (2015), pp. 232-244.

10. M. A. Meyers, O. Vohringer, and V. A. Lubarda, “The onset of twinning in metals: a constitutive description”, Acta Mater. 49, (2001), pp. 4025-4039.
11. X. Huang, K. Suzuki, Y. Chino, and M. Mabuchi, “Improvement of stretch formability of Mg-3Al-1Zn alloy sheet by high temperature rolling at finishing pass”, J. Allys. Compd. 509, (2011), pp. 7579-7584.
12. S. R. Agnew, M. H. Yoo, and C. N. Tome “Application of texture simulation to understanding mechanical behavior of Mg and solid solution alloys containing Li or Y”, Acta Mater., 49 (2001), pp. 4277-4289.
13. M. Yuasa, N. Miyazawa, M. Hayashi, M. Mabuchi, and Y. Chino, “Effects of group II elements n the cold stretch formability of Mg-Zn alloys”, Acta Mater. 83, (2015), pp. 294-303.
14. M. Gzyl, A. Rosochowski, S. Boczkal, and L. Olejnik, “The role of microstructure and texture in controlling mechanical properties of AZ31B magnesium alloy processed by I-ECAP”, Mater. Sci. Eng. A 638, (2015), pp. 20-29.
15. M. Z. Bian, and K. S. Shin, “{10-12} Twinning behavior in magnesium single crystal”, Met. Mater. Int. 5, (2013), pp. 999-1004.
16. H. L. Kim and Y. W. Chang, “An internal variable approach of orientation dependent deformation mechanism of rolled AZ31 magnesium alloy”, Met. Mater. Int. 17, (2011), pp. 721-728.
17. S. R. Agnew and O. Duygulu, “Plastic anisotropy and the role of non-basal slip in magnesium alloy AZ31B”, Int. J. Plast. 21, (2005), pp. 1161-1193.
18. A. Chapuis, J. H. Driver, “Temperature dependency of slip and twinning in plane strain compressed magnesium single crystals”, Acta Mater. 59, (2011), pp. 1986-1994.
19. Kelley EW, and Hosford WF., “Plane-strain compression of magnesium and

magnesium alloy crystals", Trans. AIME 242, (1968), pp. 5-13.

20. L. W. F. Mackenzie and M. O. Pekguleryuz, "The recrystallization and texture of magnesium-zinc-cerium alloys", Scripta Mater. 59, (2008), pp. 665-668.

21. D. H. Kang, D. W. Kim, S. Kim, G. T. Bae, K. H. Kim and Nack J. Kim, "Relationship between stretch formability and work-hardening capacity of twin-roll cast Mg alloys at room temperature", Scripta Mater. 61, (2009), pp. 768-771.

22. B. C. Suh, M. S. Shim, K. S. Shin, and Nack J. Kim, "Current issues in magnesium sheet alloys: Where do we go from here", Scripta Mater. 84-85, (2014), pp. 1-6.

23. C. E. Dreyer, W. V. Chiu, R. H. Wagoner, S. R. Agnew, "Formability of a more randomly textured magnesium alloy sheet: Application of an improved warm sheet formability test", J. Mater. Proc. Tech. 210, (2010), pp. 37-47.

24. H. Yan, S. W. Xu, R. S. Chen, S. Kamado, T. Honma, and E. H. Han, "Activation of {10-12} twinning and slip in high ductile Mg-2.0Zn-0.8Gd rolled sheet with non-basal texture during tensile deformation at room temperature", J. Allys. Compd. 566, (2013), pp. 98-107.

25. M. H. Yoo, "Slip, Twinning, and Fracture in Hexagonal Close-Packed Metals", Metal. Trans. A, 12 (1981), pp. 409-418.

26. H. Somekawa, A. Singh, and T. Mukai, "Fracture mechanism of a coarse-grained magnesium alloy during fracture toughness testing", Philos. Mag. Lett. 89, (2009), pp. 2-10.

27. D. Ando, J. Koike and Y. Sutou, "The role of deformation twinning in the fracture behavior and mechanism of basal textured magnesium alloys", Mater. Sci. Eng. A 600, (2014), pp. 145-152.

28. A.K. Rodriguez, G. A. Ayoub, B. Mansoor, A. A. Benzerga, "Effect of strain

rate and temperature on fracture of Magnesium alloy AZ31B", 112 (2016) pp.194-208.

29. M. R. Barnett, "Twinning and the ductility of magnesium alloys Part I: "Tension" twins", *Mater. Sci. Eng A* 464, (2007) pp. 1-7.

Chapter 5. Effects of alloying elements and grain size on stretch formability of Mg-Zn alloys

5.1 Introductions

A difficulty in forming Mg wrought alloys at room temperature arises from the preferred orientation that occurs when Mg alloys are rolled or extruded. Controlling microstructure has been widely considered as a way to overcome this limitation. First, various thermo-mechanical processing systems gave been designed to alter texture and microstructure. Some of these introduce high levels of shear and promote non-basal slips which randomize texture. Second, altering alloy design is considered relatively easy way to achieve the desired structures. Alloying elements that weaken the basal texture of wrought Mg include rare earth (RE) elements, Y, and Ca etc [1, 2, 3, 4, 5].

It has been reported that microstructures (grain size, texture, and alloy content etc.) affects frequency, shape, and width of twinning [6, 7, 8, 9]. Grain size is undoubtedly the critical factor in the onset and extent of twinning and slip mode as a deformation mechanism [9, 10]. Grain size refinement normally increases the yield strength of metals at low temperatures. This phenomenon is well explained by the Hall-Petch relation [11]. Like slip modes, the Hall-Petch relation also can be applied to twinning [6, 12, 13]. In addition to grain size, twinning is very dependent on strain path which is related with initial texture and Schmid Factor criterion [6, 8, 14].

The aim of this study is to elucidate the role of twinning during sheet forming of Mg alloys. Mg-Zn alloys fabricated with varying rolling conditions were studied to identify factors that improve stretch formability.

The electron back scattered diffraction (EBSD) technique, optical microstructure analysis, and texture analysis were employed to investigate the influences of grain size and texture using Erichsen tests and tensile tests. The small Erichsen test was designed to investigate the relationship between twinning and fracture behavior.

5.2 Results and discussion

5.2.1 Results of Erichsen test

Materials were prepared by extrusion with 4 nominal compositions of Z6, ZX60, ZW60 and ZA61 followed by hot rolling. In order to effects of alloying elements, Ca, Y and Al elements put in Z6 alloys. Alloy compositions are calculated in terms of atomic percent in Table 5.1. The specimens were preheated at 250^{o}C for 20min before rolling. Rolling was performed with rolling reduction of 50% per pass until a thickness of 1mm was obtained with 200^{o}C hot rolls. Specimens with different grain sizes were prepared at various temperatures ranging from 250 to 350^{o}C and annealing times varying from 1 to 48hrs. Rolling conditions and associated grain sizes and Erichsen values (IE) are listed in Table 5.2 and 5.3.

Erichsen tests were conducted on several Mg-Zn alloys with various preheating and annealing conditions, as shown in Table5.2 and Table 5.3. All the curves of IE values against grain size shows a similar tendency; they increase and then decrease. The IE values of ZX60 alloys are the highest of those tested (Fig. 5.1 (a)). Stretch formability decreases in the order: ZX60, ZW60, Z6, and ZA61. The points where the curves begin to decrease differ by

alloys. ZX60 and ZW60 alloys show peak stretch formability at smaller grain sizes than do Z6 and ZA61 alloys. And grain size of Z6 alloy increases dramatically and IE value starts to decrease at the point annealed at350^{o}C for 144hrs.

Table 5.1 List of alloy compositions in terms of weight percent and atomic percent

Specimens	Compositions (wt.%)					Compositions (at.%)				
	Mg	Zn	Ca	Y	Al	Mg	Zn	Ca	Y	Al
Z6	Bal.	6.0				Bal.	2.32			
ZX60	Bal.	6.0	0.30			Bal.	2.32	0.19		
ZW60	Bal.	6.0		0.30		Bal.	2.32		0.09	
ZA61	Bal.	6.0			1.00	Bal.	2.32			0.94

Table 5.2 Rolling conditions, grain size, and Erichsen values of Z6 and ZX60 alloys

Specimens	Preheat Temp. (^{o}C)	Annealing Temp. (^{o}C)	Annealing Time	Grain Size (μm)	Erichsen Value (mm)
Z6 250R 250A	250	250	1	6.2	3.9
Z6 250R 350A	250	350	1	76.0	4.9
Z6 250R 350A 24h	250	350	24	109.1	5.1
Z6 250R 350A 48h	250	350	48	121.3	4.8
ZX60 250R 250A	250	250	1	5.9	4.4
ZX60 250R 350A	250	350	1	35.8	5.5
ZX60 250R 350A 24h	250	350	24	82.0	5.4
ZX60 250R 350A 48h	250	350	48	93.2	5.2

Table 5.3 Rolling conditions, grain size, and Erichsen values of ZW60, and ZA61 alloys

Specimens	Preheat Temp. (°C)	Annealing Temp. (°C)	Annealing Time	Grain Size (μm)	Erichsen Value (mm)
ZW60 250R 250A	250	250	1	7.4	2.9
ZW60 250R 350A	250	350	1	12.0	4.6
ZW60 250R 350A 24h	250	350	24	22.1	5.0
ZW60 250R 350A 48h	250	350	48	58.9	5.0
ZA61 250R 250A	250	250	1	5.6	3.0
ZA61 250R 350A	250	350	1	44.7	3.9
ZA61 250R 350A 24h	250	350	24	67.2	4.0
ZA61 250R 350A 48h	250	350	48	74.7	3.8

5.2.2 Microstructures

Microstructures of various Mg-Zn alloys were obtained in ND planes. All the microstructures have recrystallized grain structures with equiaxial grains and grain sizes that are distributed homogeneously. The grain sizes of Mg-Zn alloys increase from 5.0 μm to 121.3 μm with increasing annealing temperature and time (in Fig. 5.3). The grain sizes of Z6 alloys increase much faster than those of other alloys. This phenomenon is associated with solute elements which play a significant role in controlling the growth of nucleated grains. Solute pinning can affect grain growth which is attributed to the mobility of grain boundaries during the annealing process. Thus, adding Ca, Y and Al may slow recrystallization and grain-growth. The effects of solute elements on grain growth have been defined in terms of the growth restriction factor (GRF), which equals $\sum_i m_i C_{o,i}(k_i - 1)$, where mi is the slope of the liquidus line, k_i is the distribution coefficient, and Co,i is the initial concentration of element i [16]. The concept of the GRF may explain why addition of Ca and Al suppress grain growth of Mg-6Zn. Although the GRF value of Y is low compared to that of other elements, the formation of intermetallic compounds with Y may contribute to nucleation and suppression of grain growth. There are 4 phase diagrams of Mg-6Zn alloys (in Fig. 5.4). ZW60 alloy forms much more intermetallic compounds according to thermal dynamics calculations. Small 2nd phases commonly play a key role of forming nucleation site of recrystallization. On the other hand, the grain growth rate of Mg-6Zn-1Al is not higher than that of other alloys. This may be related to its strong basal texture as shown in Fig 5.1 (b) and Fig 4.2. There are low misorientation angles between grains in strong basal texture. These

boundaries have low energy and mobility of grain boundaries [17]. Grain size affects an activation of deformation modes especially tensile twin as mentioned in previous section. Different kinds of factors may affect not only grain growth rate, but also change grain shape, distribution and texture of Mg alloys. In this study, grain size and texture are covered and equal conditions regarding to other factors are assumed.

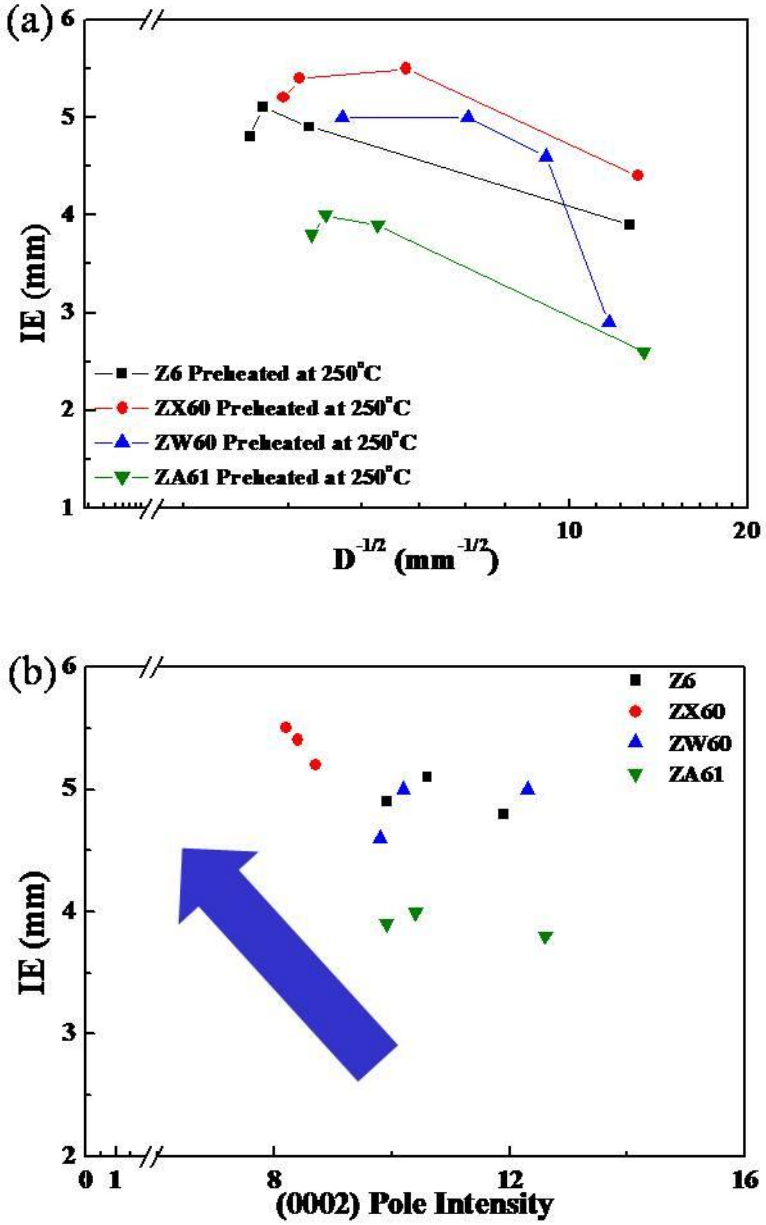

Fig. 5.1. (a) Relationship between IE value and grain sizes, (b) Relationship between IE value and basal pole intensity

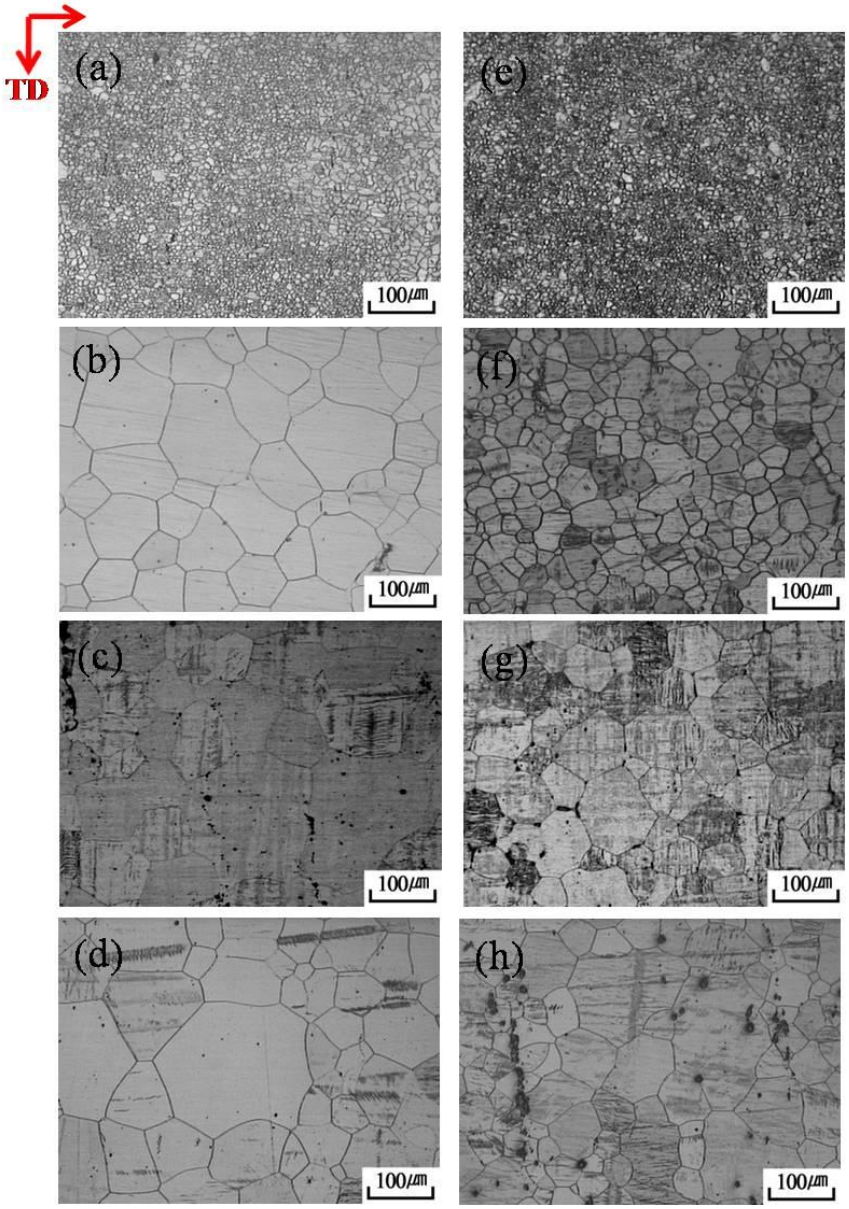

Fig. 5.2. Microstructures obtained from ND planes of (a, b, c, and d) Z6 with various annealing conditions and (e, f, g, and h) ZX60 with various annealing conditions

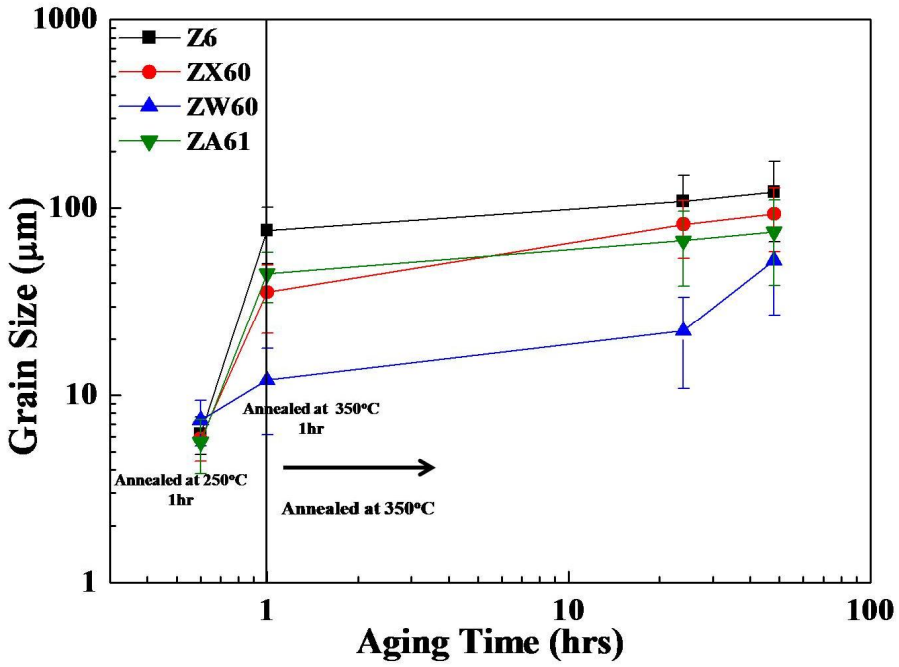

Fig. 5.3. Grain growth as a function of aging time

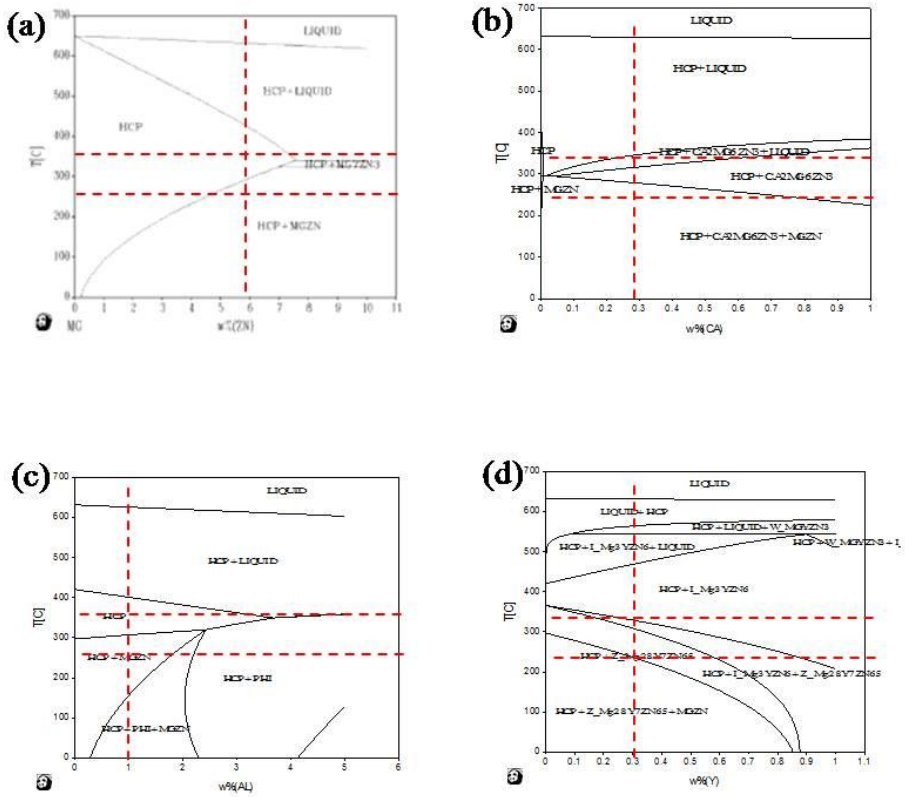

Fig. 5.4. Phase diagrams of (a) Z6, (b) ZX60, (c) ZW60, and (d) ZA61

5.2.3 Textures

The basal pole figures were also investigated. The basal pole in the typical rolling texture of Mg alloys is aligned approximately parallel to the normal direction. Maximum basal pole peaks appear in the normal direction and spread slightly towards the rolling direction (shown in Fig. 5.5). The Ca-containing alloy showed the lowest basal pole intensity. Various single crystal studies and VPSC simulation calculations have shown the critical resolved shear stress (CRSS) of non-basal slip systems decrease with the addition of Li elements [1, 18]. Moreover, Y, RE and Ca containing alloys exhibited texture weakening during thermo-mechanical processing such as rolling and extrusion [1, 2, 3, 4, 5, 19, 20]. Twinning can form strong basal texture during rolling [20]. Activation of non-basal slip modes, which leads to the deformation in the c-axis, can suppress twinning at high temperature [21]. The relationship between basal pole intensity and IE values is presented in Fig. 5.1 (b). The IE values of ZX60 are higher than those of the conditions. Weak basal texture which is favorable to basal slip mode, and tensile twinning may contribute to deformation via thickness.

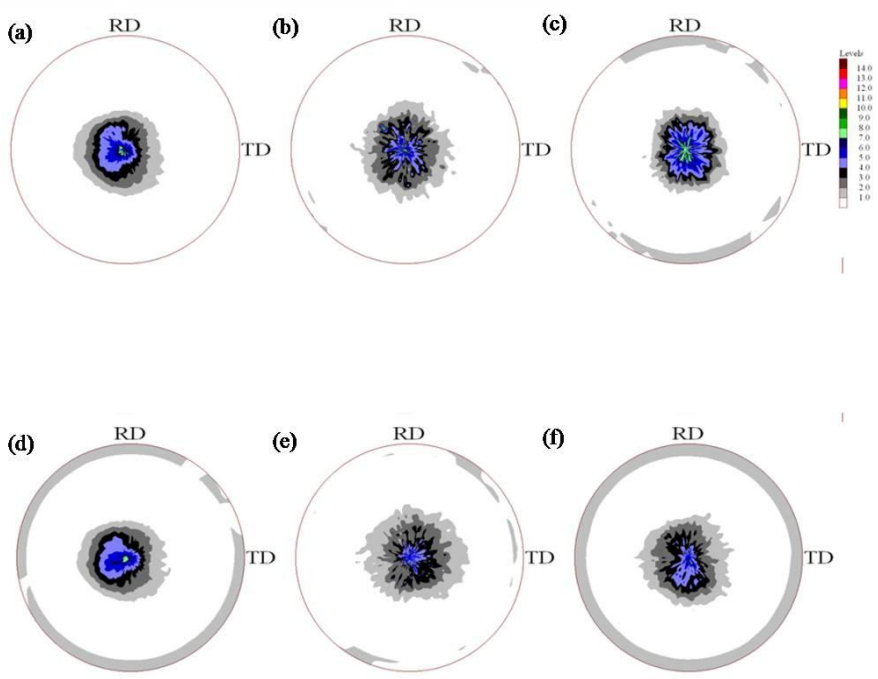

Fig. 5.5. Texture measured (a), (b) and (c) are corresponding to the pole figures of Z6 annealed at 350^{o}C for 1, 24, 48hr, respectively and the pole figures of (d), (e) , (f) obtained from ZX60, respectively

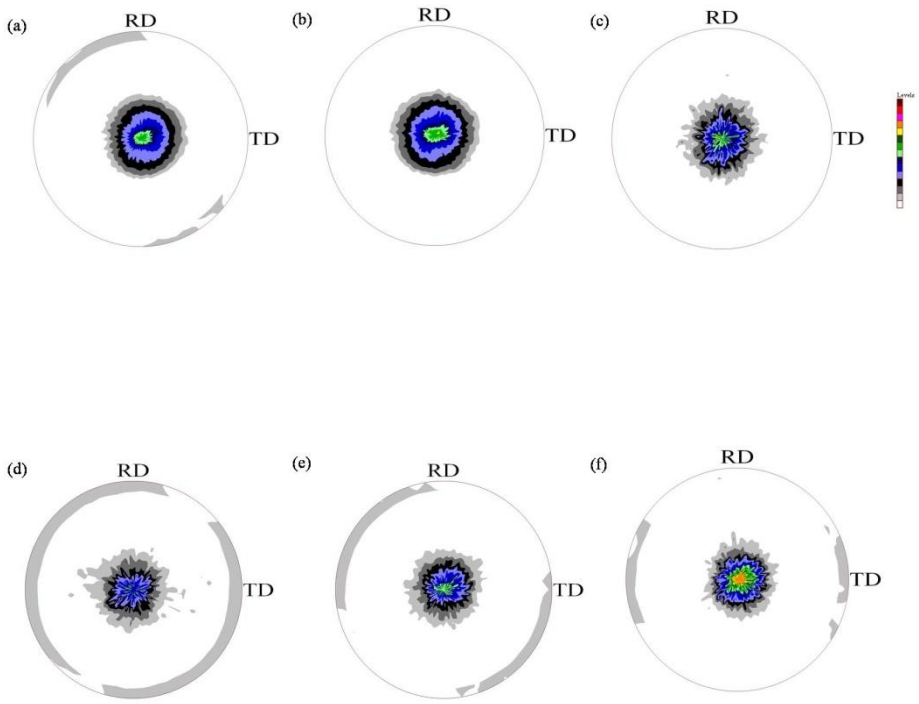

Fig. 5.6. Texture measured (a), (b) and (c) are corresponding to the pole figures of ZW60 annealed at 350^{o}C for 1, 24, 48hr, respectively and the pole figures of (d), (e) , (f) obtained from ZA61, respectively

5.2.4 Result of tensile test

The results of the Erichsen test correlates with some parameters of the tensile stress-strain curve. The variations in 0.2% yield strength, work hardening exponent, r-value, and uniform elongation against grain size for Mg-Zn alloys tested in RD are plotted in Fig. 5.7 (a), (b), (c) and (d), respectively. The parameters of all alloys show similar tendencies. The yield strength and r-value decrease, and the work hardening exponent and uniform elongation increase as grain size increases. Twinning highly dependent on grain size and twinning during deformation increases work hardening [22]. In addition, initial texture influences the activation of deformation modes including tensile twin and alters deformation behavior. It has been suggested that a high work hardening exponent was related to a high IE value via weak basal texture [23, 24]. The r-value is also related to deformation via thickness. A low r-value attributable to weak basal texture can lead to high formability [25]. However, the Ca-containing alloy did not show low yield strength or r-value. The VPSC model was applied in order to analyze the effects of grain size in more detail. The CRSS values of deformation modes and their relative activity were calculated using uniaxial tensile and compressive tests. This approach was used to simulate the stress-strain curves by varying the CRSS values of the 3 possible deformation modes (basal slip, prismatic slip and tensile twin) [11]. The CRSS values of the 3 deformation modes were calculated in Mg-Zn alloys with various grain sizes and then the Hall-Petch relations are presented in Table. 5.5. Slope (k) represents the sensitivity of grain size. The slope of tensile twin mode is higher than that of basal slip mode which indicates a decrease in CRSS ratio of tensile twin relative to basal slip. This result is in agreement with other studies [7, 11, 31]. ZX60 and ZW60 have high k values,

which indicate that tensile twin is activated well as grain size increases. Thus, these alloys have small grain sizes in the transition from basal slip mode to twinning (Table 5.4). The effect of alloying elements on {10-12} twinning is not well established because there are many factors to affect twinning. S. L. Shang et al. calculated the generalized stacking fault (GSF) of various Mg alloys and found adding Y and Ca to Mg alloys increased {10-12} twinning propensity by the first principle model [26]. On the other hand, experimental works showed that twinning was suppressed by adding Ca and Y [20, 27, 28]. And twinning in BCC metals was interrupted by solute atoms as mentioned in previous section. Twinning is affected by applied conditions and microstructures during deformation. In polycrystalline Mg and Mg alloys, grain size in the transition from twinning to basal slip decreases during the deformation with low temperatures and high strain rates [12]. The transition point slip to twinning is related to tendency of twinning. ZX60 and ZW60 have lower grain size than other alloys tested. These results are well matched with sensitivity of grain size and EBSD analysis (Fig. 5.9). There are CRSS ratios of deformation modes in Mg alloy according to VPSC calculations. <c+a> slip mode is known as contributor to enhancement of stretch formability reducing plastic anisotropy of Mg alloys. However, CRSS ratio <c+a> slip and basal slip is too large for <c+a> slip mode to activate at room temperature: more than 5 times. Moreover, CRSS ratio <c+a> slip and basal slip is larger with increasing grain size. Unlike a deformation in high temperatures, this indicates that <c+a> slip does not relate to enhance stretch formability by strain accommodation between grains. CRSS of prismatic slip mode is also too high to activate. It was reported that a ratio <c+a> to prismatic slip mode was related to r-value, but it may be difficult to activate both slip modes because of their high CRSS values [33]. On the other hand,

CRSS ration tensile twin and basal slip dramatically changes with increasing grain; CRSS of tensile twin becomes less than that of basal slip mode. Only slop of CRSS ratio tensile twin and basal slip as a function of grain size is positive. As seen in other studies, slip-twinning transition occurs because of more grain size sensitivity of tensile twin. Change preference of twinning with different grain size may strong correlate with change of stretch formability like the previous study regarding to the results of small Erichsen tests of AZ31.

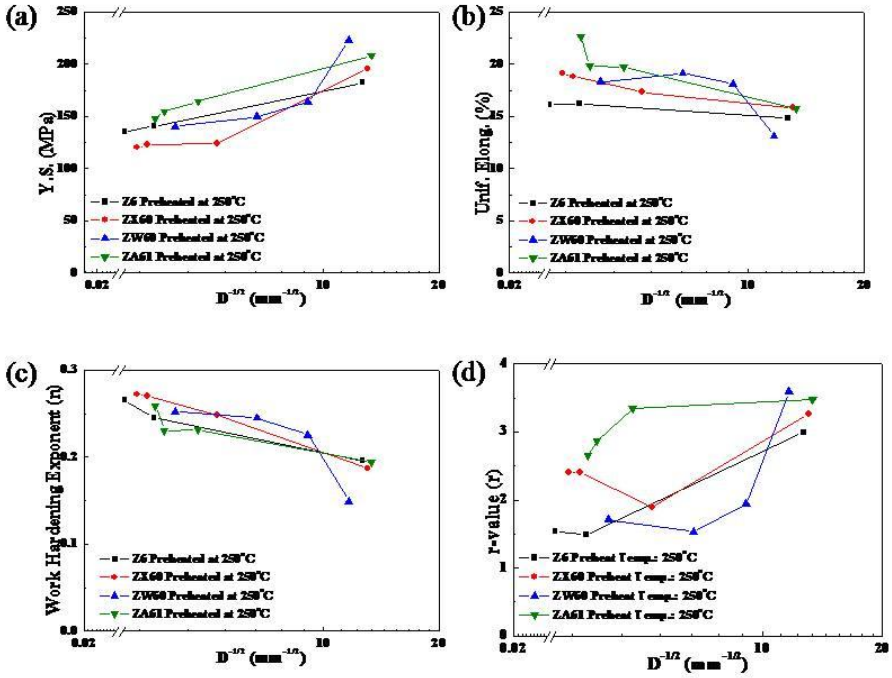

Fig. 5.7. Relationship between grain size and yield strength, (b) uniform elongation, (c) work hardening exponent, and (d) r-value

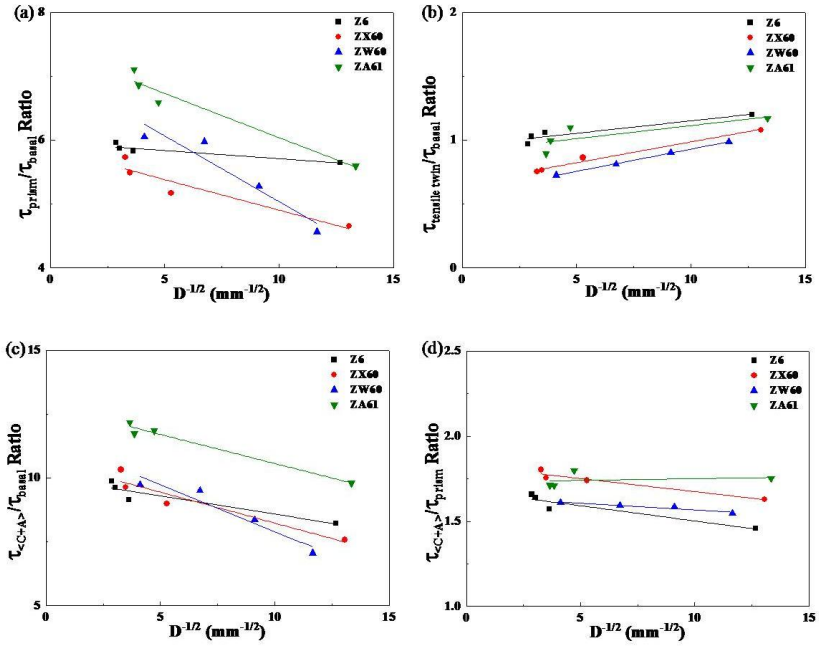

Fig. 5.8. H-P relationship obtained from VPSC calculation; (a), (b), (c) and (d) Z6, ZX60, ZW60 and ZA61 respectively

Table 5.4. Hall-Petch parameters for Mg-Zn alloys.

	Z6		**ZX60**		**ZW60**		**ZA61**	
	τ_o (MPa)	k (MPa $mm^{1/2}$)	τ_o (MPa)	k (MPa $mm^{1/2}$)	τ_o (MPa)	k (MPa $mm^{1/2}$)	τ_o (MPa)	k (MPa $mm^{1/2}$)
Basal Slip	19.26	0.66	17.05	0.74	17.86	1.02	13.70	1.69
Prismatic Slip	115.51	3.22	131.73	1.39	109.02	2.71	119.09	3.29
Tensile Twin	17.98	1.21	14.85	1.26	10.26	1.79	4.51	2.42
Slip-Twinning Transition (μm)	14.57		10.68		10.27		27.04	

5.2.4 EBSD analysis

In order to investigate the role of twinning on the results of the Erichsen test, measurements of Z6 and ZX60 TD planes were taken using EBSD. Twins are seldom seen in Z6 and ZX60 alloys with small grain sizes, but many twins form in ZX60 250R350A (Fig. 5.9). All twins were identified as {10-12} tensile twins. Even though the average grain size of ZX60 is less than half that of Z6, the tensile twins in ZX60 are considerably larger than those in Z6. This result shows that the enhancement of stretch formability is correlated with the activation of tensile twin. On the other hand, it is difficult to confirm that addition of Ca element increases activation of tensile twin because Z6 and ZX60 in this study have different texture. As mentioned in previous section, orientation is most critical factor to activate deformation modes according to Schmid law. ZX60 has weak basal texture which has the advantage to activate tensile twin mode and grow tensile twin boundaries. Twinning is formed by shuffling a group of atoms. Ca solutes, which have large atomic size, can interrupt the shuffling and play a role of pinning twin boundaries movement. J. F. Nie et al. suggested that alloying element could segregate twin boundary where it had been known as coherent boundary [27]. And segregation of elements pinned twin boundary movement during annealing. There is another thing to consider: atomic size of alloying elements. An atomic size of Ca is larger than that of Mg and can cause extension strain over Mg matrix, while that of Zn has smaller atomic size and can form contraction strain. In ZX60, a mixture of Zn and Ca segregate near twin boundary and have more advantage to move twin boundary than the cases which have only Zn or Ca solute. Z.R. Zeng et al. comments that the strain field induced by Ca or Zn solute affects twin growth [20, 27]

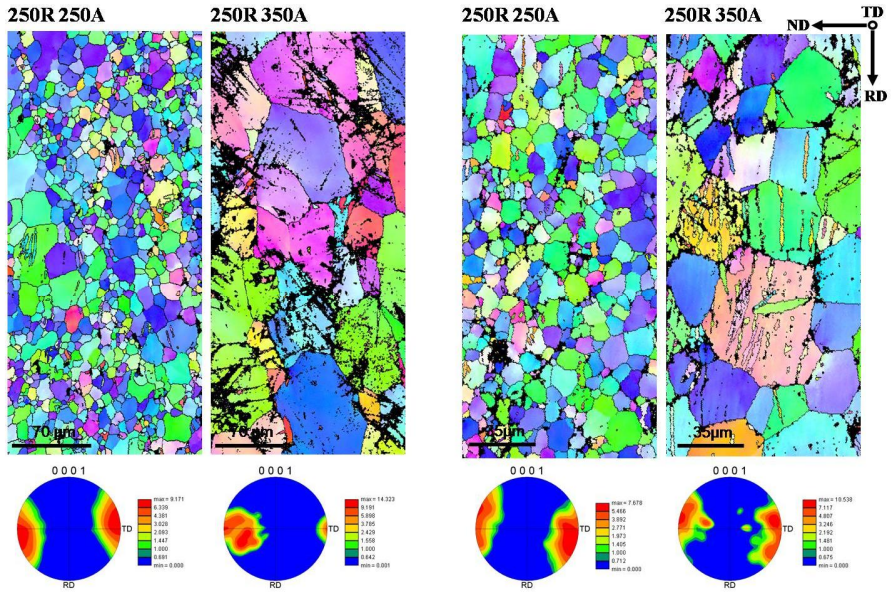

Fig. 5.9. IPF maps obtained from TD planes of (a) Z6 250R250A, (b) Z6 250R350A, (c) ZX60 250R250A, and (d) ZX60 250R350A

5.2.5 Relationship between twinning and fracture

The IE values of the Mg alloys in Fig. 5.1 (a) do not increase proportional to grain size. These results indicate that twinning plays a different role in alloys with larger grain sizes. The small Erichsen test, in which size is reduced by one tenth, was carried out in order to investigate the relationship between deformation twinning and crack formation. The grain orientations of two ZX60 specimens with different grain sizes were observed using EBSD technique. Then, SEM images were taken to observe twinning and crack propagation with punch displacements of 1/3mm, 2/3mm (Fig. 5.9). In ZX60 250R350A which showed the highest IE value, the cracks initiated at the grain boundaries of basal planes and propagated along the grain boundaries (see black line in Fig. 5.10 (a)). In addition, cracks did not form near the location of twins (see the blue circle in fig. 5.10 (b)). These results indicate that twinning enhances the stretch formability of Mg-Zn alloys. H. Yan et al. suggested that the high ductility was associated with the prevalence of tensile twin and basal slip during tensile tests [29]. D. Ando et. al. showed that low-strain grains accompanied tensile twins which formed in the grains with high schmid factors for the basal slip mode [30]. Basal slip mode is easily activated during deformation but it is restricted to the direction of the c-axis. Thus, tensile twinning may enhance strain accommodation between grains by releasing stress concentration. On the other hand, cracks formed in a different manner from those shown in Fig. 5.10 (a) in ZX60 250R350A24h. Most of the cracks seen in Fig. 5.10 (c) also formed at grain boundaries of basal planes, but some cracks were found in where twins occurred (see the blue circle in Fig. 5.10 (d)). Twinning has been identified as an origin of cracks in specimens with large grain sizes. There is a repulsive interaction between

basal dislocations and {10-12} tensile twin. It means that local stress concentration can form via a dislocation pile-up at twin boundaries [31]. H. Somekawa found that the accumulated strains at twin boundaries formed cracks that propagated along these boundaries during fracture toughness tests [32]. In Z6, there are many twins occurring during small Erichsen test. However, there is a big difference in that onset and propagation of cracks between ZX60 and Z6. In Fig. 5.11, tensile twin formed in the grain where basal plane is parallel to ND. These twins come from the cracks in grain boundary of basal plane. And cracks grow along to twin boundaries (Fig. 5.11 (b, d)). From VPSC caluculation (Fig. 5.8) CRSS of prismatic slip and <c+a> slip modes are from three times to ten times larger than that of basal slip mode. It means that basal slip and tensile twin mode can operate deformation and severe plastic anisotropy may happen. Especially, the grain in which basal plane is parallel to ND is not favored for basal slip and tensile twin modes. Therefore, strain accommodation between grains cannot be satisfied and cracks are formed in grain boundary. At this moment, twinning can release stress concentration and help meet strain accommodation. An addition of Ca in Z6 enhances twinning and twin growth according to EBSD analysis and VPSC calculation while twinning in Z6 do not grow to release stress in Fig 5.11. High formability may relate to segregation of alloying elements near twin boundary.

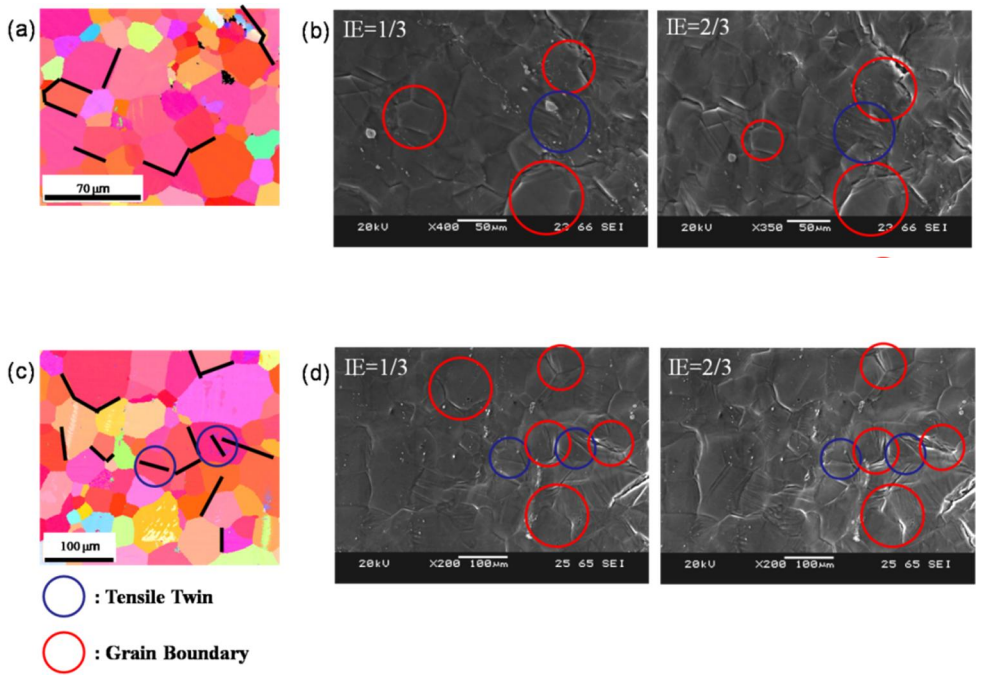

Fig. 5.10. Origin of crack and propagation during small the Erichsen test: IPF and SEM images of (a, b) ZX6 250R350A, (c, d) ZX60 250R350A24h

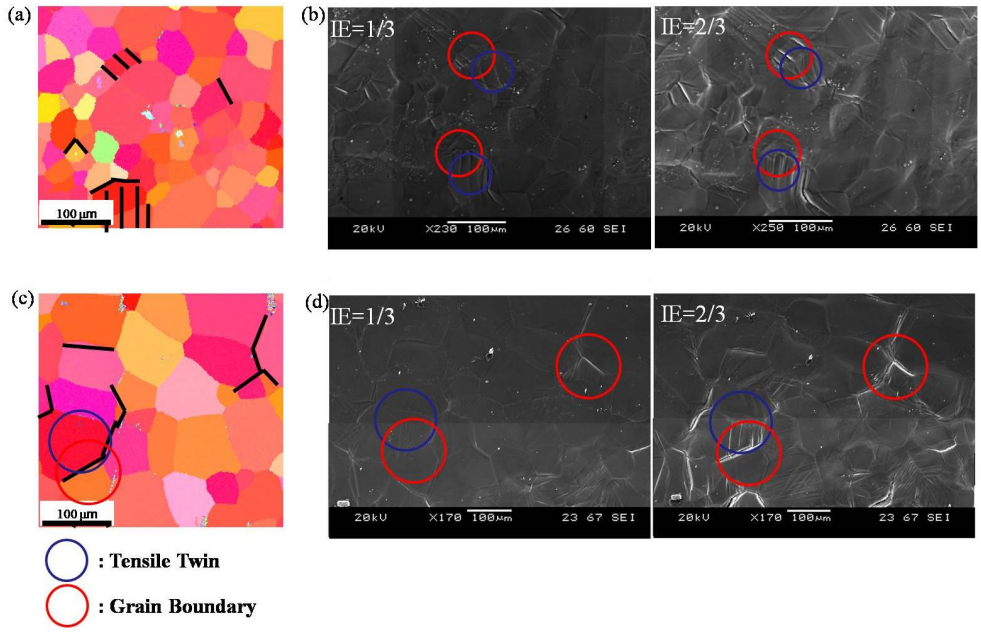

Fig. 5.11. Origin of crack and propagation during small the Erichsen test: IPF and SEM images of (a, b) Z6 250R350A, (c, d) Z60 250R350A24h

5.3 Conclusion

In the present study, the influence of twinning during the Erichsen test was investigated with various rolling conditions and alloying elements. The IE values of all alloys increased with grain size up to a certain point and then decreased. Tensile tests showed that yield strength, r-value, work hardening exponent, and uniform elongation of Mg-Zn alloys with grain sizes have similar tendencies. The Ca-containing alloy had the highest IE value. This increase in Erichsen value is associated with twinning. The results can be summarized as follows: 1) Ca weakens basal texture, which can lead to formation of tensile twin. 2) According to VPSC calculations and tensile tests, tensile twin more prevalent in specimens with Ca addition and large grains. 3) A high IE value is directly related to a propensity of tensile twinning, as assessed from EBSD images of Z6 and ZX60 after the Erichsen test. 4) The results of the small Erichsen test were agreed with the EBSD results. Cracks initiated at grain boundaries of the basal planes and twin were not origins of cracks in ZX60, which had the highest IE value. 5) However, some cracks appeared at twin boundaries as grain size increased.

Bibliography

1. S. R. Agnew, M. H. Yoo, and C. N. Tome "Application of texture simulation to understanding mechanical behavior of Mg and solid solution alloys containing Li or Y", Acta Mater., 49 (2001), pp. 4277-4289.
2. T. Al-Samman, and X. Li, " Sheet texture modification in magnesium-based alloys by selective rare earth alloying", Mater. Sci. Eng. A 528 (2011), pp. 3809-3822.
3. N. Stanford, "The effect of calcium on the texture, microstructure and mechanical properties of extruded Mg-Mn-Ca alloys", Mater. Sci. Eng. A 528 (2010) pp. 314-322.
4. R. Cottam, J. Robson, G. Lorimer, and B. Davis, "Dynamic recrystallization of Mg and Mg-Y alloys: crystallographic texture development", Mater. Sci. Eng. A 485, (2008), pp. 375-382.
5. Motohiro Yuasa, Naoki Miyazawa, Makoto Hayashi, Mamoru Mabuchi, and Yasumasa Chino, "Effects of group II elements on the cold stretch formability of Mg-Zn alloys", Acta Mater. 83 (2015), pp. 294-303.
6. J.W. Christian and S. Mahajan, "Deformation Twinning", Prog. Mater. Sci., 39 (1995), pp. 1-157.
7. M. A. Meyers, O. Vohringer, and V. A. Lubarda, "The onset of twinning in metals: a constitutive description", Acta Mater. 49, (2001), pp. 4025-4039.
8. M. Z. Bian, and K. S. Shin, "{10-12} Twinning behavior in magnesium single crystal", Met. Mater. Int. 5, (2013), pp. 999-1004.
9. M. R. Barnett, Z. Keshavarz, A. G. Beer, and D. Atwell, "Influence of grain size on the compressive deformation of wrought Mg-3Al-1Zn", Acta Mater. 52 (2004), pp. 5093-5103.

10. J. Koike, T. Kobayashi, T. Mukai, H. Watanabe, M. Suzuki, K. Maruyama and K. Higashi, “The activity of non-basal slip systems and dynamic recovery at room temperature in fine-grained AZ31B magnesium alloys”, Acta Mater. 51, (2003), pp. 2055-2065.
11. Y. Wang and H. Choo, “Influence of texture on Hall-Petch relationships in an Mg alloy”, Acta Mater. 81, (2014), pp. 83-97.
12. C. M. Cepeda-Jimenez, J. M. Molina-Aldareguia, and M. T. Perez-Prado, “Origin of the twinning to slip transition with grain size refinement, with decreasing strain rate and with increasing temperature in magnesium”, Acta Mater. 88, (2015), pp. 232-244.
13. R. W. Armstrong, “The influence of polycrstal grain size on several mechanical properties of materials”, Metal. Mater. Trans., 1A (1970), pp. 1169-1176.
14. H. L. Kim and Y. W. Chang, “An internal variable approach of orientation dependent deformation mechanism of rolled AZ31 magnesium alloy”, Met. Mater. Int. 17, (2011), pp. 721-728.
15. J.J. Jonas, S. Mu, T. Al-Samman, Gunter Gottstein, L. Jiang, and E. Martin, “The role of strain accommodation during the variant selection of primary twins in magnesium”, Acta Mater. 5 (2011), pp. 2046-2056.
16. Y. C. Lee, A. K. Dahle and D. H. StJohn, “The role of solute in grain refinement of magnesium”, Metall. Mater. Trans. A 31A (2000), pp. 2000-2895.
17. J. J. Bhattacharyya, S. R. Agnew, and G. Muralidharan, “Texture enhancement during grain growth of magnesium alloy AZ31B”, Acta Mater. 86 (2015), pp. 80-94.
18. S. Ando, and H. Tonda, “Non-basal slip in magnesium-lithium alloy single crystals”, Mater. Trans. 41 (2000), pp. 1188-1191.

19. Jong-Youn Lee, Young-Su Yun, Won-Tae Kim, and Do-Hyang Kim, "Twinning and texture evolution in binary Mg-Ca and Mg-Zn alloys", Met. Mater. Int. **20** (2014), pp. 885-891.
20. Z. R. Zeng, M. Z. Bian, S. W. Xu, C. H. J. Davies, N. Birbilis, J. F. Nie, "Texture evolution during cold rolling of dilute Mg alloys", Scripta Mater. **108** (2015), pp. 6-10.
21. A. Jain, and S. R. Agnew, "Modeling the temperature dependent effect of twinning on the behavior of magnesium alloy AZ31B sheet", Mater. Sci. Eng. A 462 (2007), pp. 29-36.
22. M. R. Barnett, Z. Keshavarz, A. G. Beer, and D. Atwell, "Influence of grain size on the compressive deformation of wrought Mg-3Al-1Zn", Acta Mater. 52 (2004), pp. 5093-5103.
23. D. H. Kang, D. W. Kim, S. Kim, G. T. Bae, K. H. Kim and Nack J. Kim, "Relationship between stretch formability and work-hardening capacity of twin-roll cast Mg alloys at room temperature", Scripta Mater. 61, (2009), pp. 768-771.
24. B. C. Suh, M. S. Shim, K. S. Shin, and Nack J. Kim, "Current issues in magnesium sheet alloys: Where do we go from here", Scripta Mater. 84-85, (2014), ppt. 1-6.
25. X. Huang, Y. Chino, M. Mabuchi, and M. Matsuda, "Influences of grain size on mechanical properties and cold formability of Mg-3Al-1Zn alloy sheets with similar weak initial textures", Mater. Sci. Eng. A 611, (2014), pp. 152-161.
26. S. L. Shang, W. Y. Wang, B. C. Zhou, Y. Wang, K. A. Darling, and L. J. Kecskes, "Generalized stacking fault energy, ideal strength and twinnability of diute Mg-based alloys: A first-principles study of shear deformation", Acta Mater. 67 (2014), pp. 168-180.

27. J.F. Nie, Y.M. Zhu, J.Z. Liu, X.Y. Fang, “Periodic segregation of solute atoms in fully coherent twin boundaries”, Science 340 (2013) 957–960.
28. N. Stanford, R. K. W. Marceau, and M. R. Barnett, “The effect of high yttrium solute concentration on the twinning behavior of magnesium alloys”, Acta Mater. 82 (2015), pp. 447-456.
29. H. Yan, S. W. Xu, R. S. Chen, S. Kamado, T. Honma, and E. H. Han, “Activation of {10-12} twinning and slip in high ductile Mg-2.0Zn-0.8Gd rolled sheet with non-basal texture during tensile deformation at room temperature”, J. Allys. Compd. 566 (2013), pp. 98-107.
30. D. Ando, J. Koike and Y. Sutou, “The role of deformation twinning in the fracture behavior and mechanism of basal textured magnesium alloys”, Mater. Sci. Eng. A 600, (2014), pp. 145-152.
31. M. H. Yoo, “Slip, Twinning, and Fracture in Hexagonal Close-Packed Metals”, Metal. Trans. A, 12 (1981), pp. 409-418.
32. H. Somekawa, A. Singh, and T. Mukai, “Fracture mechanism of a coarse-grained magnesium alloy during fracture toughness testing”, Philos. Mag. Lett. 89, (2009), pp. 2-10.
33. N. Stanford, K. Sotoudeh, and P.S. Bate, “Deformation mechanisms and plastic anisotropy in magnesium alloy AZ31”, Acta Mater. 59 (2011), pp. 4866-4874.

Chapter 6. Improvement of stretch formability of Mg-Al alloys via rolling conditions

6.1 Introductions

It has been reported that an addition of Zn and Al improve ductility and enhance strength in Mg alloys. Mg-Zn wrought alloys have been well developed because their basal textures, which lead mechanical anisotropy, remarkably weaken with addition of RE elements, Y, and Ca [1, 2, 3, 4, 5]. However, the effects of those kinds of alloying elements, which weaken basal texture, are limited in Mg-Al based alloys because Al makes intermetallic compound with them. There is another way to weaken basal texture during rolling. Thermally activated non-basal slips can compete with twinning, which form strong basal texture [6, 7, 8]. Adding small amount of Sn on Mg alloys increases the solidus line in the phase diagram. This can fabricate the Mg sheets at high temperature.

Grain size plays a critical role in the onset or extent of twinning and slip mode [9]. Grain size refinement normally increases critical resolved shear stress (CRSS) of deformation modes; this is called as the Hall-Petch relation [10]. Hall-Petch relation also can be applied to twinning because twinning is associated with stress concentration at grain boundaries [11, 12, 13]. Moreover, it is reported that non-basal slip can dominate during deformation with small grain size [14, 15].

In the present work, AZ31 and TA33 alloys have been investigated in aspects of controlling their textures and grain sizes with various rolling

conditions and identified influences of microstructures and textures on stretch formability at room temperature. The materials were prepared by extrusion with 2 nominal compositions of AZ31 and TA33 and followed by hot rolling in Table 5.1. The preheat conditions before rolling varied systematically ranging from 250^{o}C to 550^{o}C for 20min before rolling. Rolling was performed at rolling reduction of 50% per pass until a thickness of 1mm was obtained with setting 200^{o}C hot rolls for the specimens. The specimens with different grain sizes were prepared by at various annealing temperatures ranging from 250^{o}C to 550^{o}C. The rolling conditions and their grain size and Erichsen values (IE) are listed in Table 5.1. X-ray diffraction (XRD), electron back scattered diffraction (EBSD) technique and optical microstructures were used for analyzing grain sizes and textures. Visco-platic self-consistent model (VPSC) has been used in order to elucidate a role of deformation modes in Mg.

Table 6.1. Rolling conditions, grain size, and Erichsen values of AZ31 and TA33 alloys

Compositions (wt.%)	Preheat Temp. (^{o}C)	Annealing Temp. (^{o}C)	Annealing Time	Grain Size (μm)	Erichsen Value (mm)
Mg-3Al-1Zn	250	250	1	3.68	2.9
Mg-3Al-1Zn	250	350	1	3.92	3.2
Mg-3Al-1Zn	250	450	1	6.32	3.5
Mg-3Al-1Zn	350	250	1	3.81	3.1
Mg-3Al-1Zn	350	350	1	5.99	3.4
Mg-3Al-1Zn	350	450	1	11.79	3.8
Mg-3Al-1Zn	450	250	1	4.08	4.1
Mg-3Al-1Zn	450	350	1	4.80	4.4
Mg-3Al-1Zn	450	450	1	6.92	4.6
Mg-3Sn-3Al	350	350	1	4.89	3.3
Mg-3Sn-3Al	350	450	1	10.94	3.4
Mg-3Sn-3Al	350	550	1	17.38	3.4
Mg-3Sn-3Al	450	350	1	10.59	5.8
Mg-3Sn-3Al	450	450	1	16.11	6.2
Mg-3Sn-3Al	450	550	1	69.41	4.3
Mg-3Sn-3Al	550	350	1	12.34	6.1
Mg-3Sn-3Al	550	450	1	23.66	6.4
Mg-3Sn-3Al	550	550	1	55.51	6.2

6.2 Results and discussion

6.2.1 Results of Erichsen tests

Erichsen tests were conducted with AZ31 and TA33 alloys with various preheat and annealing conditions (Fig. 6.1). All the curves of IE values with annealing and preheat temperatures show similar tendency; IE values increase with increasing both annealing and preheat temperatures. An increase in preheat temperatures distinctly increases IE value while an increase in annealing temperatures slightly increase in IE value. These results indicate that annealing temperature and preheat temperature have different effects on the microstructure of Mg-Al alloys.

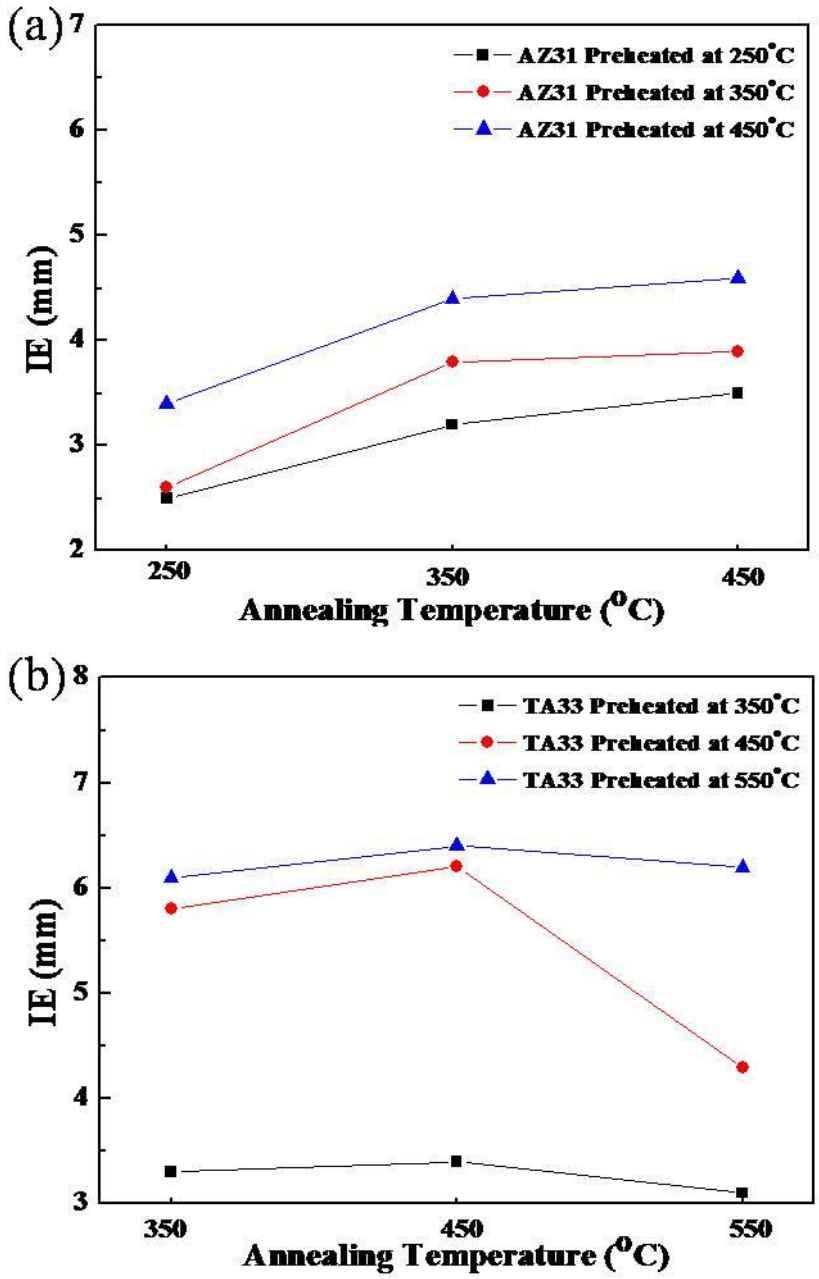

Fig. 6.1. Relationships between IE value and preheat temperature, which are obtained from (a) AZ31 and (b) TA33

6.2.2 Microstructure and Texture

Microstructures were taken from ND planes in order to identify the effects of annealing and preheat temperature. The microstructures of AZ31 and TA33 have recrystallized grain structures with equiaxial grains and the grain sizes are distributed homogeneously, while TA33s, which were annealed at 550^{o}C, have bimodal grain size distribution (shown in Fig. 6.2 and 6.3). Fig. 6.1 (c) shows that IE values of TA33 fall off in the annealing condition at 550^{o}C. These drops may be associated with abnormal grain growth in TA33. Abnormal grain growth which deteriorates formability or ductility of Mg has been found in severe deformation with high processing temperature or high annealing temperature [17]. Grain size was affected by preheat and annealing temperatures. Annealing temperature and time naturally contribute to grain growth with thermally activated diffusion. There are many factors which affect grain growth: pinning effects of solid solution and precipitation, and misorientation angles between grains etc. Solute pinning can affect the grain growth which is attributed to the mobility of grain boundaries during an annealing process. Thus, adding Sn and Al elements may slow the recrystallization and grain-growth. But amount of Sn in TA33 is very small and the diffusion coefficient of Sn atoms is higher than that of Al [18]. The strong basal texture during rolling can form low angle grain boundary between grains which, in turn the grain growth is suppressed because of the low energy and mobility of grain boundaries [19, 20]. TA33 specimens preheated at 450^{o}C and 550^{o}C have weaker basal texture than those of the other specimens. Thus, high preheat temperature and annealing temperature may contribute to high grain growth rate.

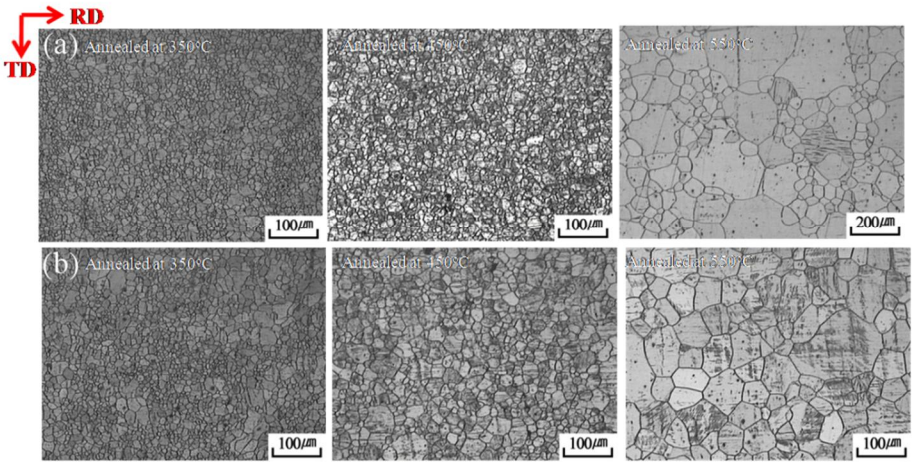

Fig. 6.2. Microstructures obtained from various rolling and annealing conditions; (a) and (b) correspond to the microstructures of TA33 450R and TA33 550R with different annealing temperatures, respectively

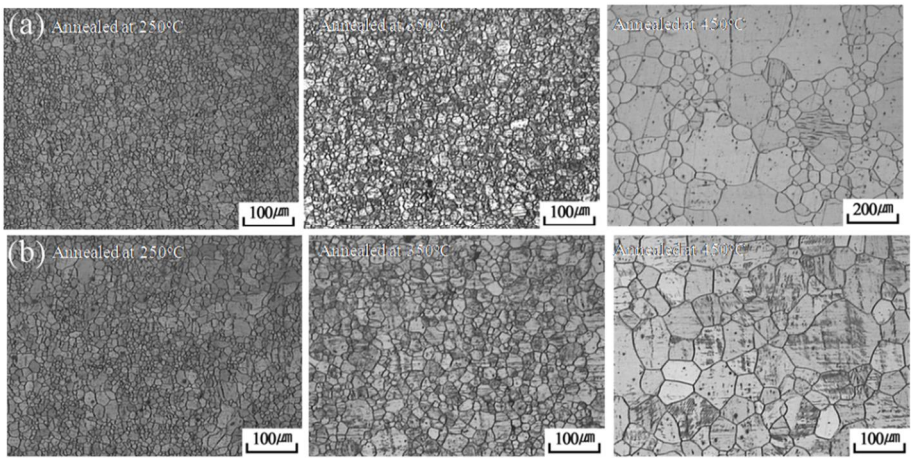

Fig. 6.3. Microstructures obtained from various rolling and annealing conditions; (a) and (b) correspond to the microstructures of AZ31 350R and AZ31 450R with different annealing temperatures, respectively

Textures are also important factor which determine stretch formability of Mg alloys. The basal poles are aligned parallel to the normal direction in the specimens rolled at low preheat temperature while in the specimen with high preheat temperature the basal pole peaks spread slightly in the rolling direction and their intensity decrease (shown in Fig. 6.4). The maximum intensity of AZ31 decreases from 7.57 to 3.41 and that of TA33 falls off from 8.25 to 3.16 with increasing preheat temperature. The evolution of texture during deformation processing is highly dependent on applied temperature [21]. Several single crystal studies and VPSC simulation have tried to elucidate the mechanism of the changing critical reserved shear stress (CRSS) of non-basal slip [22, 23]. The homologous temperature which is the applied temperature divided by melting temperature indicates the upper limit during deformation. Fig. 6.5 (a) shows that rolling at high homologous temperature decrease basal pole intensity. Twinning intensively forms basal texture during rolling. Especially, tensile twin reorient matrix orientation by 86.3^{o} at once, while reorientation induced by slip modes changes little and slow. There are two good examples to explain the relationship between activation tensile twin and basal texture. First, it was reported that Ca-containing alloy had weak basal texture after cold rolling because Ca segregation interrupt to migrate twin boundaries [8]. In addition, the activating non-basal slip modes during rolling play an important role to weaken basal texture which enhances the deformation through c-axis without twinning [24, 25]. Second, thermal vibration may help activate cross slip and non-basal slip. CRSS of non-basal slip modes dramatically drops off compared to those of basal slip and tensile twin mode (Table 6.2). Rolling at high temperatures increases an activation of non-basal slip modes which are competitors as main deformation mode. Mg-Sn alloys have a great advantage to weaken basal texture because Sn addition

increases melting temperature and enables Mg alloys to be rolled at high temperatures. It is impossible to be rolled for Z6 alloys over 400^{o}C. And the eutectic temperature of Mg-Zn binary system is slightly higher than 350^{o}C. Unless Zn solutes ideally distribute, locally melting is unavoidable. On the other hand, addition of Sn increases eutectic temperature (over 520^{o}C) and liquidus line. The advantage of rolling high temperature is that activations of non-basal slip modes and cross slip suppress a formation of strong basal texture during rolling. Fig. 6.6 (a) shows that rolling at high homologous temperature decreases basal pole intensity of Mg sheets.

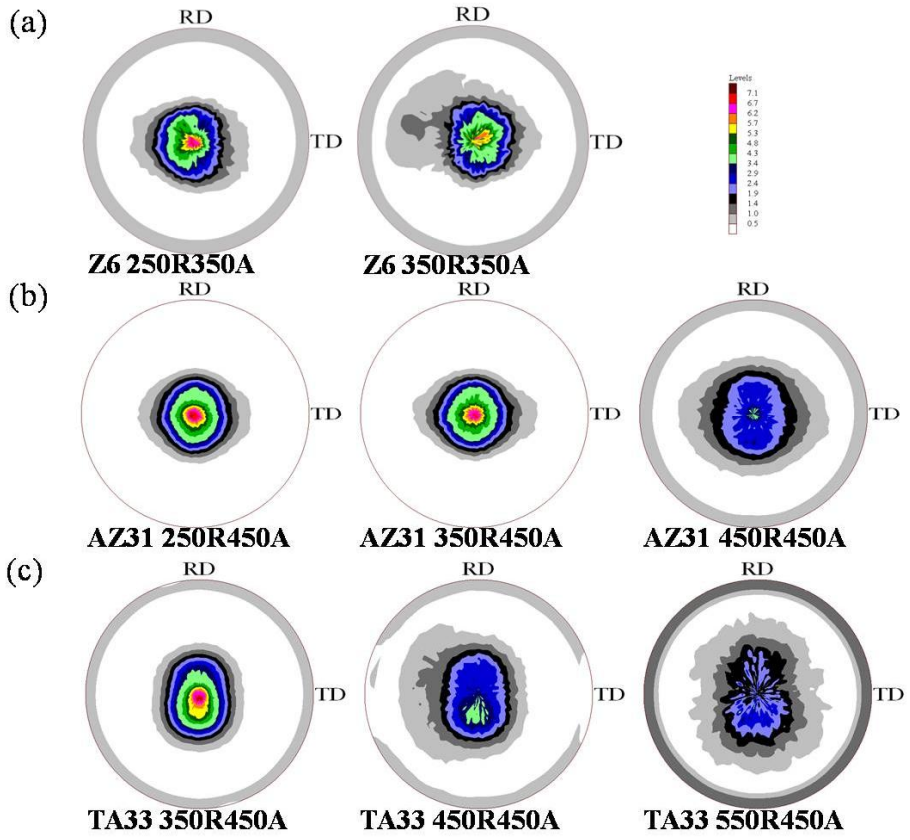

Fig. 6.4. (0001) pole figures obtained from ND planes of (a) Z6, (b) AZ31, and (c) TA33

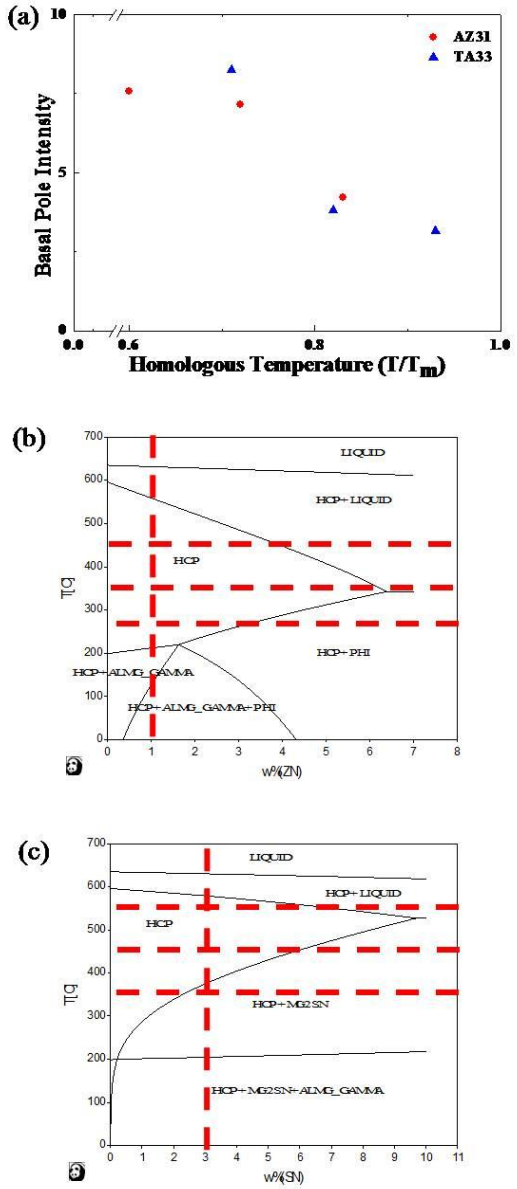

Fig. 6.5. (a) Relationship between homologous temperature and basal pole intensity, (b) phase diagram of Mg-1Al with various Sn contents, and (c) phase diagram of Mg-3Al with various Zn contents

6.2.3 Result of tensile test

Uniaxial tensile tests were carried out on Mg-Zn alloys at room temperature and nominal strain rate of 2 x 10-4 s-1 in Fig. 6.6 (a) and (b). Yield stress and r-value are correlated well with the result of textures induced by the preheat condition, while n-value and uniform elongation follow the change of grain size resulted from the annealing condition. The efforts to find the connection between the parameters of tensile test and the stretch formability have continued [7, 26]. However, high n-value and uniform elongation cannot guarantee the high formability since Mg alloys are crystallographically anisotropic. TA33 550R specimens showed high IE values but they have poor n-value and uniform elongation. In some range of Mg alloys and conditions, weak basal texture leads to high n-value and high uniform elongation. However, casting Mg alloy, which shows closely randomized texture, show high n-value but low uniform elongation. Texture of TA33 preheated at 550^{o}C has very low basal pole intensity. The condition with weak basal texture and large grain size may increase an activation of tensile twinning which reorient matrix orientation to hard orientation. VPSC model was applied in order to analyze the more detailed information about the effects of textures and grain sizes. CRSS of deformation modes and their relative activity were calculated from uniaxial tensile and compressive. This approach was used to simulate the stress-strain curves by varying the CRSS values of the 3 possible deformation modes such as basal slip, prismatic slip and tensile twin [9, 10]. The CRSS of 3 individual deformation modes were calculated from AZ31 and TA33 alloys at rolling conditions and then the Hall-Petch relations of them were in Table. 6. 2. The slope (k) of indicates the sensitivity of grain size. The slopes of tensile twin obtained from AZ31 and TA33 are higher than that of basal slip.

k value of TA33 is higher than that of AZ31. In stress-strain curves, yield strength drop off more compared to that of AZ31. An activation of tensile twin increases more in TA33 than that in AZ31. Thus, yield strength of TA33 drops off more than AZ31 (Fig. 6.8). There is another evidence to show an increase in twinning with increasing grain size. IPF maps from TD planes after Erichsen test show a number of tensile twins occur in larger grain size (shown in Fig. 6.6). TA33 550R450A and 550R550A specimens fractured earlier than other conditions. According to VPSC calculation of TA33 550Rs, more tensile twinning occurred at the beginning stage of tensile deformation (Fig. 6.7). Activation of twinning increases with an increase in a grain size. This result shows the good agreement with earlier studies [9, 24]. Twinning is affected by applied conditions and microstructures during the deformation [27]. In addition, the tensile deformation behaviors of AZ31 were calculated by VPSC model. The CRSSs of basal slip and tensile twin did not significantly change, while the change of the CRSS of prismatic slip was high. This result is well matched that the relative activity of the non-basal slip such as the prismatic slip and pyramidal slip increase when Mg alloys strained at high temperature.

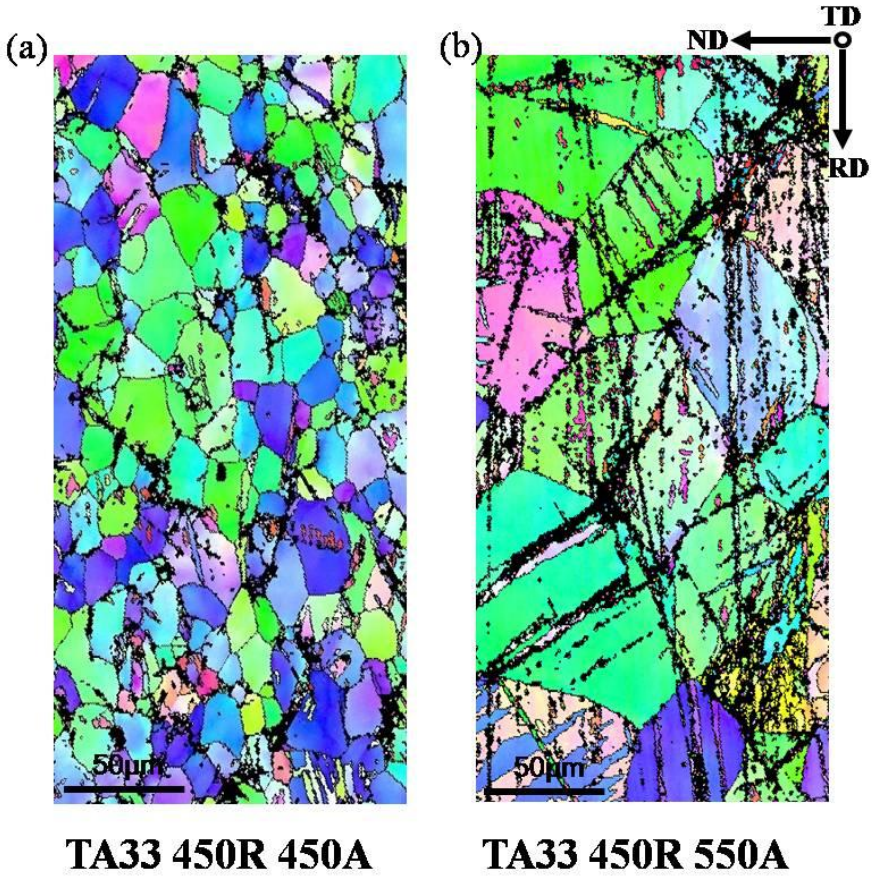

Fig. 6.6. IPF maps obtained from TD planes of (a) TA33 450R450A1H, and (b) TA33 450R550A1H

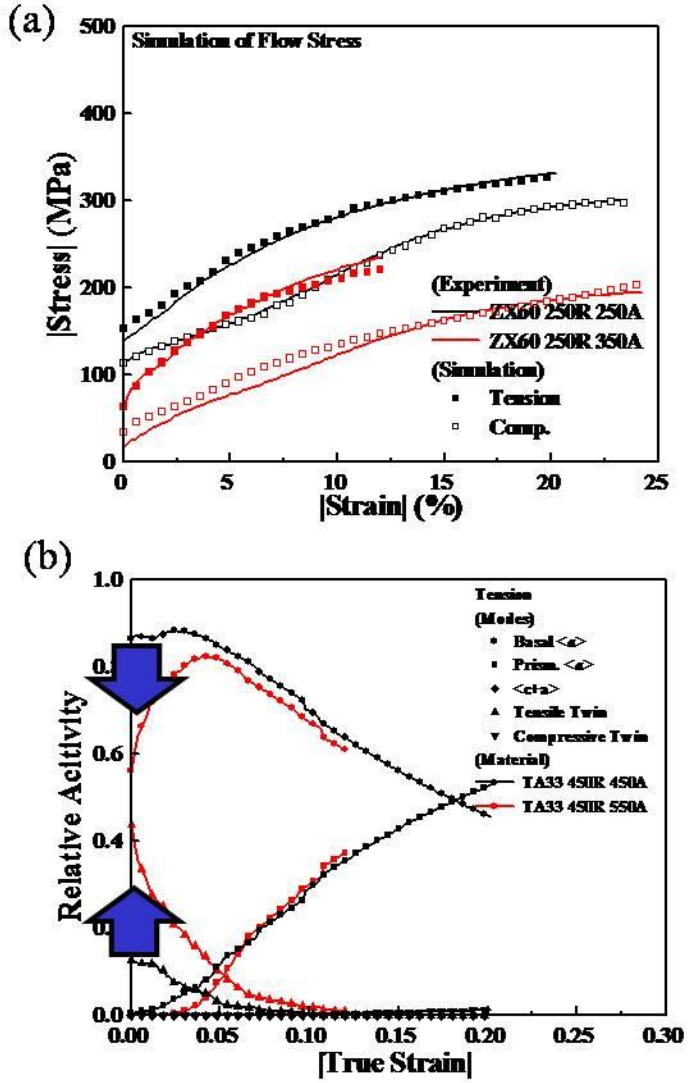

Fig. 6.7. (a) A comparison of experimental results and VPSC calculation of TA33 450R450A1H and TA33 450R550A1H, and (b) their relative activities of deformation modes from VPSC model

Table 6.2. Hall-Petch parameters of AZ31 and TA33 specimens.

	AZ31		AZ31 at 150°C		TA33	
	τ_o (MPa)	k (MPa $mm^{1/2}$)	τ_o (MPa)	k (MPa $mm^{1/2}$)	τ_o (MPa)	k (MPa $mm^{1/2}$)
Basal Slip	11.70	2.37	10.03	1.06	5.72	2.61
Prismatic Slip	40.97	4.50	18.87	3.30	74.06	6.40
Tensile Twin	5.69	3.29	5.81	2.72	-18.14	7.04

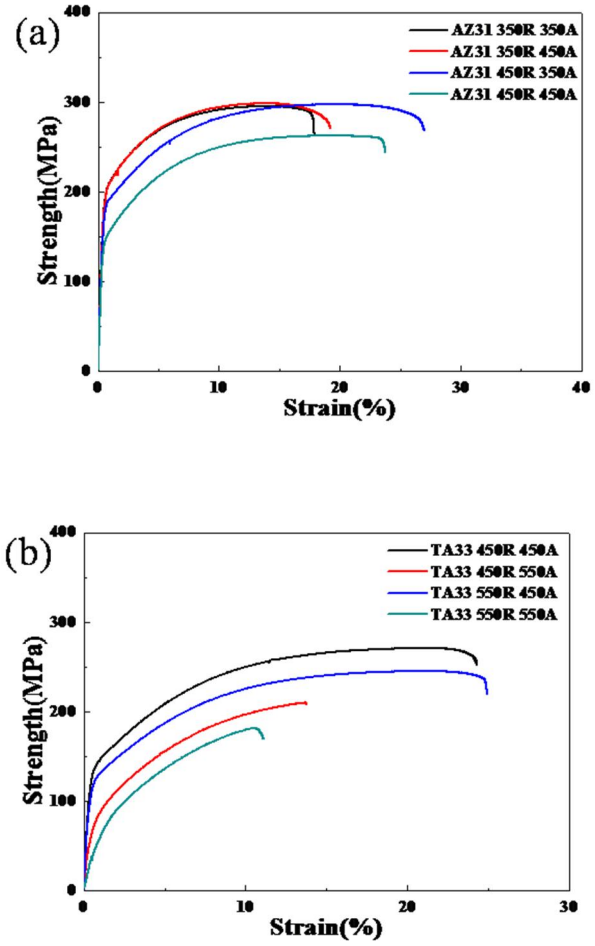

Fig. 6.8. Stress- Strain curves of (a) AZ31, and (b) TA33

The n-value, one of parameters obtained from tensile tests already dealt with in the previous sections. The specimens with high n-value show high stretch formability like other light metals such as Aluminum and Brass. Fig. 6.9 shows that Z6 and AZ31 alloys have positive relation between IE value and grain size. And work hardening coefficient (n-value) also follows positive relation with grain size. An increase in grain size increases n-value of all specimens in Fig. 6.10. In previous section, IE value increase up to certain grain size and then decrease in larger grain size; an increase in grain size obviously increase n-value of Mg alloys but twinning can enhance crack propagation. TA33, here, shows another exception of the relationship between IE value and n-value. Increasing grain size easily increases n-value by decreasing yield strength and increasing an activity of tensile twin. Fig 6.11 (a) shows well the relationship between n-value and grain size: positive relationship between them. Unfortunately, stretch formability is not simply affected by n-value. Grain size distribution highly affects stretch formability of Mg alloys. A crack induced by cleavage is not found in the results of small Erichsen test. Instead of that, onset of cracks started in grain boundaries. Homogeneous strain during deformation allows high formability. On the other hand, heterogeneous grain distribution may interrupt homogeneous strain between grains. High annealing temperature after severe deformation causes abnormal grain growth. Stored energy induced by severe deformation process such as ECAP and friction stir process is distributed heterogeneously over microstructure of Mg alloys. And annealing at high temperature makes different grain growth grain by grain. TA33 alloys preheated at 450^{o}C shows homogenous grain size distribution after annealing at 350^{o}C and 450^{o}C. However, abnormal grain growth occurred after annealing at 550^{o}C (Fig. 6.9 (b). An extent of abnormal grain growth is more severe in TA33

450R550A1H than in TA33 550R550A. Therefore, IE value severely drops in TA33 450R specimens (Fig. 6.9 (a)). And grain boundary energy, which is correlated with misorientation angles, becomes larger because applied shear force or deformation at high temperature often forms the unique texture different from basal texture.

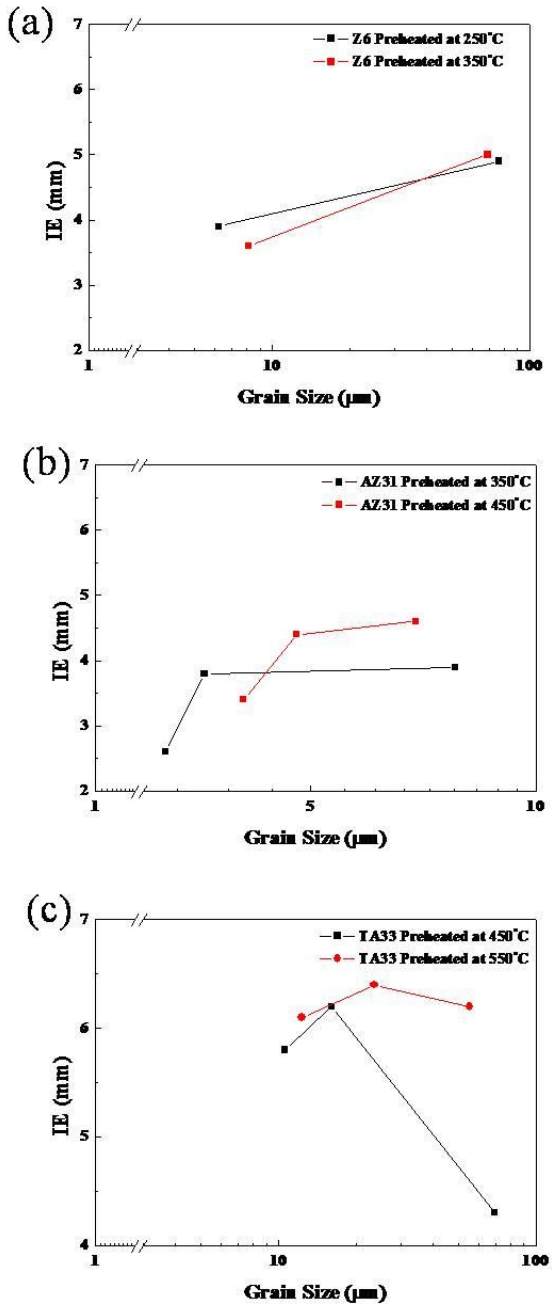

Fig. 6.9. Relationship between IE values and grain sizes: (a) Z6, (b) AZ31, and (c) TA33

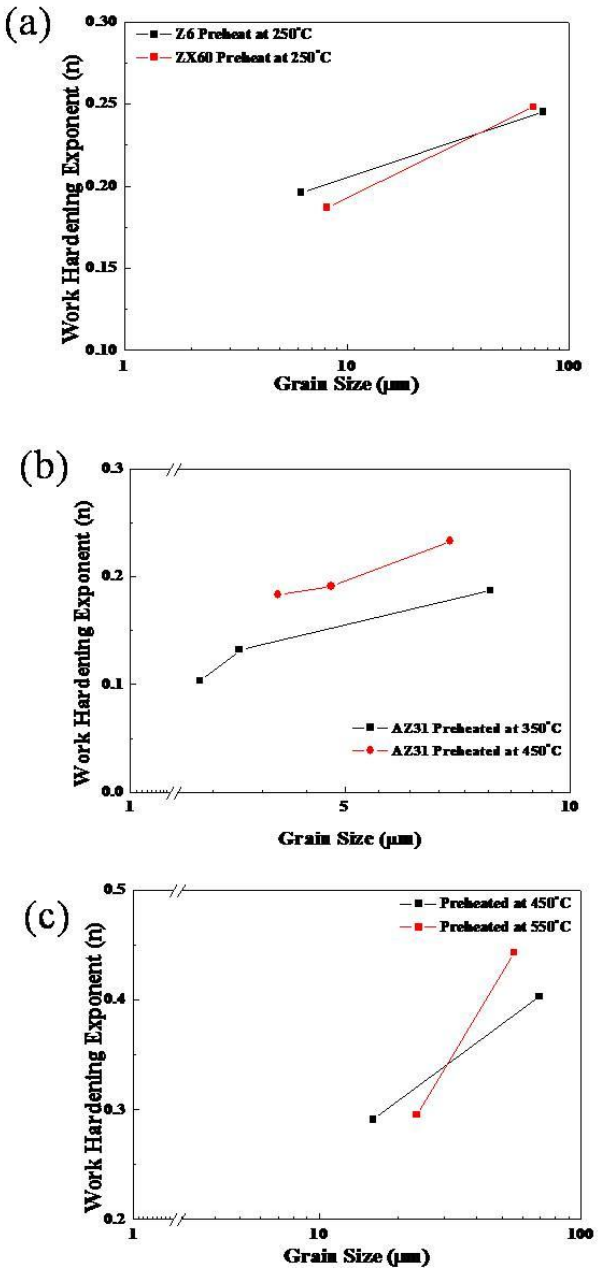

Fig. 6.10. Relationship between n-value and grain sizes: (a) Z6, (b) AZ31, and (c) TA33

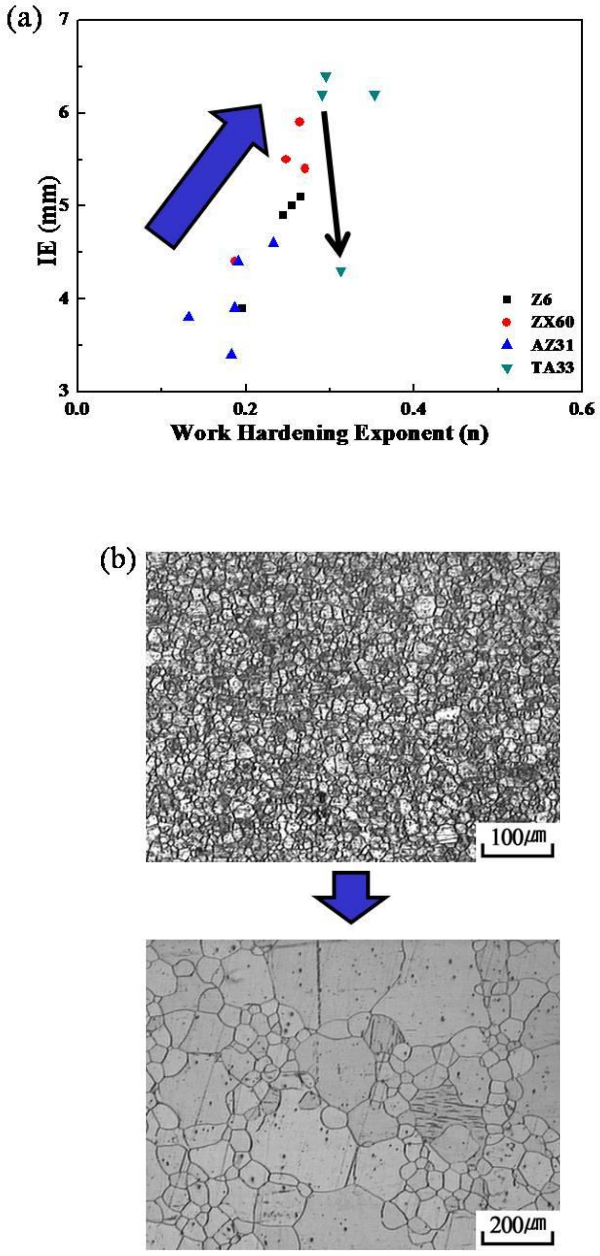

Fig. 6.11.(a) Relationship between IE values and n-value and (b) microstructures changed by annealing temperature 550°C for 1hr

6.3 Conclusions

The current study confirmed the influence of rolling conditions on stretch formability of AZ31 and TA33 alloys. The IE values of two alloys increased with increasing the preheat temperature and annealing temperature. These conditions are related with the change of texture and grain size respectively. Weakening basal texture and large grain size enhance the activation of tensile twinning according to the tensile tests and their VPSC calculation. Thus, the highest IE value of Mg alloys is associated with tensile twinning. In addition, the results of AZ31 deformation at room temperature and 150^{o}C showed that the activation of non basal slip modes is enhanced at high temperature and this weaken the typical basal texture. Work-hardening coefficient (n-value) is correlated with stretch formability in Z6 and AZ31 alloys, while TA33 alloys which shows abnormal grain growth is not in an agreement of the relationship.

Bibliography

1. S. R. Agnew, M. H. Yoo, and C. N. Tome "Application of texture simulation to understanding mechanical behavior of Mg and solid solution alloys containing Li or Y", Acta Mater., 49 (2001), pp. 4277-4289.
2. T. Al-Samman, and X. Li, " Sheet texture modification in magnesium-based alloys by selective rare earth alloying", Mater. Sci. Eng. A 528 (2011), pp. 3809-3822.
3. N. Stanford, "The effect of calcium on the texture, microstructure and mechanical properties of extruded Mg-Mn-Ca alloys", Mater. Sci. Eng. A 528 (2010) pp. 314-322.
4. R. Cottam, J. Robson, G. Lorimer, and B. Davis, "Dynamic recrystallization of Mg and Mg-Y alloys: crystallographic texture development", Mater. Sci. Eng. A 485, (2008), pp. 375-382.
5. Motohiro Yuasa, Naoki Miyazawa, Makoto Hayashi, Mamoru Mabuchi, and Yasumasa Chino, "Effects of group II elements on the cold stretch formability of Mg-Zn alloys", Acta Mater. 83 (2015), pp. 294-303.
6. J. R. Luo, A. Godfrey, W. Liu, and Q. Liu, "Twinning behavior of a strongly basal textured AZ31 Mg alloy during warm rolling", Acta Mater. 60 (2012), pp. 1986-1998
7. J. Koike, T. Kobayashi, T. Mukai, H. Watanabe, M. Suzuki, K. Maruyama and K. Higashi, "The activity of non-basal slip systems and dynamic recovery at room temperature in fine-grained AZ31B magnesium alloys", Acta Mater. 51, (2003), pp. 2055-2065.
8. Z. R. Zeng, M. Z. Bian, S. W. Xu, C. H. J. Davies, N. Birbilis, J. F. Nie, "Texture evolution during cold rolling of dilute Mg alloys", Scripta Mater.

108 (2015), pp. 6-10.

9. M. A. Meyers, O. Vohringer, and V. A. Lubarda, "The onset of twinning in metals: a constitutive description", Acta Mater. 49, (2001), pp. 4025-4039.
10. Y. Wang and H. Choo, "Influence of texture on Hall-Petch relationships in an Mg alloy", Acta Mater. 81, (2014), pp. 83-97.
11. J.W. Christian and S. Mahajan, "Deformation Twinning", Prog. Mater. Sci., 39 (1995), pp. 1-157.
12. W. Yuan, S. K. Panigrahi, J.-Q. Su, and R. S. Mishra, "Influence of grain size and texture on Hal-Petch relationship for a magnesium alloy", Scripta Mater. 65, (2011), pp. 994-997.
13. R. W. Armstrong, "The influence of polycrstal grain size on several mechanical properties of materials", Metal. Mater. Trans., 1A (1970), pp. 1169-1176.
14. S. M. Razavi, D. C. Foley, I. Karaman, K. T. Hartwig, O. Duygulu, L. J. Kecskes, S. N. Mathaudhu, and V. H. Hammond, "Effect of grain size on prismatic slip in Mg-3Al-1Zn alloy", Scripta Mater. 5 (2012), pp. 439-442.
15. Ya-Fang Guo, Shuang Xu, Xiao-Zhi Tang, Yue-Sheng Wang, and Sidney Yip, "Twinnability of hcp metals at the nanoscale", J. Appl. Phys. 115 (2014), pp. 224902
16. John J. Jonas, Sijia Mu, Tala Al-Samman, Gunter Gottstein, Lan Jiang, and Etienne Martin, Acta Mater. 5 (2011) 2046-2056
17. I. Charit and R. S. Mishra, "Abnormal grain growth in friction stir processed alloys", Scripta Mater. 58 (2008), pp. 367-371.
18. S. Ganeshan, L. G. Hector Jr., Z.-K. Liu, "First-principles calculations of impurity diffusion coefficients in dilute Mg alloys using the 8-frequency model", Acta Mater. 59 (2011), pp. 3214-3228.
19. J. J. Bhattacharyya, S. R. Agnew, and G. Muralidharan, "Texture

enhancement during grain growth of magnesium alloy AZ31B", Acta Mater. 86 (2015), pp. 80-94.

20. M. T. Perez-Prado, O. A. Ruano, "Texture evolution during grain growth in annealed Mg AZ61 alloy", Scripta Mater. 48 (2003), pp. 59-64.
21. S. R. Agnew and O. Duygulu, "Plastic anisotropy and the role of non-basal slip in magnesium alloy AZ31B", Int. J. Plast. 21, (2005), pp. 1161-1193.
22. A. Chapuis, J. H. Driver, "Temperature dependency of slip and twinning in plane strain compressed magnesium single crystals", Acta Mater. 59, (2011), pp. 1986-1994.
23. Kelley EW, and Hosford WF., "Plane-strain compression of magnesium and magnesium alloy crystals", Trans. AIME 242, (1968), pp. 5-13.
24. X. Huang, Y. Chino, M. Mabuchi, and M. Matsuda, "Influences of grain size on mechanical properties and cold formability of Mg-3Al-1Zn alloy sheets with similar weak initial textures", Mater. Sci. Eng. A 611, (2014), pp. 152-161.
25. Y. B. Chun, and C. H. J. Davies, "Investigation of prism <a> slip in warm-rolled AZ31 alloy", Metall. Mater. Trans. A 42 (2011), pp. 4113-4125.
26. D. H. Kang, D. W. Kim, S. Kim, G. T. Bae, K. H. Kim and Nack J. Kim, "Relationship between stretch formability and work-hardening capacity of twin-roll cast Mg alloys at room temperature", Scripta Mater. 61, (2009), pp. 768-771.
27. M. R. Barnett, Z. Keshavarz, A. G. Beer, and D. Atwell, "Influence of grain size on the compressive deformation of wrought Mg-3Al-1Zn", Acta Mater. 52 (2004), pp. 5093-5103.

Chapter 7. Summary and conclusions

The influence of rolling temperature and annealing temperature on the stretch formability was investigated in the present study. Mg-Al-Zn, Mg-Zn, Mg-Sn-Al alloys were examined with various rolling conditions. An increase in rolling temperature was more effective to improve IE value than annealing temperature..Basal texture in AZ31 and TA33 more weakened with increasing rolling temperature, and it might lead to increase grain growth rate. According to tensile test, the parameters of AZ31 and TA33 were differently affected by rolling temperature and annealing temperature; yield stress and n-value of AZ31 were more dependent on rolling temperature, while those of TA33 and Z6 alloys were changed by annealing temperature.

In the previous study, increasing rolling temperature weakened basal texture, and increasing annealing temperature increased grain size. To identify the effects of grain size and texture on stretch formability, various microstructures and textures were examined by EBSD analysis, VPSC calculation, and small Erichsen test. An increase in rolling temperature weakened basal texture and an increase in annealing temperature and time increased grain size in AZ31.The results of tensile tests were affected by texture and grain size; weak basal texture decreased yield strength and r-value, and increased work hardening exponent and uniform elongation. Only in 450R specimens showed that the stretch formability increased with grain size up to a certain point and then decreased. Twinning geometrically more favors in weak basal texture and in large grain size from VPSC calculations. It can be inferred that the roles of twinning is different by grain size. In addition, the EBSD images

were obtained from uniaxial and bi-axial tension test to investigate the role of tensile twin in the formability. There are two important roles for tensile twinning to contribute the high formability: twin straining by rotating orientation and activating basal dislocations in several directions by reorienting lattice or releasing stress concentration. In the tensile test of different grain sized AZ31s, the tensile twinning in M2 forms hard orientation restricted further deformation. Its tensile twin strain theoretically satisfies only 6.6% strain. Thus, activating slip systems is better way to improve formability of Mg. However, activating non-basal slip systems are significantly restricted at room temperature. According to the results of VPSC calculations, more tensile twinning occurs with increasing grain size. Specifically, tensile twinning increasingly occurs in unfavorable orientation, which indicates such tensile twins release stress concentration to accommodate grains. Tensile twinning can ease the limitation; the lattice reorientation of 86.3^{o} switch basal dislocation path and tensile twinning assists basal dislocation to activate continuously without failure. In the current experiments, the reduction in r-value comes from the tensile twinning in M1 grains, even though it cannot directly contribute to the strain through thickness. It seems that the tensile twinning aids activating basal dislocation by releasing stress concentration on grain boundaries. The relationship between tensile twin and fracture are also covered from the results of the small Erichsen test. Cracks initiated at grain boundaries of the basal planes and twinning did not become an origin of cracks in specimens with small grain size. At this moment, twinning enhances stretch formability. However, cracks originated at either grain boundaries or twins in specimens with large grain size by the interaction between twins and basal dislocations.

Alloying elements also give different the characterization of microstructures

and mechanical properties. Z6, ZX60, ZW60, and ZA61 alloys were examined. The IE values of all alloys increased with grain size up to a certain point and then decreased. Tensile tests showed that yield strength, r-value, work hardening exponent, and uniform elongation of Mg-Zn alloys with grain sizes have similar tendencies. The Ca-containing alloy had the highest IE value among them. This increase in Erichsen value is associated with twinning by weakening basal texture. In addition, VPSC calculations and tensile tests showed that tensile twin were more prevalent in specimens with Ca addition and large grains. These results indicate that a high IE value is directly related to a propensity of tensile twinning, as assessed from EBSD images of Z6 and ZX60 after the Erichsen test. The results of the small Erichsen test were the same as the test for AZ31;cracks initiated at grain boundaries of the basal planes and twin were not origins of cracks in ZX60, which had the highest IE value. 5) However, some cracks appeared at twin boundaries as grain size increased.

At last, the influence of rolling conditions on stretch formability of AZ31 and TA33 alloys was investigated. The IE values of two alloys increased with increasing the preheat temperature and annealing temperature. These conditions are related to the change of texture and grain size respectively. Weakening basal texture and large grain size enhance the activation of tensile twinning according to the tensile tests and their VPSC calculation. The specimen with high n-value showed high stretch formability except for TA33 annealed at 550^{o}C. An abnormal grain growth deteriorates stretch formability of TA33.

Weakening basal texture is the most effective way to improve stretch formability because basal dislocation, the most prefer deformation mode in Mg, can be movable in any direction. At some point, dislocation pile-up in

grain boundaries occurs and initiates cracks. According to the results of small Erichsen test, twinning can release stress concentration up to certain grain size, but twin boundary plays an origin of cracks in large grain size.